Photopolymerization in dispersed systems

Florent Jasinski, Per B. Zetterlund, André M. Braun, Abraham Chemtob

PHOTOPOLYMERIZATION IN DISPERSED SYSTEMS

Florent Jasinski,[a] Per B. Zetterlund,[a] André M. Braun,[b] Abraham Chemtob[c, d*]

[a] Centre for Advanced Macromolecular Design (CAMD), School of Chemical Engineering, University of New South Wales, Sydney, NSW 2052, Australia.
[b] Karlsruhe Institute of Technology (KIT), 76131 Karlsruhe, Germany
[c] Université de Haute-Alsace, CNRS, IS2M UMR7361, F-68100 Mulhouse, France
[d] Université de Strasbourg, France

** To whom correspondence should be addressed: E-mail: abraham.chemtob@uha.fr; Fax: +33 389 60 87 99 ; Tel: +33 389 60 88 34*

Abstract

Zero-VOC technologies combining ecological and economic efficiency are destined to occupy a growing place in the polymer economy. Today, *Polymerization in dispersed systems* and *Photopolymerization* are the two major key players. The hybrid technology based on *photopolymerization in dispersed systems* has emerged as the next technological frontier, not only to make processes even more efficient and eco-friendly, but also to expand the range of polymer products and properties. This review summarizes the current knowledge in research relevant to this field in an exhaustive way. Firstly, fundamentals of photoinitiated polymerization in dispersed systems are given to show the favourable context for developing this emerging technology, its specific features as well as the distinctive equipment and materials necessary for its implementation. Secondly, a state-of-the-art and critical review is provided according to the seven main processing methods in dispersed systems: emulsion, microemulsion, miniemulsion, dispersion, precipitation, suspension, and aerosol.

Keywords: photopolymerization, emulsion, miniemulsion, dispersion, suspension, aerosol

Table of contents

LIST OF SYMBOLS AND ABBREVIATIONS

a	radius of a single particle
AA	acrylic acid
AIBN	azoisobutyronitrile
AMP	azobis-2-methyl–propamidinium dichloride
AOP	advanced oxidation processes
AOT	aerosol-OT, sodium dioctyl sulfosuccinate
APOENPES	ammonium poly(oxyethylene)$_{10}$-p-nonyl phenyl ether sulfate
ARGET	activators regenerated by electron transfer
ATRP	atom transfer radical polymerization
BA	butyl acrylate
BAG	bis(4-methoxybenzoyl)diethylgermanium
BAPO	bis(2,4,6-trimethylbenzoyl)phenylphosphine
BPO	benzoyl peroxide
BuMA	butyl methacrylate
CLP	classification, labeling and packaging
cmc	critical micellar concentration
CTA	chain transfer agent
CTAB	cetyl trimethyl ammonium bromide
DBK	dibenzylketone
DHA	dihydroxyacetone
DMPA	2,2-dimethoxy-2-phenylacetophenone
DPE	1,2-diphenyl-ethane
DTAB	dodecyltrimethyl ammonium bromide
DTBK	di-*tert*-butyl ketone
DS	dodecylsulfonate
DTBA	p-(4-diethylthiocarbamoylsulfanylmethyl) benzoic acid
DVB	divinyl benzene
E_i	activation energy of initiation [kJ mol^{-1}]
E_λ	extinction coefficient [m^{-1}]
EGDMA	ethylene glycol methacrylate
FTIR	Fourier transform infrared
GPC	gel permeation chromatography
HDTCl	hexadecyltrimethylammonium chloride
HMB	hydroxymethyl butanone
I-PDMS-I	diiodo-poly(dimethylsiloxane) macrophotoiniferter
ICAR	initiators for continuous activator regeneration
INISURF	molecule combining the properties of initiator and surfactant
ISC	intersystem crossing
K_λ	absorption coefficient [m^{-1}]
KPS	potassium persulfate
l	optical path length [m]
λ	wavelength [nm]
λ_0	wavelength of the incident radiation [nm]
L_p	photon radiance emitted per unit solid angle in a given direction [photon m^{-2} sr^{-1} s^{-1}]
LED	light-emitting diode
LVREA	local volumetric rate of energy absorption
m	ratio of the refractive index of the particle (n) to that of the surrounding water
μ	chemical potential
MA	methyl acrylate
MDEA	methyldiethanolamine
MMA	methyl methacrylate
N	number density of droplets (or particles) [cm^{-3}]

n	refractive index of the particle
NHC	N-heterocyclic carbene
NIR	near-infrared
Ω	solid angle [steradian]
P_{abs}	volumetric absorbed photon flux [photon m^{-3} s^{-1}]
$P_{abs}(s)$	polychromatic volumetric absorbed photon flux at any point of the irradiated system
$P_{abs,\lambda}(s)$	monochromatic volumetric absorbed photon flux at any point of the irradiated system
$P_0(\lambda, s)$	monochromatic incident photon flux as a function of λ and s
$P_{0,\lambda}$	monochromatic incident photon flux [photon L^{-1} s^{-1}]
$P_{t,\lambda}$	monochromatic transmitted photon flux [photon L^{-1} s^{-1}]
$P(\theta)$	phase function (angular distribution of irradiance scattered by a particle at a given wavelength)
PDMS	poly(dimethylsiloxane)
PEG-DA	poly(ethylene glycol) diacrylate
PEO	poly(ethylene oxide)
PETA	pentaerythritol triacrylate
PET-RAFT	photochemical electron transfer reversible addition-fragmentation chain transfer
photoINISURF	molecules combining the properties of a photochemical initiator and surfactant
PISA	polymerization-induced self-assembly
PLP	pulsed laser photopolymerization
PMMA	poly(methyl methacrylate)
PNAEI	poly(*N*-acetylethylenimine)
PPEGMA	poly(poly(ethylene glycol) methyl ether methacrylate
POENPE	poly(oxyethylene)$_{20}$-p-nonyl phenyl ether
PSA	pressure sensitive adhesives
PVA	poly(vinyl alcohol)
PVAc	poly(vinyl acetate)
PVP	poly(vinyl pyrrolidone)
$Q_{s,\lambda}$	Mie scattering efficiency
RAFT	reversible addition-fragmentation chain transfer
REACH	registration, evaluation, authorization and restriction of chemicals
RTE	radiative transfer equation
s	distance between a point on the surface of the radiation source and a point in the irradiated system [m]
S_λ	scattering coefficient [m^{-1}]
$\sigma_{s,\lambda}$	scattering cross-section [cm^2]
SDS	sodium dodecyl sulfate
TERP	tellurium mediated radical photopolymerization
T_λ	internal transmittance
θ	angle relative to the direction of the incident beam
TFSA	trifluoromethanesulfonic acid
UV	ultra-violet
UVA	spectral domain from 315 to 400 nm
UVB	spectral domain from 280 to 315 nm
UVC	spectral domain from 200 to 280 nm
VAc	vinyl acetate
VIS	visible
VOC	volatile organic compound
X	size parameter for the dispersion
ZnTPP	zinc tetraphenylporphyrin

1. INTRODUCTION

Polymerization in dispersed systems – mostly suspensions and emulsions – accounts for 20 % of the world polymer production. In most cases, water is used as continuous phase, resulting in two major advantages with regards to process conditions. Firstly, volatile organic compounds (VOCs) are avoided, making the process environmentally friendly; and secondly, the viscosity of the system is kept at a moderate level, facilitating polymerization heat removal, and therefore, the achievement of high throughput rates [1]. Heterogeneous waterborne polymerization has been a tremendous success story at both industrial and academic levels, and market growth is expected in all segments and regions. In the domain of waterborne coatings only – a leading product derived mainly from emulsion polymerization – the market size was estimated in 2015 at 17.7 million tons worth EUR 52.4 billion [2]. The main drivers identified for polymerization in dispersed systems are (i) regulatory pressure based on environmental concerns, (ii) increasing awareness among consumers of plastic products, and (iii) growth in its broad applications spectrum, particularly in the Asia-Pacific region. This very buoyant context is anticipated to create opportunities for future innovations, breakthrough polymerization processes and launches of novel waterborne polymer products.

To upgrade this technology, ultra-violet (UV)-visible (VIS) photopolymerization [3] – to date implemented primarily as a film curing process [4] – has emerged as one of the most promising methods. Although research in this field began some 35 years ago, recent developments on energy-efficient light-emitting diodes (LEDs), photoinitiators absorbing in the VIS spectral domain, low scattering monomer miniemulsions, and new designs of photochemical reactors, to name but a few, have shed new light on the possible improvements and innovations provided for a *photochemically initiated polymerization in dispersed systems*. In the foreground, photochemical initiation opens avenues for improved process conditions in regards to reaction efficiency, energy consumption and safety. Additionally, original latexes can be achieved resulting from photoinitated thiol-click, controlled radical photopolymerizations or photopolymerization-induced self-assembly (photo-PISA) with unusual composition, functionality, architecture or morphology compared to those obtained by conventional means (using redox or thermal radical initiators).

The aim of this review is to summarize for the first time the current knowledge in research relevant to this field in an exhaustive way, from the first photopolymerization in emulsion reported in the 1980s by Turro's group [5] to the most recent developments in photoinitiated radical polymerization in miniemulsion using VIS light [6]. Some fundamentals of photoinitated polymerization in dispersed systems are given in the first section to show the favorable context for developing this emerging technology, its specific features and issues as well as the distinctive equipment and materials necessary for its implementation. The second section is a state-of-the-art and critical review organized according to the processing method in dispersed systems: emulsion, microemulsion, miniemulsion, dispersion, precipitation, suspension, and aerosol photopolymerization. Didactically, each sub-section begins with a short description of the process and the general principles governing particle formation. Even when discussing each process separately, the diversity of experimental conditions often makes direct comparison of results difficult. For this reason, we have attached particular importance to provide detailed irradiation conditions as much as is reasonably practical. Whenever possible, radiation data are reported systematically as follows: [*type of radiation source*, *electrical and/or radiant power, spectral distribution, irradiance].* When only partial irradiation conditions are provided by authors, either assumptions have been made from experimental data, or the missing data have been clearly noted. As a final comment, note that this review will not cover photochemically initiated functionalization of particles, UV post-curing and cross-linking of waterborne heterogeneous systems such as paints or lacquers. Additionally, only the electromagnetic spectrum corresponding to UV-VIS wavelengths

will be considered for triggering polymerization; gamma rays, X-rays or ultrasound initiated polymerization in dispersed systems will not be discussed.

2. FUNDAMENTALS OF PHOTOINDUCED POLYMERIZATION IN DISPERSED SYSTEMS

2.1 POLYMERIZATION IN DISPERSED SYSTEMS MAKES THE SHIFT TOWARDS RADIATION CONTROL

2.1.1 The context: A mature technology facing new challenges

In polymer industry, there are currently considerable societal and legislative constraints to become compliant with more stringent environmental and health regulations: formulations with low or no VOCs, less energy-intensive processes, greater integration of renewable resources, and minimal waste production [7]. Polymerization in dispersed systems is today at the forefront of this polymer economy of the future which must be sustainable but also eco-efficient. In fact, polymerization in dispersed systems encompasses a number of distinct processes such as emulsion, suspension, microemulsion, miniemulsion, or dispersion polymerization, to cite the most important, where water is generally the continuous phase [8]. In addition, inverse heterophase polymerization techniques in continuous organic media have been developed for the preparation of a number of very important water-soluble industrial polymers, such as poly(acrylic acid) or poly(methacrylic acid) used in wastewater treatment, detergents, and super-absorbent polymers [9].

Polymerization in dispersed systems has a number of key advantages: first, VOCs are obviated, making the process and the final waterborne product environmentally friendly. Second, the viscosity of the system is low, enabling an efficient heat transfer from exothermic polymerization reactions. Therefore, high yields may be achieved in reasonable times. Central to this technology is chain-growth radical polymerization performed in stirred tank reactors using thermal or redox initiators, and a wide majority of polymerizations in dispersed systems is based on this water-tolerant polymerization mechanism. Among the variety of techniques, only emulsion and suspension have been applied industrially at a very large scale.

● *Suspension polymers* are estimated to be produced at 30 million metric tons (dry basis), i.e. nearly 13 % of the total polymer production. Suspension polymerization yields some of the most important commodity thermoplastics, which are produced as dry solid beads (0.1 - 10 mm) after filtration and washing. The most emblematic polymers derived from this process are poly(vinyl chloride), poly(methyl methacrylate), expandable polystyrene, and styrene-acrylonitrile copolymers [10].

● *Emulsion polymers* are stable waterborne polymer dispersions, with a typical particle size spanning 50 – 200 nm. They are often referred to as polymer colloids or latex. The annual production was estimated in 2016 at 12.7 million metric tons (dry basis) with an annual growth rate of 5.1 % [2]. *Emulsion polymers* account for over 80 % of the waterborne dispersions produced annually. Step-growth polymers (polyurethane, polyester…), alkyd and silicone are completing the list. Although the latter are waterborne products, they do not result from a polymerization performed in a dispersed system but in organic solution. Adequate functional groups introduced during the synthesis or surfactant addition make them dispersible in water, as a second stage after synthesis. Their specific properties - low viscosity, no VOC, film-forming ability - make them essential in many industrial sectors including coatings, adhesives, paper coating, inks, additives for construction materials, and non-woven textiles. Although the level of production is lower than for suspension polymers, emulsion polymerization offers higher versatility, in particular more latitude in achieving broad and customized properties, because the polymer microstructure and composition can be easily tuned in semi-continuous operation. *Emulsion polymers* can be used in dry form or directly as waterborne dispersions for film formation (coatings and adhesives). Industrial formulations are characterized by high solid or polymer contents (> 50-60 % by weight). The principal advantages are an increased space-time yield of the reactor, more efficient product transport, and faster drying times during film application.

Today, the most common *emulsion polymers* include copolymers based on styrene-butadiene (approx. 37 % of the market share), (meth)acrylates (30 %), vinyl acetate (28 %) and so-called specialty monomers (5 %) such as vinylidene chloride for high barrier coatings [11].

Although polymerization in dispersed systems has proved to be a tremendous success at both academic and industrial levels, there are mainly two incentives to go beyond the current technology:

- Broadening the range of latex products and properties available. Waterborne systems account for nearly 75 % of the architectural coatings (building and construction industries) , but they hold a much lower share of the industrial coatings market (< 20 %). Industrial coatings (automotive, protective, marine, wood, coil, packaging...) generally require higher performance, and are still heavily dominated by solvent borne products. For many coating manufacturers, the most important technological improvement would be the generalized usage of waterborne products in every possible area [12]. In addition, more than 90 % of waterborne coatings prepared from *emulsion polymers* contain acrylic monomers. Although acrylate monomers have high structural versatility, broadening the range of latex and properties available as well as improving the waterborne products' performance are needed to meet future societal challenges. The penetration of new markets such as high barrier, maintenance coating applications is expected to drive innovations. Furthermore, the implementation of European's REACH legislation and new regulations on hazard classification and symbols will act as strong incentives for the displacement of solvent borne polymer products. Many of these products authorized today may be labelled hazardous in the near future, even without change in their safety datasheet.

- Making the process even more efficient, eco-friendly and safer. Most industrial polymer dispersions are produced under semi-continuous operations with typical polymerization times of several hours. Although some conventional monomers such as acrylates have high propagation rate coefficients (k_p), the highly exothermic nature of radical polymerization makes heat dissipation a critical issue. Controlled addition of monomers in semi-continuous processes is thus mandatory for most polymerizations, not only to master polymer composition, but also to obviate that the resulting accelerating reaction may proceed to the point of loss of control (runaway), leading to drift in polymer architecture, fire or explosion. To overcome this limitation, the development of reactors for continuous processes (tubular and continuous-stirred tank reactors referred to as CSTR) featuring higher heat removal has been investigated [13]. CSTRs in series is the main commercial continuous process implemented today for the large scale production of styrene–butadiene rubber latex. Nonetheless, prone to plugging (coagulation), tubular reactors have not been implemented commercially except for the production of vinyl acetate homopolymers and ethylene-acrylate copolymers. Reduction in energy consumption is a second key challenge. Indeed, heating is necessary in a majority of polymerizations in dispersed systems as the thermal homolytic dissociation of initiators carried out at 75–90 °C is today the most widely used mode of generating initiating radicals. Water has about two times the heat capacity of a common organic solvent such as acetone. This means that heating and cooling at the end of the reaction as well as temperature regulation during polymerization require a large amount of energy. Consequently, possible improvements cover a more extended use of polymerization at ambient temperature and a wider use of more economical energy sources.

2.1.2 Photopolymerization: From film curing to waterborne dispersions

The use of radiation to initiate polymerization in dispersed systems may appear prima facie as a very unconventional alternative, or at least a choice far from being intuitive. Obviously, except from optically transparent or translucent microemulsions, the first difficulty has to do with the strong turbidity of most monomer or polymer dispersed systems. In addition to *scattering*, *absorption* (from photoinitiator but also monomer or surfactant) causes a significant attenuation of the radiation penetration within the reactor,

particularly for the short UV wavelengths (UVC: 200 - 280 nm). Based on this challenge, it seems logical that photoinitiated polymerization has developed essentially as a cross-linking technology for films having a maximum thickness of 50-100 µm (Fig. 1) [4]. Radiation–curing is applied today in many industrial areas, including mainly graphic arts (inks, overprint varnishes), optoelectronics (photoresists) and industrial coatings [14].

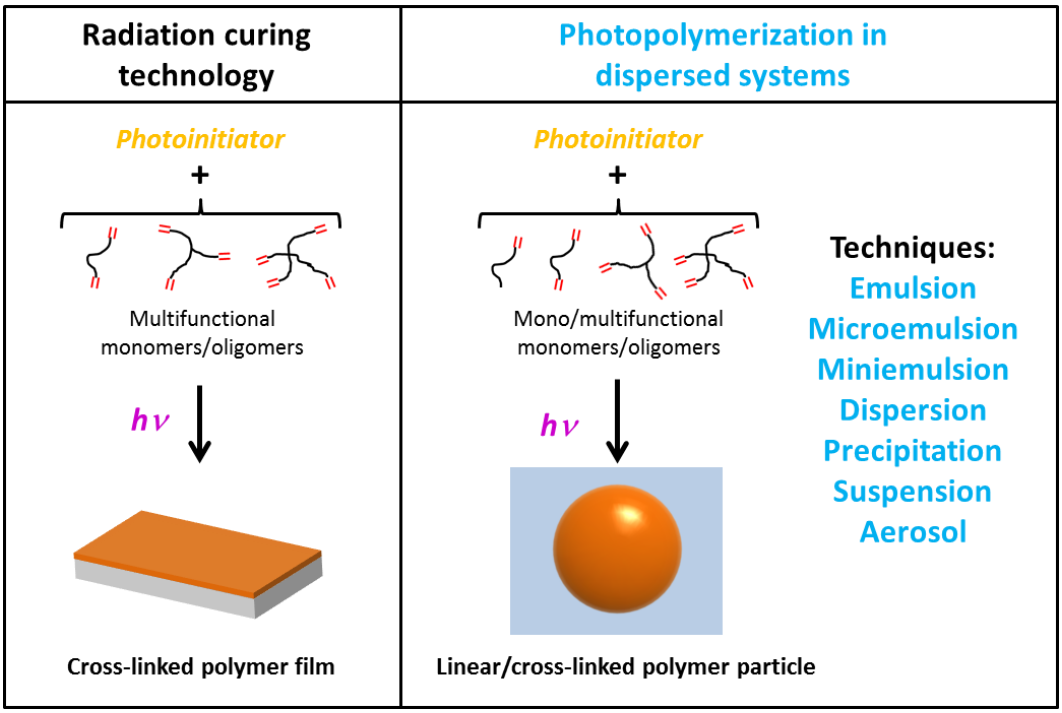

Fig. 1: Types of processes and products of photopolymerization in dispersed systems

Despite this morphological limitation, UV-VIS curing technology features many interesting advantages, a number of which are relevant for improving energy-efficiency and the green credentials of polymerization in dispersed systems: 100 % solid content formulation (no solvents or volatiles), ambient temperature process, high energy savings and production speed process, and small space requirement. As proof of the interest generated by this technology, UV-curable coatings were expected to grow at 9 % from 2015 to 2020, compared to 6 % for waterborne coatings [15]. Radiation curing and polymerization in dispersed systems thus have in common being two VOC-free technologies, performed respectively in water and without organic solvent (the other VOC-free processes include powder polymer technology and reaction in ionic liquids or compressed (supercritical) fluids). By "merging" these two approaches, there is the expectation of a synergistic eco-efficient technology based on *photopolymerization in dispersed systems*. Obviously, one of the main challenges in this turbid medium is to cope with heterogeneous distribution of radiation and the consequent spatial variations in the generation of initiating radicals. This may undermine the polymerization activity, raise problems of local overheating or polymer precipitation in limited irradiated regions.

Research on photopolymerization in dispersed systems started more than 35 years ago [16], but cutting–edge technologies remain to be developed. However, recent developments in photochemical engineering, energy-saving radiation sources, photoinitiators and photoinitiated radical-based polymerizations based on photocatalytic processes or click reactions constitute a sound basis from which to re-assess the potential of these systems. Historically, the first photopolymerizations in a heterogeneous environment were reported by Turro et al. in the early 1980's using styrene macroemulsions [5]. Meanwhile, Fouassier et al. photopolymerized methyl methacrylate-based microemulsions, investigating mainly kinetic aspects [17]. Following these pioneering studies, the technology has been implemented in various dispersed

systems such as aerosol, suspension, dispersion and other emulsion-type processes, which are for the first time not only gathered, but also inter-linked and commented on in this review. While there are more than 200 examples proving its feasibility, the question of the applicability of this novel platform in modern-day society remains a crucial issue. Meeting the challenge of radiation penetration requires paying greater attention to photochemical engineering aspects (design of reactor, choice and geometrical arrangement of radiation sources), and also to colloidal properties and composition of the dispersed systems. In practice, most photopolymerizations in dispersed systems described in the literature were conducted without any serious attempt being made to optimize utilization of radiation or colloidal dispersed system characteristics. Consequently, there is still plenty of scope for further development in this area, and many opportunities to seize at both industrial and university levels.

2.1.3 Photoinitiation, when a tiny change creates great opportunities!

Unlike a conventional method where initiation is triggered by the addition of active substances (oxidizing/reducing agent pair) or thermolatent agent (peroxides or azo compounds), a photoinitiated radical polymerization involves, in most instances, a photochemically reactive initiator able to generate initiating species when irradiated to trigger polymerization. Consequently, except for the primary step of creating the active centers, the mechanism and final products remain unchanged. Despite this seemingly insignificant change, photopolymerization in dispersed systems can open avenues for many improvements:

• **Photochemical polymerizations have several advantageous features**:

- Contactless stimulation [18];
- Specific reactivity of electronically excited states compared to ground states resulting in a greater range of initiation pathways: fragmentation, electron transfer, energy transfer, or hydrogen abstraction;
- Temporal control of reaction (ms);
- High spatial resolution (μm);
- Reaction rate and molecular weights tunable by precise energetic and spatial dosage of radiation;
- Higher decomposition rates of photochemical initiators compared to their thermal analogues;
- No effect of temperature on initiation stage.

• **A technology potentially scalable towards industrialization.** Today, one of the principal industrial applications of photochemistry lies in the area of radical chain reactions including chlorination and sulfochlorination of alkanes. Although these reactions allow the preparation of low-molecular weight compounds, they have two important points in common with chain-growth radical polymerization: the mechanism (initiation, propagation, termination) and very high quantum yields, larger than 1000, meaning that one photon absorbed induces the addition of more than 1000 monomer units.

• **Low energy consumption and safety.** Photoinitiated polymerizations can occur at ambient temperature and rely on the use of energy-saving UV or VIS radiation sources. In addition, some reactions may even be carried out using sunlight as renewable energy source. Because chain-growth polymerization reactions are exothermic in nature, the issue of heat removal should also be taken into consideration given it may negatively impact the energy efficiency of the process (see section 2.2.6 on *Photoreactor* for details).

• **A range of polymerization reactions can be facilitated under radiation activation.** Radiation-initiation has attracted growing interest for performing controlled/living radical polymerization in dispersed systems due to the mild reaction conditions. The synthesis of novel water-borne materials based on thiol-click chemistry is also a promising contemporary research area. Additionally, some thiol-ene or acrylate photopolymerizations can even occur without initiator by appropriate choice of the irradiation wavelength, which minimizes the formation of by-products.

2.2 CONSIDERATIONS FOR THE DEVELOPMENT OF PHOTOPOLYMERIZATION IN DISPERSED SYSTEMS

2.2.1 Temporal control

• **Control of polymerization in terms of time.** A first key feature of photoinitiated polymerization is temporal control of the reaction. Given that initiating radicals cannot be generated without electronic excitation of a photoinitiator, polymerization initiation by carbon-centered radicals will stop instantaneously when the incident radiation is switched off. However, polymerization will continue as long as there are primary or propagating radicals present whose lifetimes are controlled by their electronic structure, the concentration of potential reaction partners and temperature. The lifetimes of these radical species might span from only a few hundred nanoseconds to fractions of seconds. Consequently, the generation of initiating radicals can be performed in a controlled fashion by switching on and off the radiation source, or by using a shutter, which is a distinctive feature compared to the use of thermal or redox initiators. In this way, reactions can be stopped almost instantly. As a result, the risk of runaway reaction is strongly mitigated while for thermal polymerization, the thermal inertia continues to generate radicals in the reaction medium even after the heat source has been stopped. A broad range of radical photoinitiators are commercially available from *e.g.* IGM Resins, Lamberti, Lambson and BASF. Although a minority of initiators are water-soluble (necessary condition for *e.g.* emulsion polymerization, see section 2.3.4 on *Photoinitiators* for details), most of the oil-soluble initiators originally developed for UV-curing technology may also be used for photopolymerization in dispersed systems. The unique characteristic of temperature-independent decomposition rates yields a more robust process since a temperature deviation is unlikely to alter the overall initiator radical concentration photochemically generated in the medium. Furthermore, the radical generation can be controlled by the emission characteristics, the power of the radiation source and by the absorption conditions set by the geometry of the photochemical reactor.

• **Excellent temporal resolution (≈ ms or even less).** This opens an avenue for non-steady state radical polymerization conditions since the change of radiant power or frequency of a pulsed emission can cause the radical concentration to deviate from a constant, steady-state value. The consequence of a tunable rate of change of the concentration of radicals is to obtain defined conversions (synthesis of pre-polymers) [19]. For *e.g.*, pulsed-laser photopolymerization (PLP) was reported in the late 1980s [20]. Involving alternating light and dark periods, it has been mainly exploited for the determination of propagation rate coefficients in radical chain polymerization. It was also shown that the variation of the frequency of pulsed irradiation affected the molecular weight dispersity of the prepolymer [21]. Today, the instant on/off capacity of LEDs opens new horizons to use radiation to control polymer architecture and composition. By contrast, traditional UV arc radiation sources (other than xenon flash arcs) are switched on and off only when needed, not only due to the warm up time to reach stable exitance but also due to the negative impact of switching on their lifetime.

2.2.2 Spatial control and in situ photopolymerization

• **Control of polymerization in terms of space.** Spatial control in photopolymerizations refers to the ability to control precisely where the polymerization reaction occurs at 2D or 3D level [22]. One of the most common and successful applications is photolithography, a widely disseminated process in industry used to photochemically generate (micro)structures, *e.g.* at the surface of semiconductor (mostly silicon) wafers [23]. In dispersed systems, spatial control is largely expressed through the use of microfluidic devices, taking advantage of the UV transparency of quartz or poly(dimethyl siloxane)-based microreactors. In a conventional process, microsized multifunctional monomer droplets are generated, at the junction of two microchannels or at the tip of a capillary, to be cross-linked downstream under short UV-exposure. Polymer microparticles with a narrow size distribution and complex morphologies (Janus, core-shell…) have been

realized, taking advantage of complex flow fields and high spatial resolution (µm) as reported by many authors including Serra [24], Kumacheva [25], or Doyle [26]. These studies, close to a suspension polymerization (described in section 3.6), have been discussed elsewhere [27].

• **Miniaturization and online monitoring.** As an extension, spatial control also enables *in situ* (localized) polymerization through the use of focalized radiation performed by *e.g*. a waveguide. A first benefit is the down-scaling of the polymerization reactor that could lead to the use of very small microreactors (see details in section 2.2.6). Additionally, online monitoring of the reaction progress can be facilitated. While fiber optic probes for spectroscopic sensors (near-IR or Raman spectroscopy) are necessary in emulsion processes, the low dimensions of the irradiated sample (small optical path) may allow the use of conventional transmission FTIR spectroscopy, making possible the contact-free measurement of monomer conversion during irradiation. Furthermore, the modest cost and standard availability of time-resolving features on commercial FTIR spectrometers also make the implementation of time-resolved studies (sub-second time scale) possible, which is particularly relevant to assess online very fast photopolymerization kinetics of thiol-click polymerization reactions occurring in the matter of seconds. Real-time FTIR spectroscopy has been widely implemented for in situ monitoring of very fast cross-linking of UV-curable coatings mainly based on acrylate monomers [28].

2.2.3 Radiation penetration and distribution

• **An "optically thick" medium.** Like (nano)composite or pigmented UV-curable coatings, dispersed monomer or polymer systems are mostly "optically thick" media due to the conjugated effect of *absorption* and *scattering*. However, the issue is likely to be exacerbated in the case of polymerization in dispersed systems because of two factors:

1. With the exception of microreactors (having an internal channel diameter ≤ 1 mm), the optical path of most reactors is much larger than the thickness of coatings.

2. Dispersed monomer systems of practical utility (*e.g.* monomer emulsions) are highly scattering due to several effects: (i) a concentration effect because industrial standards impose solids content greater than 50 wt%; (ii) the difference of refractive indices between the dispersed phase and the continuous aqueous phase is usually marked. While this difference is relatively small for a monomer such as methyl methacrylate (0.081 at 20°C), it is almost three times higher for styrene (0.213); (iii) most monomer emulsifications result in broad droplet size distributions, with a significant proportion of highly scattering particles with a diameter larger than 100 nm.

To understand the effect of *absorption,* one must note that most UV-curable varnishes, which are non-scattering and only a few tenths of micron thick, are already considered as "optically thick". This means that a significant amount of radiant energy is absorbed within a few micrometers from the irradiated surface of the material. The second challenge is *backscattering* opposing radiation entry due to monomer droplets (except for dispersion polymerization, in which case no droplets are initially present) and particles. Scattering being an elastic phenomenon, forward scattering contributes to light penetration in contrast to backscattering. Characterized by high organic phase concentration (> 50 wt%) and broad droplet size distributions (100 -10 µm), acrylate monomer macroemulsions as used industrially for emulsion polymerization exhibit very high scattering coefficients (vide infra). The corollary is that irradiance falls off very rapidly with increasing distance from the irradiated surface. Generally, UVB (280 – 315 nm) and UVA (315 – 400 nm) do not exceed the first 50 µm from the reactor wall in such a system, resulting in a minimal irradiated reactor volume fraction. Radiation of even shorter wavelength is absorbed or scattered in a much thinner layer, implying that polymers can only be formed in the close vicinity of the irradiated surface. It is therefore hardly surprising that some authors mention the formation of a tarry deposit on the wall of the

cooling well or plugging when using tubular-type reactors. Therefore, the question of how far the emitted radiation penetrates the dispersed reaction medium is important not only from a reactivity point of view but also to preserve colloidal stability and constant process characteristics.

• **Concomitant absorption and scattering.** Inside an efficiently stirred reactor, a thermal reaction is carried out statistically throughout the reactor. By contrast, a photochemical chemical reaction is only possible in irradiated volumes. In a heterogeneous or dispersed medium, the incident photon flux is attenuated in accordance with:

$$P_{t,\lambda} = P_{0,\lambda} 10^{-E_\lambda l}$$

where $P_{0,\lambda}$ the monochromatic incident photon flux [photon L^{-1} s^{-1}], $P_{t,\lambda}$ the monochromatic transmitted photon flux [photon L^{-1} s^{-1}], E_λ the extinction coefficient [m^{-1}], and l the optical path length [m].

The extinction coefficient E_λ is usually defined as the sum of the absorption K_λ [m^{-1}] and scattering S_λ [m^{-1}] coefficients:

$$E_\lambda = K_\lambda + S_\lambda$$

These two variables are usually difficult to obtain individually. For dispersions, K_λ and S_λ, can be determined experimentally by nonconventional spectrophotometric methods using diffusive reflectance and transmittance requiring typically spectrophotometers equipped with an integrating sphere [29, 30]. For more details on optical properties of particles, we refer interested readers to two reference publications in this field: one general from van de Hulst [31], and a second more advanced by Bohren [32]. To reveal the impact of scattering on radiation penetration, Figure 2 shows more simply the results of internal transmittance $T_\lambda = \frac{P_{t,\lambda}}{P_{0,\lambda}}$ (obtained with a conventional UV-VIS spectrophotometer) between a photoinitiator emulsion system – combining scattering and absorption – and a concentration equivalent solution system where only absorption is effective.

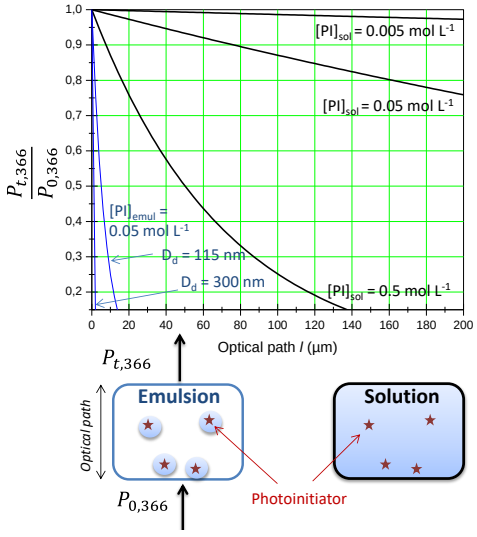

Fig 2: Internal transmittance measured at 366 nm by spectrophotometric analysis in regular transmission for two concentration equivalent systems in solution and emulsion containing 2,2-dimethoxy-2-phenylacetophenone (DMPA, see Table 1). Only this photoinitiator absorbs at the incident wavelength. The emulsion system contains DMPA droplets (average diameter: 115 or 300 nm) dispersed in water and pre-dissolved in CH_2Cl_2 (2 vol.%) having an overall concentration of 0.05 mol L^{-1}. The solution system corresponds to DMPA dissolved in CH_2Cl_2 at three different concentrations (0.005 – 0.5 mol L^{-1}). The dispersed system shows a significantly higher shielding effect assigned to scattering while the radiation penetration of the solution system can be modulated upon changing the initiator concentration because only absorption occurs.

• **Scattering by particles: General considerations.** The scattering coefficient can also be related to the scattering cross-section $\sigma_{s,\lambda}$ [cm^2]:

$$S_\lambda = \sigma_{s,\lambda} N,$$

where N is the number density of droplets (or particles) [cm^{-3}].

Interestingly, $\sigma_{s,\lambda}$ can be estimated by Mie theory calculations which are valid for spherical particles of any size provided that their concentration is dilute enough to avoid multiple scattering. Multiple scattering takes place when some light scattered out of the original beam by a particule might be scattered again by another and reach finally the detector. Prediction of the extent of Mie scattering involves complicated calculations (complex mathematical expression is detailed in ref [33]), but computer codes are readily available online [34] and offer a highly useful overview of the effect of particle size and the refractive indexes of the two non-miscible media, or of the wavelength of excitation on scattering. Figure 3A shows the evolution of the *Mie scattering efficiency* (solid curve) $Q_{s,\lambda} = {}^{\sigma_{s,\lambda}}/_{\pi a^2}$ (dimensionless) which is related to the scattering ability of a single particle of radius *a* as function of the quantity *mx*, where *m* is the ratio of the refractive index of the particle (*n*) to that of the surrounding water (n_{water}), $x = {}^{2\pi a n_{water}}/_{\lambda_0}$ is the *size parameter* for the dispersion (polystyrene), and λ_0 the wavelength of the incident radiation (500 nm) [35].

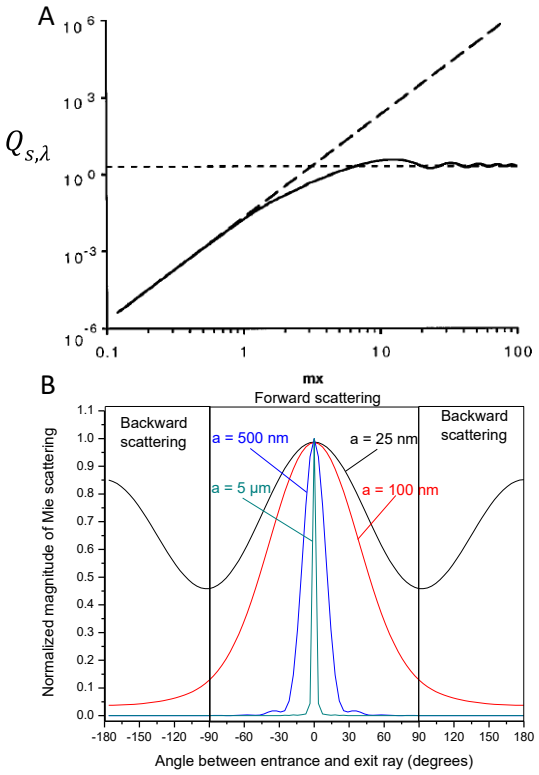

Fig. 3: A) Plot of scattering efficiencies $Q_{s,\lambda}$, for Mie scattering (solid curve) and Rayleigh scattering (dashed curve) vs *mx* for a polystyrene dispersion of radii ranging from 5 to 5000 nm, *m* = 1.59/1.33, λ_0 = 500 nm (data from [35]). The dotted line indicates the limiting value of $Q_{s,\lambda}$ for large particles. **B**). Graph showing the phase function $P(\theta)$ (unpolarized radiation) for four different radii of single polystyrene particles (50, 200, 500 and 5000 nm) as a function of angle θ which is relative to the direction of the incident beam. The values have been normalized so that the value of the peak at 0° (angle with incident beam) is one. These values were calculated using the interactive Mie Scattering Calculator at http://omlc.org/calc/mie_calc.html [34].

For *mx* < 1 (a < 50 nm for polystyrene), an excellent correlation with the Rayleigh approximation (dashed curve in Fig. 3A) offers a simple analytic solution for $Q_{s,\lambda}$:

$$Q_{s,\lambda} = \frac{8\pi}{3} a^4 \left(\frac{m^2-1}{m^2+2}\right)^2 \left(\frac{2\pi n_{water}}{\lambda_0}\right)^4$$

For low *mx* values, the scattering efficiency varies with the fourth power of the particle radius (a) and inverse fourth power of the wavelength (λ_0). Therefore, scattering and thus radiation attenuation may be minimized in this range by (i) shifting towards higher irradiation wavelengths and/or (ii) by relying on smaller polymerizable entities. With regard to this last point, monomer microemulsions (a < 25 nm) and miniemulsions of very small droplet sizes (a < 50 nm) may be interesting candidates to improve radiation penetration [36]. These two types of emulsion feature indeed the lowest monomer droplet sizes among the range of polymerization processes considered in dispersed systems.

In the intermediate size range (1 < *mx* < 4 involving a particle radius range of 50 - 200 nm), the increase of the scattering efficiency diminishes and becomes proportional to the second power of the particle size. The particles are getting even larger (*mx* > 10, *a* > 500 nm), the scattering efficiency levels off and settles to a value close to 2. This means that under these conditions $Q_{s,\lambda}$ is much less impacted by particle size and can even increase with larger wavelength. Even if this threshold value means that individually, a large particle has a higher scattering efficiency than a small particle, at similar polymer concentration, the dispersion made up of large particles has much less entities leading to minor scattering compared to a small particles dispersion.

Another characteristic of scattered radiation which may be of importance for radiation penetration is that it takes place in all directions, but usually with different intensities in different directions. Fig. 3B shows the results of the phase function $P(\theta)$ for polystyrene particles of radii *a* = 50, 200, 500 and 5000 nm. $P(\theta)$ is the angular distribution of irradiance scattered by a particle at a given wavelength (see Fig. 3B: λ_0 = 500 nm). It is given for angles θ which are relative to the direction of the incident beam. When *mx* < 1 (*a* < 50 nm), the signal is not isotropic. With minima at θ = 90°, $P(\theta)$ is practically symmetric in the fore (θ = 0°) and aft direction (θ = 180°) implying a significant portion of back-scattering (θ > 90° or θ < -90°). By contrast, when scattering entities become larger (*mx* > 1), the anisotropy is more pronounced and scattering is strongly biased toward the forward direction. This result is also useful for the understanding of the higher radiation penetration in polymer suspensions exhibiting radii >> 5 µm. As a final comment, it is important to underscore that Mie theory does not apply to systems where multiple scattering takes place, which is the majority of polymerizations in dispersed systems, even if concentrated emulsions are left apart. Scattering effects of photopolymerizations may, however, be evaluated by using the approach of Kubelka-Munk that has already been found to be very useful in atmospheric science to understand scattering of aerosols [37, 38].

• **Absorbed photon flux and radiation distribution.** The main challenge is the correct evaluation of the *volumetric absorbed photon flux*: P_{abs}[photon m^{-3} s^{-1}], corresponding to the amount of photons absorbed per unit time and reaction volume, that will determine eventually the rate of a photochemical reaction. The radiometric equivalent of P_{abs} is identical with the *local volumetric rate of energy absorption* (LVREA) as introduced by Whitaker and Cassano [39]. In a heterogeneous reaction system, the absorbed flux quantities depend on K_λ (vide supra) and the diminution of radiation due to forward- and back-scattering. The monochromatic incident photon flux $P_0(\lambda, s)$ at any point of an irradiated heterogeneous system may be calculated in applying the radiative transfer equation (RTE) [48, 49] leading to

$$P_0(\lambda, s) = \int_{\Omega=0}^{\Omega=4\pi} L_p\,(\lambda, s, \Omega) d\Omega$$

where s [m] is the distance between a point on the surface of the radiation source and a point in the irradiated system, and Ω [steradian], the solid angle [40]. L_p is the photon radiance emitted per unit solid

angle in a given direction [photon m^{-2} sr^{-1} s^{-1}] [80]. Combined with the absorption coefficient, the monochromatic volumetric absorbed photon flux at any point of the irradiated system may be obtained by.

$$P_{abs,\lambda}(s) = K_\lambda \int_{\Omega=0}^{\Omega=4\pi} L_{p,\lambda}(s,\Omega)d\Omega$$

For polychromatic irradiations, $P_{abs,\lambda}(s)$ has to be integrated over the spectral domain of interest.

$$P_{abs}(s) = \int_{\lambda_1}^{\lambda_2} K(\lambda)d\lambda \int_{\Omega=0}^{\Omega=4\pi} L_{p,\lambda}(s,\Omega)d\Omega$$

Although spectroscopic evidence for such calculations were so far never attempted in the field of photopolymerization in dispersed systems, this approach has been extensively investigated in other heterogeneous photochemical systems [41]. Photochemical reactors containing aqueous suspensions of TiO_2 particles are a prime example aiming at an optimization of advanced oxidation processes (AOP) used for oxidative degradation of pollutants in aqueous systems. The most popular numerical solutions of the integrodifferential Radiative Transfer Equation (RTE) has involved Monte Carlo [42], discrete ordinate model [43] and finite volume methods [44]. It is expected that a useful transfer of knowledge between radiation optimized reactor modeling, design and application might occur shortly.

• **Mitigating the effect of radiation attenuation or living with it?** The empirical approach accumulated over 35 years by chemists is already sufficient to demonstrate that photopolymerization in dispersed systems is feasible over a broad range of conditions despite a non-uniform radiation distribution. As proved experimentally in many instances, strong radiation attenuation does not necessarily lead to low polymerization rates. For emulsion polymerization involving “optically thick” systems (see section 2.2.3), some good results may be rationalized on the basis of high diffusion rates and low viscosity making dispersed systems an excellent medium to avoid mass transfer limitations. Clearly, problems of diffusion limitations are minimized compared to UV-curable coatings where cross-linking strongly reduces molecular mobility. Another reason is that radical photopolymerizations have rather high quantum yields. They are initiated by a single photochemical process yielding a pair of primary radicals and subsequently amplified by a large number of consecutive thermal reactions, i.e. monomer propagation in the case of polymerization. Consequently, a photochemical radical chain reaction can generally take place in a reaction system where relatively few photons are absorbed per unit volume, and even at low temperatures. Many radical organic chain reactions (*e.g.* chlorination, bromination, sulfochlorination, some oxidations) have been developed to large scale applications since the 1940s [45]. Finally, note that a number of monomer containing entities such as micelles or droplets, although not absorbing incident photons (dark area), can indirectly contribute to polymerization. When a monomer is sufficiently soluble in water, which is the case even for hydrophobic monomers like styrene, it can diffuse through the aqueous phase to reactive entities containing an oligo- or macroradical.

To date, only few works are published with the aim of mitigating the detrimental effect of radiation attenuation in photopolymerization in dispersed systems. The current level of knowledge is largely insufficient to meet the standards of modern technology and to adapt it to the requirements and challenges of industrialization. However, several actions can be implemented as “guidelines” to minimize radiation attenuation:

(i) ***Reducing the optical path length:*** The most relevant approaches rely on photochemical reactor design (see section 2.2.6) [46].

(ii) ***Increasing the wavelength of irradiation:*** The shift to higher wavelength (VIS or even near-infrared (NIR) radiation and two-photon excitation) provides a significant decrease of the level of scattering, in

particular when the Rayleigh approximation is valid ($mx < 1$). Therefore, this approach may be relevant for dispersed systems composed of nanodroplets or nanoparticles (a < 50 nm). One illustrative example is the use of photoredox systems, active at visible wavelength [47], for the initiation of miniemulsion polymerization [6].

(iii) ***Decreasing the droplet diameter and size distributions:*** On the contrary of the argument above, scattering may also be reduced by adapting a dispersed system to a given irradiation. In such a case, the droplet radius should be made much smaller than the wavelength of irradiation ($mx < 1$). Reducing the droplet diameter is experimentally possible by relying on miniemulsion or microemulsion polymerization techniques, where the colloidal properties of the dispersed systems can be optimized using high pressure homogenizers, static mixers or ultrasonifiers to narrow the droplet size distribution

(iv) ***Decreasing the solids content:*** The concentration of droplets affects the scattering properties of a medium by increasing the probability of multiple scattering events (clustered spaces). Thus more radiation is lost for initiation in the first layers of the dispersed system.

(v) ***Matching the refractive index of the two phases:*** As shown in Fig. 5, a lower m value can reduce the scattering coefficient under certain conditions, mostly for small particles sizes relative to the wavelength of irradiation. The feasibility of this approach has been shown for conventional miniemulsions [48] and Pickering emulsion polymerization [49], but was never harnessed in a photochemically induced process.

(vi) ***Mathematical modelling***: The use of advanced numerical tools could provide accurate modelling of the radiant distribution within an irradiated volume of given shape and thus enables optimization of irradiation conditions.

2.2.4 Radiation-initiated polymerizations

At present, most polymerization processes in dispersed systems rely on thermal radical generation, photochemical initiation opens the door to a number of applications either unattainable by thermal means (because of the specific reaction manifold of excited molecules) or because the photochemical process might be easier to realize.

- **Thiol-X reactions.** Examples worth highlighting are thiol-ene and thiol-yne polymerizations proceeding via an initiated addition of a thiyl radical, RS$^{\bullet}$, generated by hydrogen abstraction from RSH, to a carbon–carbon π-bond (alkenes) or triple (alkynes) bonds. Although thermal or redox initiators can be used, radical photoinitiators (in particular α-cleavable initiators, see section 2.3.4 on *photoinitiators*) are highly effective at initiating thiol-ene polymerizations either by hydrogen abstraction from a thiol functional group or by addition of the initiator radicals to an alkene. For dithiol-dialkene monomer miniemulsions, the step growth mechanism resulted in a 1:1 stoichiometric consumption of thiol and ene functional groups, yielding a linear [50], or cross-linked [51] poly(thioether) latex in the matter of seconds, but only small reaction volumes and solid contents were addressed so far. Harnessing the enormous potential of the thiol-based "toolbox" may in the near future create a novel portfolio of sulfur-containing polymer latexes.

- "**Self-initiated" polymerization.** Photochemical monomer (substrate) activation may also occur without addition of initiators, thus minimizing the formation of by-products. A broad range of conventional monomers such as acrylates may undergo radical polymerization at ambient temperature from their $n\pi^*$-excited state. Such "self-initiated" photopolymerization in miniemulsion was for example demonstrated in 2012 with using irradiation sources emitting a part of their radiation spectrum in the UVC and UVB spectral range [52]. Unfiltered radiation of a conventional Hg medium-pressure arc (λ > 220 nm) was employed to prepare initiator-free polyacrylate nanolatex. By contrast, most monomers used for radical polymerization cannot undergo thermal "self-initiated" polymerization below 100 °C when properly purified.

• **Photo-catalyzed initiation.** Very recently, photoredox catalysts have emerged as highly efficient initiators for polymerizations in dispersed systems, with very specific advantages: (i) only low irradiance required (a few mW cm^{-2}), (ii) electronic excitation in the VIS spectral region, (iii) only catalytic amounts of photosensitizer required (because regenerated in the process), and (iv) high specificity (no unwanted side reactions). Jung et al. showed that the well-known and commercially available Ir complex $Ir(ppy)_3$ (tris[2-phenylpyridinato-*C*2,*N*]iridium(III)) can photo-catalyze controlled/living radical polymerization of a styrene miniemulsion [6]. In this example, a photochemical electron transfer reversible addition-fragmentation chain transfer (PET RAFT, vide infra) process plays a key role in the activation/deactivation of radical species. Radical polymerization has also been carried out using colloidal or supported TiO_2 as non-extractable and recyclable heterogeneous photocatalyst [53].

2.2.5 Low energy consumption and increased safety

• **Comparison with thermal and redox initiators.** Thermal decomposition (homolysis) of peroxides and azo compounds is the industry standard to initiate radical polymerization in dispersed systems, generally requiring a minimum temperature of 75 °C. Thermal redox initiation may be exploited at room temperature, but its implementation has rarely been driven to increase the green credentials of the process. Its use served primarily to broaden the scope of achievable polymer microstructures, that are temperature-dependent [54]. For redox initiators systems, such as hydrogen peroxide (oxidant) and ferrous salts (reductant), the activation energy of the initiation step (E_i) is about 40–60 kJ mol^{-1} *i.e.* approx. 80 kJ mol^{-1} less than for thermal initiator decompositions. Consequently, energy and equipment costs can be reduced. Nevertheless, the heat of polymerization needs to be diverted via *e.g.* an "adiabatic process", where an increase of the reactor temperature is leading to a faster rate of initiation and reasonable cycling time can thus be achieved [55]. For the photochemically induced polymerization, the initiation step is temperature independent (E_i = 0 kJ mol^{-1}) since the energy of the electronically excited state of the initiator chromophore is higher than the energy of homolysis required to generate the primary radicals. The overall activation energy of the subsequent radical polymerization is approximately 20 kJ mol^{-1}. This value indicates that the polymerization rate will be rather insensitive to temperature changes, thus improving robustness and reliability of the polymerization process.

• **Benefits.** The photochemically initiated polymerization involves a source of radiation to trigger polymerization at room temperature without external heat. The possibility of initiating polymerization at room temperature is very interesting (i) for monomers whose polymerization is highly exothermic (vinyl acetate and most acrylates), that may cause a runaway reaction, or (ii) when the reaction system includes a highly volatile organic continuous phase (e.g. dispersion polymerization), an unstable (emulsion) or kinetically stable (miniemulsion) dispersed system. Furthermore, more recently developed radiation sources allow repeated switching on and off (*e.g.* LEDs, excimer sources) and may provide the possibility of non-steady state radical polymerization conditions and a higher factor of safety due to the absence of any hot-spot. In contrast to a widespread presumption, that radiation is generally more expensive to produce than heat, because of considerable losses that occur in the production of electrical energy and its conversion into useful radiation energy. These newly developed radiation sources exhibit high radiation efficiencies while consuming much less electrical energy. However, medium-pressure Hg arcs emitting a broad line spectrum extending from UVC to VIS spectral domain and being recognized as the workhorses in industrial applications of photochemistry, consume a significant amount of energy and represent, with operating temperatures of more than 850 °C, hot-spots that are subject to particular safety requirements. Beside the higher radiant efficiency of LEDs, their narrow spectral emission allows optimization of the fraction of emitted radiation to be absorbed by a given redox initiator (see section 2.3.1 for details on *irradiation sources*). In addition,

excitation in the VIS spectral range often circumvents interactions with other components mostly absorbing in the UV spectral domain such as monomers, surfactants and polymers.

2.2.6 Photoreactors and continuous flow operations

• **Batch photoreactors.** Photopolymerizations in dispersed systems were often carried out in improper reaction vessels such as round bottom flasks or Schlenk tubes implying major drawbacks such as significant losses of incident radiation and indeterminable and fluctuating irradiance values (irradiance means radiant power or photon flux arriving at the surface per unit area for a specific wavelength ou within a specific wavelength range). Modern research conditions call for photochemical reactors to optimize incident radiation, improve reproducibility and increase the uniformity of radiation distribution within the reactor. The results of the development of photochemical technology are already extensively exploited in preparative organic photochemistry, for the disinfection of drinking water, and the oxidative treatment of waste water and air. Large scale applications of photoreactors in the domain of polymer chemistry are only implemented for polymer modifications (*e.g.* chlorination of poly(vinyl chloride) [56], but are yet to be developed for proper photopolymerization. In 2011, Chemtob et al. used an immersion-type photoreactor ([57], Fig. 4) equipped with a medium-pressure Hg arc for acrylate miniemulsion photopolymerization [66]. Such compact batch reactor designs have been employed for more than 50 years to carry out preparative photochemistry on scales of milligrams to up to tens of kilograms. The radiation source is contained in a double-jacketed water-cooled well immersed into a stirred or recirculated reaction system, with the key advantage that the emitted radiation is entirely incident to the photochemically reactive system. Because irradiance falls off very rapidly with increasing distance from the radiation source due to absorption and scattering, non-homogeneous radiation distribution is often observed in conjunction with poor turbulence and insufficient control of irradiation time per unit volume. Development in photochemical engineering led to designs and geometries of photoreactors where these parameters can be controlled. Practically all recently developed and applied photochemical reactors are designed for processes in closed circuit or continuous regimes [58].

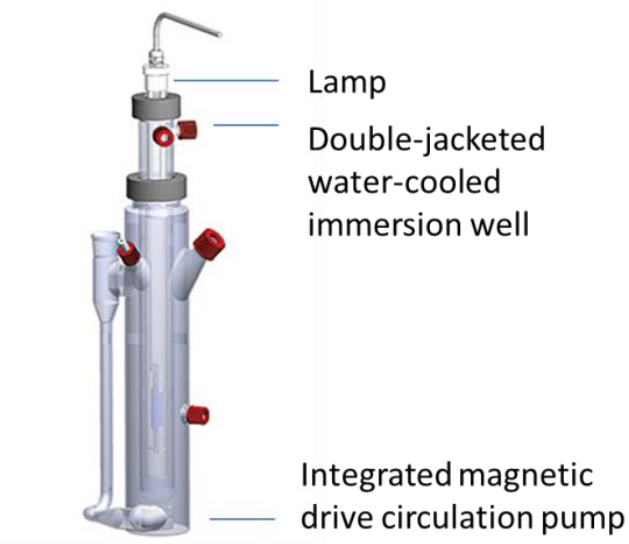

Fig. 4: Immersion-type closed circuit photoreactor (Peschl Ultraviolet GmbH, Mainz, Germany).

• **Closed and open circuit photoreactors.** These reactors consist of one or multiple UV and/or VIS radiation transparent channels through which a reaction system is circulated continuously. Their length and optical path may vary from several meters to a few millimeters and from tens of centimeters to some tens of micrometers, respectively. For dispersed systems with high extinction coefficients, down-scaling of the optical path to the micrometer scale in precisely engineered channels will lead to a quasi-uniform volumetric

incident photon flux [59]. Such tubular microflow reactors with channels of internal diameters < 1 mm and typical flow rates < 1 mL min^{-1} were used for miniemulsion photopolymerization [60]. To ensure such low but constant flow rates, syringe pumps are ideally suited. Down-scaling the production of latexes from monomer miniemulsions to volumes of microscale photoreactors keeps the advantages of open circuit photochemical reactors and continuous processing (control of all primary process parameters: irradiance, flow rate, temperature) and opens the possibility to use radiation sources that may be dedicated for irradiating small surfaces (LEDs, excimer sources, fibers). However, micro channel plugging might occur and is attributed to adhesion wetting [61]. "Macroflow reactors" (internal channel diameter $\geq$ 1 mm) were more adapted to provide high throughput, while still offering a large surface-to-volume ratio to ensure an acceptable irradiated volume fraction. For *e.g.*, a tubular photoreactor [46] (Fig. 5) was employed for the photopolymerization of miniemulsions. Externally irradiated tubular reactors bear the disadvantage of considerable loss of radiant energy, even when radiation sources are equipped with reflectors [57]. In addition, very high rates were achieved with a helix-type tubular reactor (Fig. 6) made up of UV-transparent fluoropolymer tubing wrapped at a defined distance around a radiation source of low electrical power (*e.g.* "black light" fluorescent tube) and with flow rates usually > 1 mL min^{-1} [62]. However, a transfer from batch to continuous process mode is by no means trivial. As recently highlighted by Asua et al. [13], the main challenges include run-to-run irreproducibility, clogging and variability in polymer architecture. At present, a wide choice of photochemical reactors is commercially available with different designs and volumes to be used for a large scope of radiation sources and flow rates, hence, providing superior versatility and compactness compared to conventional thermal reactors. It is expected that photochemical reactors will be one of the main levers and tools to stimulate future development of photopolymerization in dispersed systems.

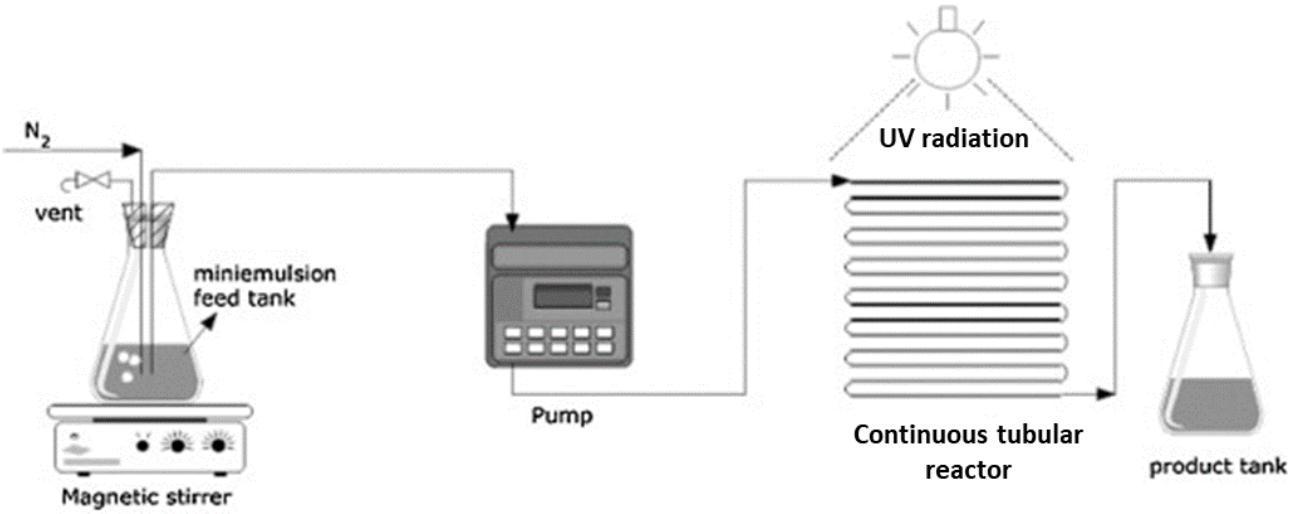

Fig 5: Laboratory scale set-up for a continuous process of photopolymerization of an aqueous polyurethane/acrylic hybrid miniemulsion using a tubular reactor with an inner diameter of 1 mm. This figure has been reproduced from [46] with permission of the copyright owners.

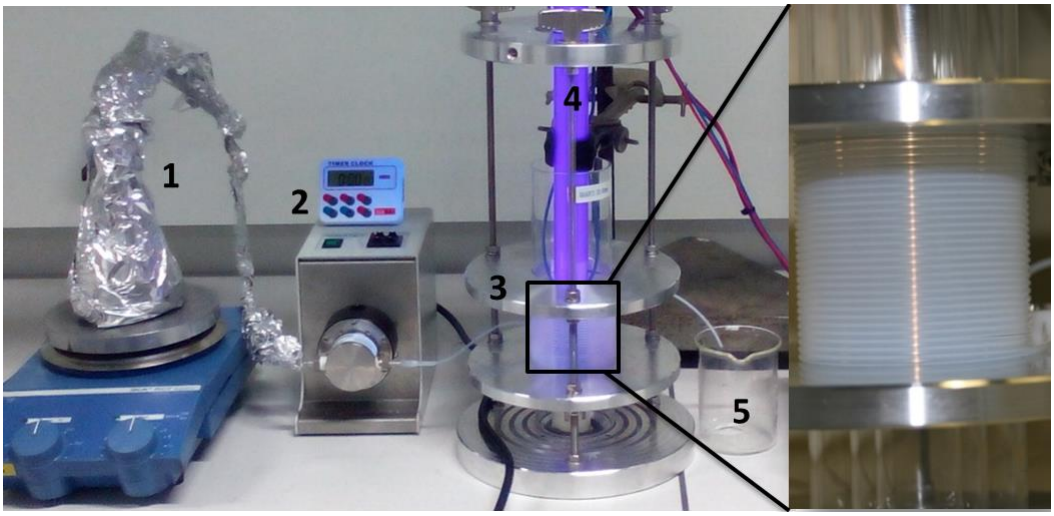

Fig 6: Photochemical helix minireactor in macroflow conditions: monomer miniemulsion tank (**1**), pump (**2**), helical photoreactor (**3**), UVA "black light" fluorescent tube (**4**) and collecting flask (**5**). The inset shows a magnification of the helically coiled tubing constructed by winding a PTFE tubing (1.5 mm inner diameter) around a quartz cylinder. This figure has been reproduced from [62] with permission of the copyright owners.

• **Managing heat removal in photoreactors.** A common feature to all above mentioned examples is that reactions may be performed at ambient temperature as a means to reduce energy consumption. However, polymerizations being mostly exothermic processes, heat removal is typically required. In order to maintain ambient temperature, the use of a cooling fluid, a very low polymerization rate or a sufficient heat transfer area may be required. On industrial scale, exothermic photochemical processes (e.g. chain reaction of photo-chlorination) are mostly performed as batch processes in tank reactors with negative irradiation geometry which may be reduced in volume, multiplied and/or mounted in parallel to limit the heat removal rate per reactor. For smaller installations, tubular reactors with positive irradiation geometry and much higher cooling areas are used. Tubular reactors in closed circuit batch or continuous regime may be associated with heat exchangers at the reactor exit, from where the heat may be transferred to other installations. For now, all these solutions concern examples of the organic preparative photochemistry, but the accumulated experience is considered with confidence to be transferable to exothermic photopolymerization reactions in dispersed systems.

2.3 Materials and Equipment

2.3.1 Radiation sources

The efficiency of the initiation step depends strongly on the characteristics of the source of excitation: *radiant power*, *spectral distribution* and *geometry.* Photopolymerization, primarily exploited as a thin film curing technology for coatings, inks and adhesives, has finally expanded to preparative projects with an increased scope of radiation sources and an expanded spectrum of irradiation reaching from UVC (> 200 nm) to VIS (< 800 nm). Aside from the emission range of these sources, polymerization in dispersed systems can be carried out using other means of radiation. Several examples include ionizing radiation such as γ-rays to achieve polymerization in emulsion [63]. On the low energy side of the electromagnetic spectrum, emulsion polymerization processes of conventional monomers (styrene, acrylates) can be triggered by ultrasound [64-67]. In a very limited way, microwaves have been used to realize polymerizations in emulsion [68]. For photopolymerization in dispersed systems, wavelengths of excitation are generally > 250 nm because radiation of lower wavelengths is strongly absorbed by other components of the formulation, and may also cause photodegradation reactions involving dissolved molecular oxygen [69]. The primarily used radiation

sources to trigger polymerization emit in the UVA (315-400 nm), UVB (280-315 nm) and in part of the UVC region (250-280 nm). The two former regions are the main absorption areas of commercial radical photoinitiators. Over the last 10 years, the attractiveness of the VIS domain for radiation-curing has substantially increased due to several advantages compared to UV radiation: safe use (provided that irradiance and exposure are reasonable), better through cure opening the way for cross-linking of millimeter-thick materials, and lower cost. Given that photopolymerization in dispersed systems employs the same photoinitiators as used for radiation-curing, it is logical that the same type of radiation sources are used: mainly medium-pressure Hg-arcs and, to a minor extent, high-pressure Xe arcs, compact fluorescent tubes, LEDs, excimer sources, lasers, and laser diodes [57].

• **Medium-pressure Hg arc: The workhorse among radiation sources.** Medium-pressure Hg-arcs emit a wide spectral distribution (220-600 nm) of lines whose importance and wavelengths can be varied by doping with metal halides [80]. In addition, different qualities of the surrounding quartz or borosilicate materials decide on the lower spectral limit of the incident radiation [70]. The use of the polychromatic radiation of a medium-pressure Hg arc allows selecting photoinitiators within a wide range of absorption spectra. Air- or water-cooling of the operating arc is compulsory but the heat released is not always fully dissipated. Consequently, the temperature of the irradiated reactor volume may be higher than ambient temperature, and should eventually be regulated, but must be in any case specified because it can significantly affect the polymerization.

• **Fluorescent tubes.** Fluorescent tubes emit the luminescence of a solid located at the inside surface of the tube. The luminescing solid is excited by a low-pressure Hg arc, the emission of the latter is absorbed by the solid and the glass tube and cannot penetrate the latter [57]. As fluorescent tubes have been developed for electric lighting, their emission is a white light (wide polychromatic emission from 380 to 700 nm) with shades of blue, red, green or yellow depending on the luminescent solids employed. If a luminescent solid emitting in the UVA and VIS spectral domain is attached to the inner surface of the tube, the latter acting as a filter absorbing the VIS luminescence, the fluorescent tube emits only between 315 and 400 nm, sometimes 430 nm. These tubes are called actinic fluorescent lamps or “black light” tubes and have proven very useful for the photochemical initiation of polymerizations in dispersed reaction systems [71].

• **LED systems.** The adoption of LEDs for applications using visible radiation such as television, communication, sensor or lighting has been extremely prolific. Their commercial adoption for UV/VIS-curing technology is rather recent, and the result of intense efforts to mitigate many barriers: cost, limited availability, low output, and thermal management. Although LEDs do not really have a higher luminous efficiency compared to conventional medium-pressure Hg arcs (≈ 70 lm/W versus ≈ 50 lm/W), their polychromatic emission is narrow and may be matched with the absorption spectrum of the photoinitiating system. This is a key point to improve energy efficiency in addition to their instantaneous switching on/off ability. Furthermore, LEDs are now offered with higher peak irradiances (> 50 mW cm^{-2}) and longer lifetimes (≈ 30000 h *vs* 10000 h for medium-pressure Hg arcs). Monochromatic LEDs emit in the UVB, UVA and VIS spectral domains. With lines (half width < 15 nm) in the UVA domain at 365 nm, 385 nm, 395 nm and 405 nm, they may be used for photopolymerization in dispersed systems. Although, there are currently only very few examples known of LED utilization in this field, UV LED business is expected to grow from $45M in 2012 to $270M in 2017 and LEDs are likely to be important equipment component driving the development of polymerization technology.

2.3.2 Continuous phase

• **Water.** The majority of photopolymerizations in dispersed systems are conducted using water as continuous phase. Water is ideal because of its abundance, low cost, negligible environmental impact, and

high heat capacity (4.18 J g^{-1} K^{-1}) [72] which is amenable to energy dissipation during polymerization. An additional advantage is the high transparency of pure water over a large UV spectral range. Residual absorption in the range between 200 and 340 nm is lower than 10^{-3} cm^{-1} and may be partially explained by Rayleigh scattering [73]. The absorbance remains below 1 cm^{-1} until 187 nm but the line emitted by a low-pressure Hg arc (in Suprasil®) at 185 nm is already used for the photochemical homolysis of water, which is exploited for the oxidative degradation of organic pollutants in waste water. Thus, water offers a broad spectral window to work with UV irradiation, in sharp contrast with many organic solvents.

• **Organic solvents.** An organic solvent transparent to the wavelengths required for the photochemical polymerization must be selected. In dispersion or precipitation photopolymerization (see sections 3.4 and 3.5, respectively) starting from a solution, the choice of an organic continuous phase is very limited because it must also fulfil specific solubility criteria (good solvent for monomer, poor solvent of polymer). Consequently, mainly mixtures of water, ethanol and acetonitrile have been used [74]. Ionic liquids have also been considered but are generally highly absorbing in the UV range [75].

• **Gases.** Gas, *e.g.* nitrogen or helium, have also been used as continuous phase, in particular for aerosol photopolymerization (see section 3.7 on *aerosol photopolymerization*) because of their inertness and transparency over the total UVC to VIS spectral range [76].

2.3.3 Emulsifiers

The stability of a dispersed system such as an emulsion or suspension is ensured by electrostatic and/or steric interactions, provided by use of ionic or non-ionic surfactants [77]. In the case of photopolymerization in dispersed systems, a very limited scope of surfactants has been used to date. The most common ionic types are sodium dodecyl sulfate (SDS) and cetyl trimethyl ammonium bromide (CTAB), widely found in conventional emulsion polymerization. With regard to non-ionic surfactants, poly(ethylene oxide) (PEO) and poly(vinyl pyrrolidone) (PVP) have been used in dispersion photopolymerization [78] and poly(vinyl alcohol) (PVA) in suspension polymerization [79]. There are also examples of polymeric surfactants including photocleavable groups [80]. Molecules combining the properties of initiator and surfactant (INISURFS), were also used [81]. An interesting example is Dowfax 2A1, a branched C_{12}-alkylated diphenyl ether disulfonate surfactant widely used in industrial emulsion polymerization. The photoINISURF properties of Dowfax 2A1 can be rationalized in terms of an electronic excitation of the diphenyl ether group to the first excited singlet state and a subsequent homolysis to intermediate phenoxyl and phenyl radicals, able to initiate polymerization, in a manner similar to type I photoinitiators (see next section 2.3.4) [82].

2.3.4 Photoinitiators

• **Overview of photoinitiators used for photopolymerizations in dispersed systems.** There is a great diversity of photoinitiating systems mainly developed for UV-curing technology [14]. However, three types of photoinitiators are mainly employed for the photopolymerization in dispersed systems and will be described and classified in accord with the mechanism of the generation of the intermediate reactive species, their nature and their chemical reactivity, as shown in Fig. 7.

a. Type I radical photoinitiators. Compounds reacting upon electronic excitation by homolysis to yield mainly C-centered radicals might be considered as type I photoinitiators, if (i) they absorb in a convenient spectral region, (ii) exhibit a high quantum yield of homolysis and (iii) generate radicals of lifetimes and reactivity enabling them to initiate polymerization rather than to deactivate by disproportionation. Some examples are given in Table 1. Among the many examples, monoaryl ketones with electronegative substituents linked to the α-position are taking a particular position. Usually, the lowest triplet state of the carbonyl chromophore ($^3n,\pi^*$) reacts by hydrogen abstraction if adequate hydrogen

donor molecules are present. However, the homolysis of the C–C bond adjacent to the electronically excited chromophore (α-cleavage, Norrish I reaction) would be favoured when adequate substituents bound to the α-position are stabilizing the alkyl radical to be generated (see Fig. 7a) [83]. Consequently, in order to exploit α-cleavage of electronically excited monoaryl ketones as a mechanistic concept for the generation of primary radicals initiating polymerization, functional groups, such as hydroxy, alkoxy, alkylamino groups, are linked to the α-C-position to enhance the rate of α-cleavage by stabilizing the corresponding α-hydroxy-alkyl-, α-alkoxyl-alkyl- and α-(alkylamino)-alkyl radicals generated in slightly exothermic reactions.

b. Type II radical photoinitiators are mixtures of hydrogen acceptors (oxidant) and donors (reductant, see Fig. 7b). The first are usually chosen from ketones that react from their first triplet state ($^3(n,\pi^*)$-state) with high quantum yield and predominantly by abstracting hydrogen from reducing molecules (DH, route ①). In order to avoid electronic excitation but to ensure high reactivity, the latter are chosen from aliphatic tertiary amines, thiols or secondary alcohols [83, 84]. The "Type II" makes reference to the bimolecular reaction between an electronically excited oxidant (which should not be confused with photosensitizer, because it is not regenerated), and a reductant, called co-initiator (or co-synergist). Generally, ketyl radicals react rapidly by disproportionation, and it may be assumed that the radicals generated from the co-initiator ($D^{\bullet}$) trigger the polymerization. The mechanistic details of the hydrogen abstraction might vary with the nature of the oxidant, and electron-transfer might occur upon electronic excitation of the oxidant with a subsequent proton transfer (*e.g.* with tertiary amine as reductant, route ②).

c. Photoacid generators are mostly based on onium salts that consist of a triarylsulfonium (Ar_3S^+) or diaryliodonium (Ar_2I^+) cation and an anion (X^-) with the characteristics of a weak nucleophile and weak base (typically the anion of a super acid such as BF_4^- or PF_6^-). Upon electronic excitation, the cations undergo homolysis to yield iodonium ($ArI^{\bullet+}$) or sulfonium ($ArS^{\bullet+}$) radical cations and C-centered radicals (see mechanism in Fig. 7c for the specific case of iodonium salts). The C-centered radicals are highly reactive phenyl radicals ($Ar^{\bullet}$) that react with organic compounds (DH) by hydrogen abstraction to yield benzene (ArH) or recombine to form biphenyl (Ar_2). The iodonium (or sulfonium) radical cations also react by hydrogen abstraction from DH to generate the corresponding hydroiodonium ($ArIH^+$) (or hydrosulfonium $ArSH^+$) cations where the first subsequently deprotonate to yield more or less stable aryliodides (ArI) and bisaryliodides (Ar_2I). The combination of proton and the original anion (X^-) act as Brønsted superacid capable of protonating *e.g.* epoxy or vinylether monomers thus initiating cationic polymerization. Basically, cationic reactions are precluded in the presence of water, but Crivello described in 2003 the synthesis of epoxy functionalized polyether beads by way of a cationic photopolymerization in suspension [85] (see section 3.6 on *suspension photopolymerization*).

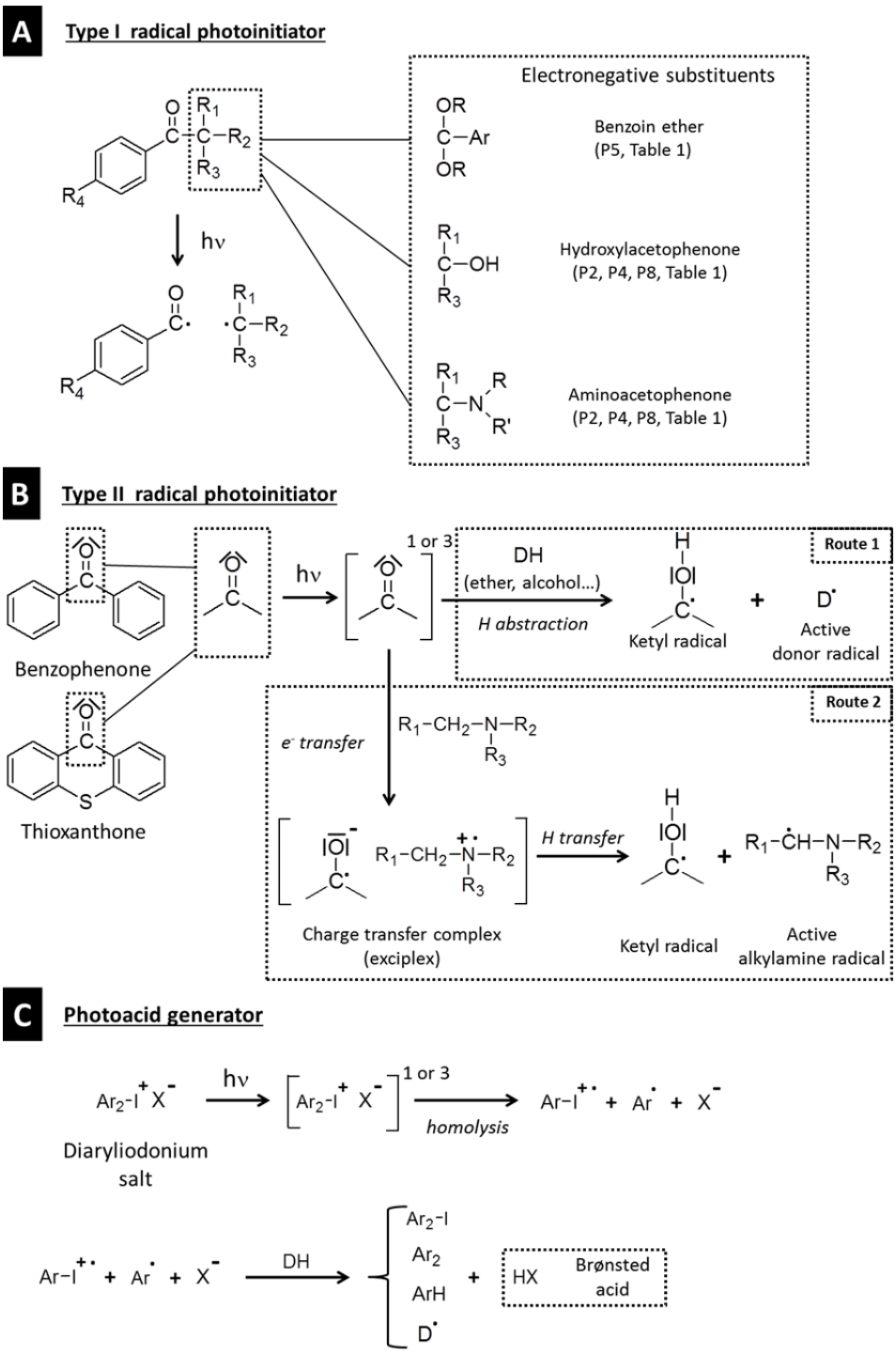

Fig. 7: Mechanistic schemes of the initiating processes of radical (A and B), and cationic photopolymerizations (C).

• **Requirement of water-solubility of radical photoinitiator.** Table 1 lists the photoinitiators mainly employed for photopolymerizations in dispersed systems. Oil-soluble Type I photoinitiators are most commonly employed due to their wide availability. However, within the context of this review, oil-soluble initiators may not always be the best choice. When the initiator radical pairs are produced in a very confined space (polymer particles, monomer swollen micelles or monomer nanodroplets), the probability of recombination is higher than that of being scavenged by a monomer molecule. Consequently, water-soluble photoinitiators may be better suited under these conditions. In fact, it was observed that conventional emulsion polymerization relies primarily on primary radicals located in the continuous phase [86]. However, only a limited range of water-soluble photoinitiators is commercially available, and currently, 2-hydroxy-1-[4-(2-hydroxyethoxy) phenyl]2-methyl-1-propanone (Irgacure 2959, P4) is used almost exclusively when

water solubility is required, although, its water-solubility is rather limited (≈ 1 g/100 mL). Recent developments were directed to the modification of acylphosphine oxides (*e.g.* P7 and P15) with hydrophilic poly(ethylene oxide) chains or carbohydrate residues [87, 88], and very recently, Li- and Na-salts of mono-acylphosphine oxide and bis-acylphosphine oxide (P14) exhibiting good water-solubility and high reactivity were reported by Liska et al. [89].

• **Alternative photoinitiatinng systems.** To overcome the challenge of designing water-soluble photoinitiator, we foresee the development of alternative approaches: firstly, innovative methods to convert conventional water-insoluble photoinitiators into water-dispersible nanoparticles. For example, spray-drying of a volatile TPO (P7) nanoemulsion led to a water-dispersible photoinitiator powder used recently in the 3D printing of hydrogels [90]. Alternatively, aqueous colloidal dispersions of semiconductor nanoparticles, best known as photocatalysts for advanced oxidation processes, could also be implemented for photopolymerization in dispersed systems. Upon excitation, subsequent photoinduced electron-hole pairs have been reported to contribute to the formation of initiating radicals in aqueous solution [91], but also in miniemulsion [53].

Table 1: Main type I radical photoinitiators used for photopolymerizations in dispersed systems. Further data on photoinitiators can be found in [92]. Photoinitiators P2, P4, P5, P6 and P8 are commercial and contain a common aryl alkyl ketone group: R_1-Ph-C(=O)-Alkyl-R_2. The nature of R_1 and R_2 will change the absorption wavelength and the efficiency of cleavage process. P7, P14 and P15 are also commercial structures based on phosphine oxides. They absorb in near UV-vis region, and produce both benzoyl and phosphinyl initiating radicals.

Photoinitiator	Chemical structure	Initiating radicals	Abbreviation
Azobisisobutyronitrile (AIBN)	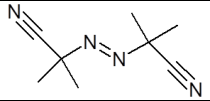	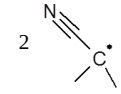	P1
2-Hydroxy-2-methyl-1-phenylpropan-1-one (Darocure 1173)	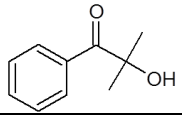	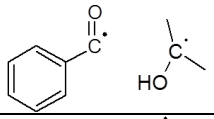	P2
1,3-Diphenylacetone (DBK)	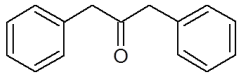	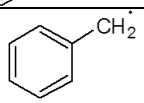	P3
1-[4-(2-Hydroxyethoxy)-phenyl]-2-hydroxy-2-méthyl-1-propane-1-one (Irgacure 2959) *Water-soluble*	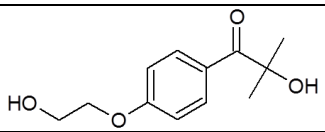	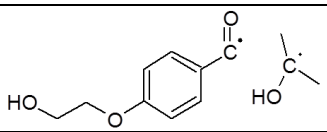	P4
2,2-Dimethoxy-2-phenylacetophenone (DMPA)	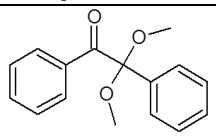	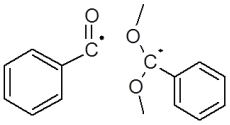	P5
2-Methyl-4'-(methylthio)-2-morpholinopropiophenone (Irgacure 907)	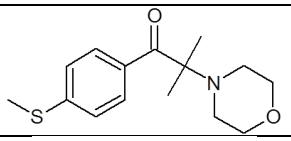	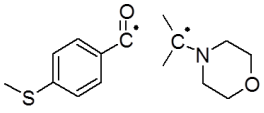	P6
Diphenyl(2,4,6-trimethylbenzoyl)phosphine oxide (TPO)	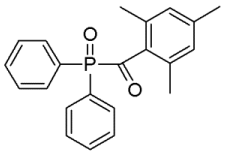	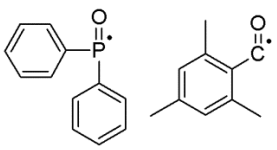	P7
1-Hydroxycyclohexyl phenyl ketone (Irgacure 184)	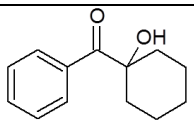	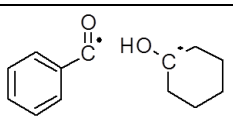	P8
Di-tert-butyl ketone (DTBK)	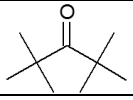	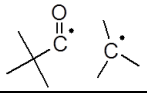	P9

3-Hydroxy-3-methyl-2-butanone (HMB)	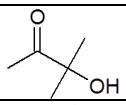	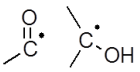	P10
Potassium persulfate (KPS) *Water-soluble*	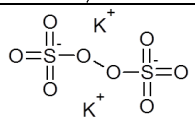	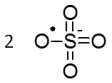	P11
α-ketoglutaric acid (KGA) *Water-soluble*	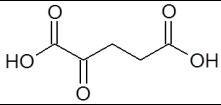	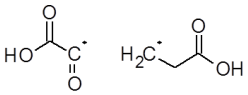	P12
Dihydroxyacetone (DHA) *Water-soluble*	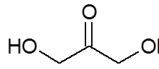	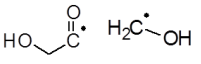	P13
Sodium salt of bis(mesitoyl)phosphinic acid (Na-BAPO) *Water-soluble*	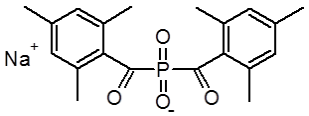	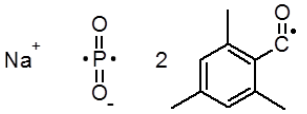	P14
Bis(2,4,6-trimethylbenzoyl)phenylphosphine oxide (BAPO) *Oil-soluble*	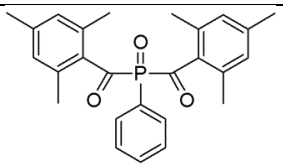	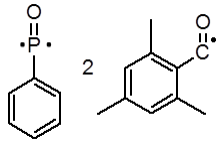	P15

3 PHOTOINDUCED POLYMERIZATION PROCESSES IN DISPERSED SYSTEMS

3.1 EMULSION PHOTOPOLYMERIZATION

3.1.1 General considerations

Emulsion polymerization is a well-established latex manufacturing process that is employed extensively for the production of conventional linear polymer colloids such as *e.g.* poly(vinyl acetate) (PVAc), styrene-butadiene copolymers, styrene-acrylate copolymers and poly(acrylate) [86, 93]. As a result of the high demand of polymers produced by emulsion polymerization, process development has long been a major economic issue in chemical industry. Although emulsion polymerization has been known since the end of World War II, photochemical initiation of this process has only been a subject of research since the 1980s, and to date, only rather few research has in fact been conducted. A summary of the investigations published is shown in Table 2. In general, laboratory scale photochemically initiated emulsion polymerization is relatively straightforward to implement. It is important to consider the partitioning behavior of the photoinitiator to ensure a conventional emulsion polymerization mechanism (main polymerization locus in polymer particles as opposed to in monomer droplets). It is therefore essential that the photoinitiator is located in the aqueous phase.

The polymerization in a conventional O/W emulsion requires special conditions of implementation: (i) aqueous medium used as the continuous phase, (ii) micron-sized monomer droplets dispersed in the aqueous medium, (iii) a surfactant providing effective stabilization of the monomer droplets in water and forming micelles (not required for *e.g.* in surfactant-free emulsion polymerization), and (iv) an initiator soluble in the aqueous phase. The mechanism of emulsion polymerization is complex, and one of its main features is that polymerization does not occur in the monomer droplets, but in polymer particles generated in the aqueous phase. As the monomer is consumed in the polymer particles, it is replenished by monomer diffusion from the droplets to the particles. The progression of an emulsion polymerization may be divided into three distinct intervals (Fig. 8) [86, 93].

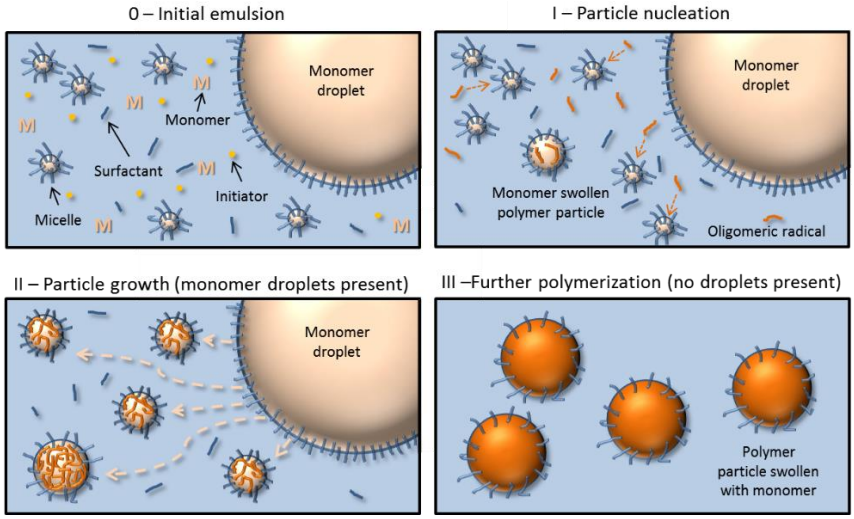

Fig 8: Schematic illustrations of the initial monomer emulsion and of the three different intervals of an emulsion polymerization.

Initially, (stage **0**, Fig. 8), the emulsion contains monomer-swollen micelles and predominantly micron-sized monomer droplets (1 - 20 μm). Under the effect of heat or radiation, the water-soluble initiator generates radicals in the aqueous phase. These radicals add to monomers present in the aqueous phase, the growing (oligo)radicals (so called "z-mers") become surface active and enter the monomer-swollen micelles where polymerization occurs (micellar nucleation). During interval **I** (Fig. 8, typically 0 - 10% conversion), the number of polymer particles increases gradually to reach a constant value marking the end of the nucleation period. In the absence of surfactant, or when the surfactant concentration is below the critical micellar concentration (cmc), particle formation may also occur via homogeneous nucleation (which may involve precipitation of oligomers in the aqueous phase). In Interval **II** (Fig. 8, typically 10 - 40 % conversion), new polymer particles are no longer formed, and particle growth occurs as monomers diffuse through the aqueous phase from droplets to particles. During this interval, the monomer concentration in the particles remains approximately constant. In Interval **III** (Fig. 8, typically 40 - 100 % conversion), all monomer droplets have been consumed, but polymerization continues within the polymer particles. An emulsion polymerization typically yields nanoparticles in the size range of 50 - 500 nm.

3.1.2 Adaptation to photoinitiation: O/W emulsion

The first photochemically initiated emulsion polymerization was reported by Turro et al. in 1980 [5], who conducted polymerizations using the system styrene and SDS and employing a number of oil-soluble ketone photoinitiators including 1,3-diphenylacetone (dibenzylketone (DBK), P3), benzoin and di-*tert*-butyl ketone (DTBK, P9). Polymerization rates and molecular weights obtained were comparable to those determined when using thermal initiators, but the resulting particle sizes were not analyzed. As outlined above, in the presence of surfactant at concentrations above cmc, the emulsion polymerization involves particle formation via micellar nucleation. Due to low water solubility, photoinitiators commonly used in radical photopolymerization tend to be predominantly located within micelles [16] and in monomer droplets in contrast to typical water soluble initiators such as potassium persulfate (KPS, P11). Oil-soluble initiators are often associated with low initiator efficiencies in emulsion-type reaction systems due to a fast bimolecular termination (recombination) of the radical pair generated upon initiator decomposition occurring within the confined space of monomer-swollen micelles or small monomer droplets [86, 94, 95]. The effect of this phenomenon on the kinetics of styrene, methyl methacrylate (MMA) and acrylic acid (AA) emulsion polymerization was studied by Turro et al. in the 1980s [5, 96-98].

In fact, electronic excitation of a C=O-chromophore is leading, depending on the substituents, to a nπ*-transition with a subsequent, mostly quantitative singlet to triplet intersystem crossing to generate the corresponding triplet state (^{3}(nπ*)-state). ^{3}(nπ*)-states react preferentially by hydrogen abstraction (see Fig. 7B, Type II photoinitiators), but introducing appropriate substituents at the α-position(s) of the carbonyl compound (see Fig. 7A, Type I photoinitiators), the ^{3}(nπ*)-state undergoes homolysis of a σ-bond adjacent to the excited chromophore to generate a triplet radical pair [99]. A recombination of a triplet radical pair requires a preceding triplet to singlet intersystem crossing, as only spin paired radicals can reform a σ-bond. The rate of a (bimolecular) singlet radical pair combination depends on the (local) concentration of the radicals and is particularly important if the reaction is taking place in a confined space (micelle). Given the rate of triplet to singlet intersystem crossing, the probability that radicals of the triplet radical pairs would initiate polymerization with monomers present within the aggregate or would exit from the micellar aggregate into the aqueous bulk phase is rather low, and emulsion photopolymerization using hydrophobic initiators is known to be inefficient. In order to minimize radical recombination within micelles, Turro et al. applied an external magnetic field [5, 96] to shift the equilibrium of the reversible fast intersystem crossing process (Fig. 9) toward the triplet radical pairs. In fact, already a low magnetic field (< 500 G [5]) is leading to a Zeeman splitting of the triplet sublevels ($T_{\pm}$) [100], hence creating an energy sink that increases the lifetime and, consequently the probability of initiation within the aggregate or of a radical escape into the bulk phase. An increase of the magnetic field to values > 1000 G had no impact on yield or molecular weight of *e.g.* polystyrene, but may affect the molecular weight distribution. In fact, Turro et al. could show that the technique of applying a magnetic field of ≥ 1000 G would allow to use suitable hydrophobic photoinitiators (for *e.g.* aromatic ketones) to initiate emulsion polymerizations of styrene, MMA and AA emulsions, with efficiencies similar to processes employing water-soluble photoinitiators.

As predicted, the magnetic field effect on the polymerization can only be observed for photoinitiators generating triplet radical pairs (typically aryl ketone, see Table 1), but is non-existent for singlet radical pairs generated by azo type initiators such as AIBN [99,[101].

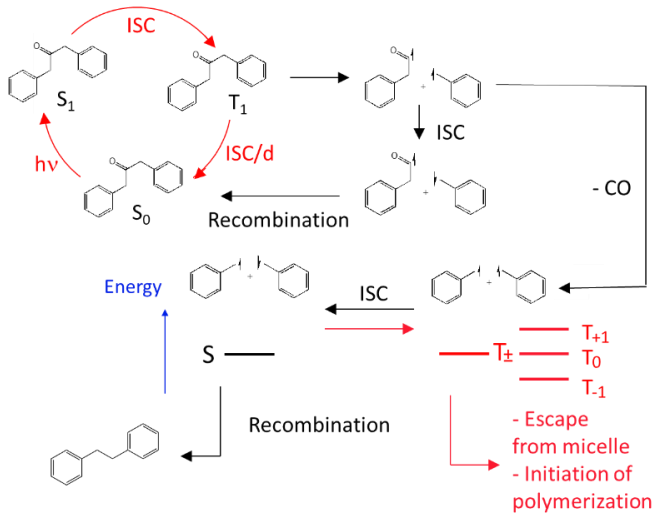

Fig. 9: Effect of an external magnetic field on the intersystem crossing (ISC) of benzyl radical pairs putting the fast rate of recombination of singlet radical pairs at a disadvantage by creating an energy sink at the triplet levels. Turro et al. could not determine the effect of an external magnetic field on the primary radical pair (before decarbonylation) but assume that the quantum yield of DBK consumption increases [96].

The hypothesis of a magnetic field effect on the radical pairs generated within micellar aggregates is supported by replacing Na^+ as counterion of dodecylsulfonate (DS) aggregates by Mg^{2+}, La^{3+} or Gd^{3+} [97]. It is assumed that larger counterions would increase the size of the micelles and therefore lower the rate of radicals initiating polymerization within the aggregates or exiting the micelles, and, in fact, in the absence of

a magnetic field, the yield of polystyrene was found to decrease by factors from 5 to 10. Applying a magnetic field of 2000 G afforded for Na^+, Mg^{2+} and La^{3+} the same high yields of 80 to 90 %. The paramagnetic Gd^{3+} enhances the intersystem crossing while shielding the aggregates from the external magnetic field, and the yield of polystyrene was equivalent to that found in the absence of a magnetic field. However, the presence of either of the ions mentioned (in the presence or absence of an external magnetic field) had no effect on the photoinitiated emulsion polymerization of methyl methacrylate (MMA). The authors speculated that this striking difference compared to the styrene system may be caused by the fact that initiation occurs primarily in the aqueous bulk phase, since MMA exhibits a significantly higher solubility in water. Emulsion polymerization of styrene using water soluble initiators was confirmed later [86], and further work would be required to differentiate between initiation within micellar aggregates and in the continuous aqueous phase.

Investigating in more detail the magnetic field effect on recombination within and escape from the micelles of the benzyl radicals generated by decarbonylation (Fig. 9), Turro et al. [99] focused analyses on the product of recombination (1,2-diphenyl-ethane (DPE), Fig. 9) and defined with a cage effect (ratio between the concentration of DPE and the concentration of DPK consumed after a given time of photolysis) the efficiency of recombination, or, inversely, the efficiency of initiation by or of escape from micelles of benzyl radicals. For experiments made in hexadecyltrimethylammonium chloride (HDTCl) micellar systems, cage effects for DPK of 32 and 17 % were observed in the absence and presence of a magnetic field (500 G), respectively. System inherent magnetic effects were found in investigating two differently ^{13}C-labeled DBKs (Fig. 10). For DBK-1-^{13}C, the dibenzylketone ^{13}C-enriched (90 %) at the carbonyl function, the cage effect was practically identical (33 %). The result could be anticipated, as the ^{13}C-labeling at the carbonyl function is no longer system relevant after decarbonylation. However, the cage effect increased to 46 % for DBK-2,2'-^{13}C, the dibenzylketone ^{13}C-enriched (90 %) at the two α-methylene positions, due to the faster triplet-singlet intersystem crossing of the germinal ^{13}C-radical centers.

The investigations of the Turro group exhibit the large potential for the application of low magnetic fields to optimize efficiency, molecular weight and molecular weight distribution of photochemically initiated emulsion polymerizations.

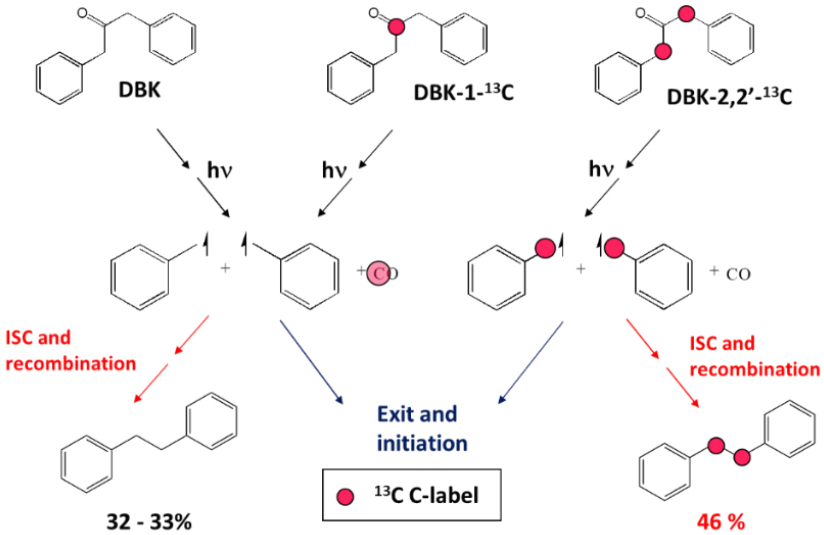

Fig 10: The efficiency of polymerization initiation in micellar systems depending on system inherent magnetic effects (^{13}C-labeling) [96].

One of the obvious advantages of photopolymerization is the fact that elevated temperature is not a requirement. This has been exploited in the production of poly(vinyl acetate) in emulsion, the final goal being the synthesis of poly(vinyl alcohol) (saponification of PVAc). The final product exhibited improved mechanical properties as a result of less branching, as the relative rate of chain transfer to polymerization decreases with

decreasing temperature [102]. In 2002, Mah et al. prepared PVAc using an anionic surfactant, ammonium poly(oxyethylene)$_{10}$-p-nonyl phenyl ether sulfate (APOENPES) and its nonionic equivalent poly(oxyethylene)$_{20}$-p-nonyl phenyl ether (POENPE; see Fig. 11) [103, 104], KPS (P11) having been used as photoinitiator. The experiments were conducted in the absence of molecular oxygen using a round bottom flask (Pyrex®) into which an immersion well (glass quality undefined) containing a Hg arc (500 W) was placed. More details concerning the arc are not known, since the cited arc does no longer exist in the product line of Ushio. In addition, the authors do not describe, how the emulsion has been agitated. Nevertheless, the experiments yielded polymers with low degrees of branching and high molecular weights when vinyl acetate (VAc) was photopolymerized at 0 °C. Similar results were obtained using the non-ionic surfactant POENPE [104].

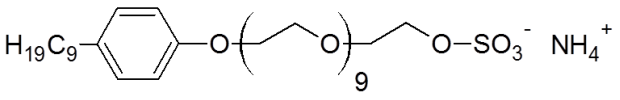

APOENPES

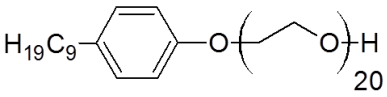

POENPE

Fig. 11: Ionic and non-ionic surfactants used by Mah et al. in the emulsion photopolymerization of VAc [103, 104].

In 2003, Lacroix-Desmazes and coworkers synthesized poly(methyl methacrylate) (PMMA) by radical photopolymerization in emulsion using p-(4-diethylthiocarbamoylsulfanylmethyl) benzoic acid (DTBA; see Fig. 12) as photo-surf-iniferter, i.e a molecule able to act as surfactant, photoinitiator and control agent at the same time [105]. The molecular weight data indicated some controlled/living character as anticipated considering previous work on iniferter systems, *e.g.* the pioneering work of Otsu [106, 107]. The controlled/living character was negatively impacted by addition of a conventional surfactant (SDS) due to the formation of micelles. Aside from providing some level of control/livingness during the polymerization, another advantage of the use of DTBA is the functionalization of PMMA chain ends by carboxylic acid groups, as the initiating radical adds to the C-C-double bond of monomer and oligomer. This feature enabled grafting of PMMA on a poly(ethylene-*b*-glycidyl methacrylate) copolymer, demonstrating how this synthetic approach can be used effectively to modify polyolefins.

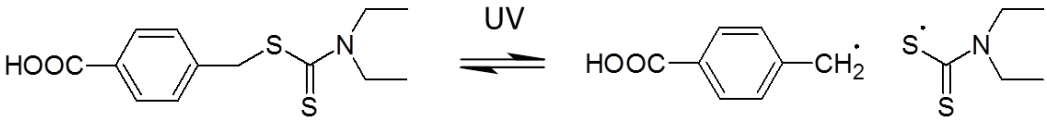

Fig. 12: UV photocleavage of DTBA photo-surf-iniferter used by Lacroix-Desmazes and coworkers in emulsion photopolymerization [105].

Shim et al. [108] performed UV-induced controlled/living radical polymerization of MMA in an emulsion using a surface active reversible addition-fragmentation chain transfer agent (CTA) or RAFT agent, whereby the surface activity was imparted by a carboxylate (COO^-) moiety of the RAFT R-group agent. Radical generation presumably occurs by homolysis of the C-S bond of the RAFT agent [109]. Good control/livingness was obtained with polymeric nanoparticles of narrow size distribution in the submicron range. Very recently, Yamago and coworkers carried out controlled/living radical photopolymerization of MMA employing a water-soluble organotellurium CTA (photo-TERP) [110]. Taking advantage of the Te-C bond's reversible photoinduced homolysis under visible light, polymerization was initiated through a white LED. Controlled/living characteristics were demonstrated as well as good temporal control through a series of "on-

off" cycles. Nevertheless, the conditions to achieve control over molecular weights were challenging since the authors mentioned the importance of precise radiation filtering (without providing irradiance data) and the need for heating (65 °C) for 9 h to obtain full conversion.

In 2009, Yang et al. carried out emulsion polymerization of styrene under UV irradiation in a beaker shaped container covered by a quartz cap through which the magnetically stirred reaction system was irradiated under a nitrogen blanket by a short high pressure Hg arc (375 W) [111]. Two radical photoinitiators were employed: the water-soluble Irgacure 2959 (P4, Table 1) and the hydrophobic DMPA (P5). After irradiation for 2 h, the styrene emulsion (10 wt%) polymerized with DMPA exhibited high turbidity with an average particle size of 80 nm, while the one initiated by Irgacure 2959 was completely transparent with an average particle size of only 30 nm (Fig. 13). This latter approach provides an attractive route to very small particles without the use of excessive amounts of surfactants (as in microemulsion polymerization. Strategies for the synthesis of high-solids-content, low-surfactant/polymer ratio nanolatexes has have already been reported [112]. Since the chosen range of wavelengths of irradiation is not selective for the excitation of either one of the two photoinitiators, excitation of the monomer cannot be excluded. Nevertheless, the results may indicate that experiments with Irgacure 2959 led to hydroxylated polystyrene chains would enhance the colloidal stability. The same equipment was used to initiate the emulsion polymerization of MMA by electronic excitation of Fe^{3+} ions that are known to react from their excited state with H_2O yielding hydroxyl radicals [113] as initiating species. The fast thermal reversibility of the photochemical Fe^{3+}-reduction and the high rates of hydrogen abstraction and addition to π-bonds ensure a high efficiency of the MMA polymerization (90 %) within 10 min of irradiation with particle diameters in the range 20-90 nm depending on conditions [114].

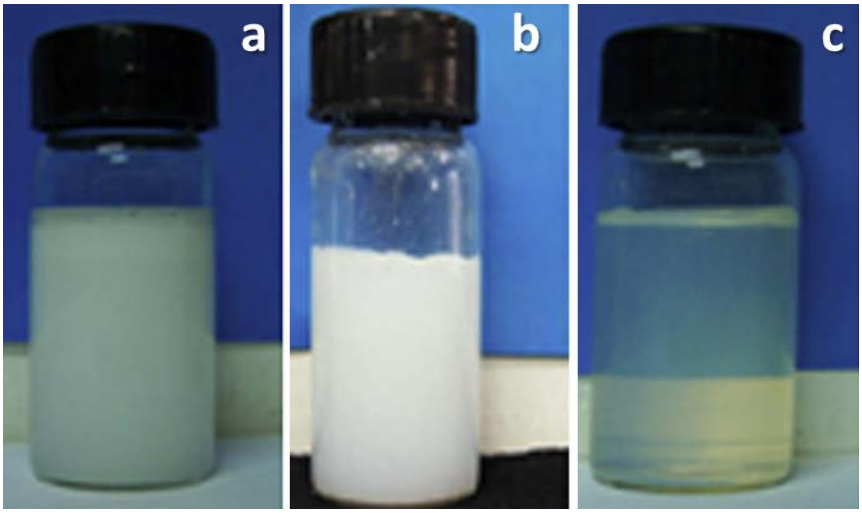

Fig. 13: Initial styrene emulsion (a), PS latex prepared using DMPA (b, turbid) and I 2959 (c, transparent). This figure has been reproduced from [111] with permission of the copyright owners.

Muller et al. [115] conducted surfactant-free emulsion polymerization of styrene using Na-BAPO. (P14) under blue light (LED emitting at 465 nm). If blue light is used, the resulting particles were quite monodisperse with diameters ~100 nm, although the molecular weights were unusually low with M_w = 1500-3500 g/mol. More anecdotic, photochemically induced seeded emulsion polymerization has been reported for the synthesis of core-shell particles, whereby the shell-polymer is polymerized using photoinitiation [116, 117].

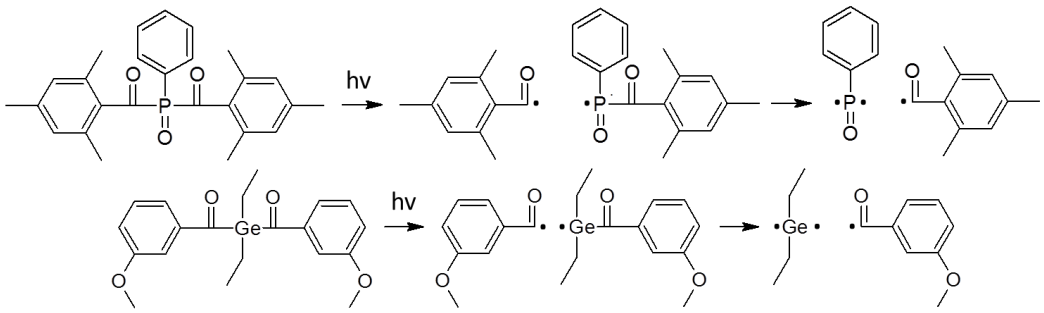

Fig 14: Photoinitiators (and decomposition pathways) used by Tauer/Yagci and coworkers for styrene emulsion photopolymerization (BAPO (top) and BAG (bottom)). Reproduced from [118] with permission of the copyright owners.

In 2011, Tauer, Yagci and coworkers investigated photoinitiated emulsion and bulk polymerizations of styrene using two different Type I photoinitiators (bis(2,4,6-trimethylbenzoyl)phenylphosphine (BAPO, P15) and bis(4-methoxybenzoyl)diethylgermanium (BAG) (Fig. 14) [118] employing two white fluorescent lamps (18 W; fluorescence tubes also used for indoor illumination).

The use of these hydrophobic photoinitiators leads to two types of polymerization mechanisms: (i) polymerization in growing particles (largely accepted emulsion polymerization mechanism; final particle diameter approx. 100 nm) as well (ii) as polymerization in very large polydisperse monomer droplets (100 nm - 200 µm), the latter eventually forming a coagulum. The two-stage decomposition patterns of BAPO and BAG (Fig. 19) might lead to the attachment of an initiator moiety to a polymer chain being able to further decompose and generate a polymer radical at the end of the polymer, where the initiator residue is located. Consequently, the molecular weight is increasing with conversion in a manner similar to a controlled/living radical polymerization. In fact, the authors observed that photopolymerization also occurs after consumption of the initiators or in the absence of the two initiators investigated. Upon total consumption of the photoinitiators, phenacyl chromophores bound to the polymer might act after homolysis as photochemical radical generators by hydrogen abstraction or addition to π-systems. The effect of molecular oxygen adding to C-centered radicals and the subsequent initiation by peroxyl radicals may also explain part of their results. But the increase of molecular weight of polystyrene under similar conditions and in the absence of molecular oxygen might indicate additional mechanisms of initiation. For experiments, where no photoinitiators were added, the authors suggested that electronic excitation of the styrene monomer would lead in the presence of polystyrene to an electron transfer generating a styrene radical cation and a polystyrene radical anion that react to yield a radical pair by hydride transfer. Branching along the polystyrene chain would be in favor for such a mechanistic hypothesis, but radical ions and hydride transfer seem highly improbable in aqueous systems, unless these intermediates would be strongly protected in the organic phase. In fact, the photoinitiated polymerization rates in emulsion were higher than those in the corresponding homogeneous (bulk) systems, and the rate enhancement may be explained by compartmentalization.

Tauer and co-workers [119] later described, based on a somewhat similar concept, an emulsion-type photopolymerization of styrene using a water-soluble acetic acid-modified BAPO photoinitiator (phenyl group adjacent to the P=O group in BAPO is substituted with acetic acid) in a flow reactor under UV irradiation. A rather large amount of SDS (0.17 mol L^{-1}) was employed, and extremely high polymerization rates and molecular weights were obtained. Calculations indicated that the average number of propagating radicals per particle exceeded one, despite the small particle size, thus not consistent with zero-one kinetics. The authors interpreted this result with photoinitiator end chain fragments (phenacyl groups) incorporated into the polymer backbone (as already mentioned above) generating upon electronic excitation new initiating radicals by hydrogen abstraction and called it a “snowballing radical generation” effect. Very recently, Lacôte and coworkers described the first use of visible light in emulsion photopolymerization using styrene as monomer and a photoinitiating system based on three different water-soluble compounds [120]. Although

not studied, the mechanistic details may involve a first step of electron-transfer upon electronic excitation of a dye (acridine orange), leading to the photoreduction of a disulfide compound, further decomposed into thiyl radicals. While these latter are not able to trigger the polymerization, proton transfer with a third compound (N-heterocyclic carbene borane) may generate NHC-boryl initiating radicals.

Table 2: Summary of main studies describing emulsion photopolymerization.

Monomer	Continuous phase	Surfactant	Photoinitiator	Polymerization time/ Irradiation system	Particle diameter	Ref.
Styrene or MMA/AA	Water	SDS	P1/P3/P9/P13	[5][96]: 450 W, Hanovia, medium pressure Hg-arc, immersed, Pyrex®, l = 313 nm (K_2CrO_4). [101] : no details concerning irradiation	-	[5, 96-98]
Vinyl acetate	Water	APOENPES, POENPE (Fig. 11)	P11	Degassed, 500 W, high(?)-pressure Hg arc, immersed, most probably: quartz, irradiation time: < 180 min	-	[103, 104]
MMA	Water	DTBA (Fig. 12)/SDS		N_2 purged, 125 W, medium-pressure Hg arc Philips HPK, external, most probably Pyrex®, irradiation time: 24 h	-	[105]
MMA	Water	Surfiniferter (4-thiobenzoyl sulfanylmethylsodium benzoate)		UV (no details), 6 h, N_2 purged, 375 W, high(?)-pressure Hg arc, external, quartz, irradiation time: 150 min, λ = 365 nm	300 – 400 nm	[108]
MMA	Water	Brij98/SDS/ CTAB	Organotellurium, CTA/4,4'-azobis(4-cyanovaleric acid)	Up to 9h, LED Visible range, 50% Filter, 6 W	45-350 nm	[110]
Styrene	Water	SDS	P4/P5	150 min, high-pressure Hg arc, λ = 365 nm, 375 W	24 – 139 nm	[111]
MMA	Water	CTAB	$FeCl_3$	N_2 purged, 1000 W, high-pressure Hg arc, quartz, external, irradiation time: 10 min, radiant exitance: 20 mW cm^{-2}	20 – 90 nm	[114]
Styrene	Water	Surfactant-free	P14	LED, 465 nm (60 LEDs per meter), UV (no details)	80 – 400 nm	[115]
Styrene/MMA	Water	SDS	Benzoin	125 W, medium-pressure Hg arc, N-HPL 125W, Peschl Ultraviolet GmbH, Duran, immersion, irradiation time: 180 min	100 – 700 nm	[116]
Styrene/n-isopropyl acrylamide	Water	-	2-[p-(2-hydroxy-2-methylpropiophenone)]-ethylene glycol methacrylate	N_2 purged, 150 W, doped medium-pressure Hg arc, Heraeus TQ 150 Z3,), immersed, most probably Pyrex®, irradiation time: 60 min,	260 nm	[117]
Styrene	Water	SDS	P15/BAG (Fig. 14)	< 300 h, 2 fluorescent tubes (white light), 2 x 18 W, 0.5 mW cm^{-2}	100 nm (latex). 0.1-10 µm (coagulum)	[118]
Styrene/Butyl methacrylate (BuMA)/MMA	Water	SDS	P15/acetic acid-modified BAPO	450 W, medium-pressure Hg arc, Hanovia, external (centered on minireactor,), residence time: 36.5 to 146 s,	50 nm	[119]
Styrene	Water	SDS	Acridine orange (dye)/Disulfide (oxidant)/NHC borane	Conventional stirred tank reactor surrounded by a visible LED strip (?), external, no details concerning irradiance, irradiation time: 6 – 10 h.	60 – 330 nm	[120]

3.2 MICROEMULSION PHOTOPOLYMERIZATION

3.2.1 General considerations

A microemulsion [121-124] is a macroscopically homogeneous mixture of two immiscible liquids (of main interest here: water and vinyl monomer), a surfactant and sometimes a cosurfactant (a medium-chain length aliphatic alcohol) that forms spontaneously without external shear forces, *i.e.* it is thermodynamically stable. The interfacial tension between the two liquids must be close to zero. Due to the high surfactant content of microemulsions, the micelles are able to incorporate all monomer in the system within their hydrophobic cores by swelling. Before polymerization (stage **0** in Fig. 15), the system contains monomer-

swollen micelles (diameter ≈ 1-10 nm [125, 126]), and some of these micelles are transformed into polymer particles during the polymerization. Only a fraction of monomer-swollen micelles is getting nucleated - the remaining monomer-swollen micelles provide monomer to the growing particles via diffusion across the continuous phase (stage **I** in Fig. 15). Taking into account that some coalescence will also occur, the final particle size is typically in the range 20-60 nm (stage **II** in Fig. 15). In general, among polymerization processes in heterogeneous media, microemulsion polymerization yields the smallest particles, but also works with by far the highest surfactant concentrations, typically as much as 100 – 300 wt% of the monomer concentration. Depending on the relative amounts of the two liquids and the type of surfactant, microemulsions can exist either as oil in water (O/W) or as W/O microemulsions. By varying the surfactant content, the formation of bicontinuous systems may be observed with a random organization with interconnections between the different phases. At high surfactant concentrations, monophasic lamellar structures might be present. Microemulsion polymerization directly relates to conventional monomers such as styrene [124, 127], or acrylates [128, 129]. Inverse systems mainly involve water-soluble monomers such as acrylamide [130]. O/W microemulsion polymerization of styrene is illustrated in Fig. 15.

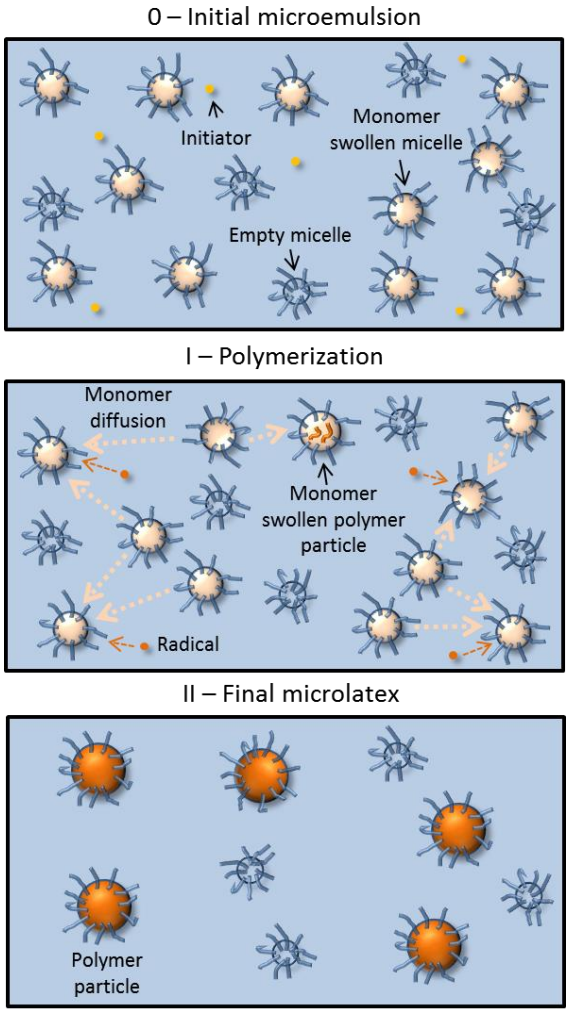

Fig. 15: Main stages of a typical O/W microemulsion polymerization.

The kinetics of microemulsion polymerizations are characterized by the compartmentalization of propagating radicals – it is a zero-one system (as in zero-one emulsion polymerizations), where monomer-swollen micelles and particles never contain more than 1 radical for a kinetically significant period of time [121, 124] (stage **I** in Fig. 15). In general, the polymerization rates are high and the molecular weight typically reaches the chain transfer to monomer limit [131] (very high molecular weight), *i.e.* chain transfer to monomer is the main end-forming event. The final polymer particles (20-60 nm) are larger than the initial

monomer-swollen micelles, as a result of monomer diffusion from non-nucleated monomer-swollen micelles to polymer particles during the course of the polymerization (stage **I** in Fig. 15). Non-nucleated monomer-swollen micelles remain in the system to high conversion (stage **II** in Fig. 15).

3.2.2 Adaptation to photoinitiation: O/W microemulsion

Microemulsion polymerizations are highly suited for photochemically induced initiation. They are typically optically transparent/translucent, especially at low conversion, as a result of the small size of the monomer-swollen micelles and polymer particles. Various studies reported on photoinduced polymerization processes in microemulsion are summarized in Table 3.

Merlin and Fouassier reported the first photochemically initiated polymerization in a microemulsion in 1981 [17]. These authors referred to their system as an emulsion polymerization – however, given the very high surfactant:monomer ratio (260 wt% sodium lauryl sulfate relative to MMA), it is likely that this was in fact a microemulsion polymerization. Photochemical initiation was carried out using various saccharides (fructose, glucose, sucrose…). The authors used mono- and disaccharides that may be represented as α-hydroxylated aliphatic carbonyl compounds, and as such, may undergo α-cleavage upon electronic excitation. α-Hydroxylated ketones and aldehydes absorbing at wavelengths > 300 nm, photopolymerizations of MMA were observed for excitations at 313 and 365 nm using medium-pressure Hg arcs. A scission of carbohydrate bonds was already earlier postulated [132]. Irradiation with the same unfiltered radiation sources (*i.e.* including the spectral range from 200 to 300 nm) resulted in much higher polymerization rates due to a significant contribution from MMA self-initiation. Encinas et al. [133] investigated the MMA/SDS system employing the radical photoinitiators dihydroxyacetone (DHA, P13 Table 1), DTBK (P9, Table 1) and hydroxymethyl butanone (HMB, P10, Table 1), the latter two being hydrophobic. The experiments carried out with quasi-monochromatic radiation at 313 nm (Hg-line) confirm the earlier results concerning the use of substituted aliphatic carbonyl compounds as photoinitiators. DHA, soluble in the aqueous phase, provided the highest polymerization rate and highest initiation efficiency. But this study also highlights a recurring problem of the photoinitiation in emulsion-based systems: the inefficiency of hydrophobic radical photoinitiators. As already mentioned in the previous section on emulsion polymerization (section 3.1), fast bimolecular termination (recombination) of the radical pair generated from a single initiator molecule in the confined space of a monomer-swollen micelle/polymer particle is thought to be the major cause [5, 96-98].

Turro and El-Aasser conducted photoinitiated polymerizations of styrene in a microemulsion using SDS as surfactant, irradiating with the 313 nm-line of a high-pressure mercury arc (radiant exitance: 3.6 mW cm^{-2}) and using DBK (P3) as oil-soluble initiator [134]. The polymerization rate increased with increasing initiator concentration and with increasing radiant power. The increase of the polymerization rate was accompanied by a decrease in molecular weight, rationalized by increased triplet radical pair concentration and consequently a greater termination rate. An increase of the initiation rate (by varying initiator concentration or radiant power) also led to larger particles, proposed to be caused by enhanced coagulation of primary particles at high initiation rates. The particle diameters were in the range 35-56 nm. Larpent and Tadros studied the photoinduced microemulsion polymerization of styrene, MMA and vinyl acetate using KPS (P11, Table 1), azobis-2-methyl–propamidinium dichloride (AMP) and AIBN (P1, Table 1) as initiators [135]. The stability of the final emulsions was evaluated by addition of electrolyte to determine the critical flocculation concentration. revealing that charged particles (from ionic initiators such as the KPS or APM) were less stable than particles (diameters 23-61 nm) obtained with the non-ionic initiator (AIBN).

The mechanism of photoinduced microemulsion polymerization of butyl acrylate (BA) using SDS as surfactant was examined in detail by Capek et al. in the mid-1990s [136-138]. Photochemical initiation was

first carried out using AIBN under UV irradiation at 365 nm. Polymerization did not occur when BA itself or BA/SDS was irradiated. However, polymerization did proceed when irradiating microemulsions of BA/SDS/water without any photoinitiator. Interestingly, the authors found that the polymerization continued for a significant time period even after the irradiation was switched off (post-polymerization; Fig. 16). Similar data were later reported for other systems [139]. The rate of radical decay contained a significant contribution from first-order kinetics (as opposed to second-order kinetics for "normal" bimolecular termination) [136]. This effect was proposed to originate from the existence of relatively immobile high molecular weight radicals that could only terminate via reaction diffusion [140]. Another significantly contributing factor is the segregated environment afforded by nanoparticles as in a typical zero-one emulsion polymerization system [86, 93]. In addition, the number of particles increased during post-polymerization, which is evidence of chain transfer to monomer followed by exit and subsequent re-entry into (non-nucleated) monomer-swollen micelles.

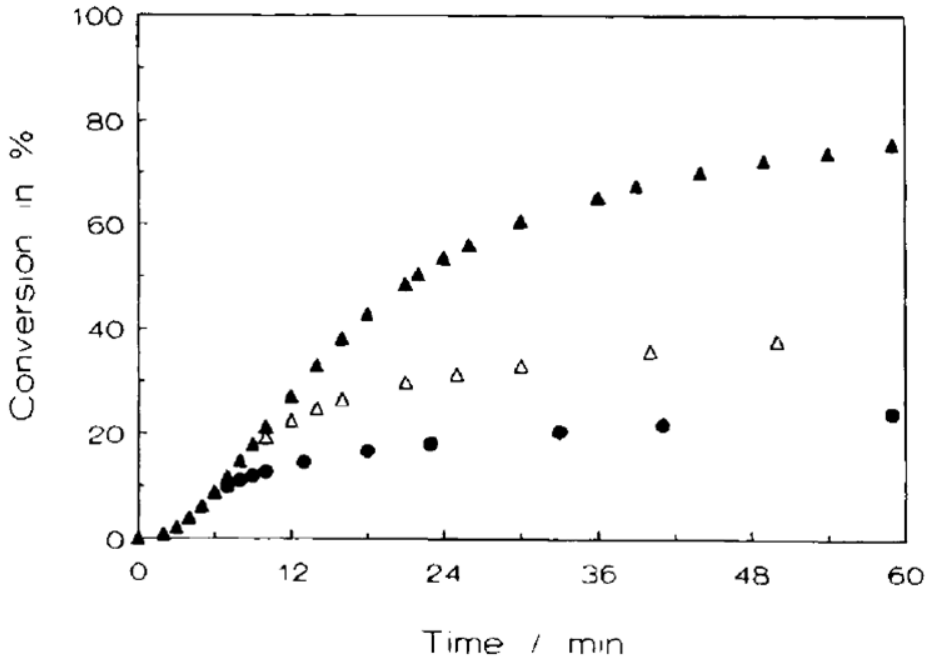

Fig. 16: Post-polymerization in the photoinduced microemulsion polymerization of BA. Continuous irradiation (▲), stop 5 min (●), stop at 10 min (△). Reproduced from [136] with permission of the copyright owners.

Wang et al. [125] conducted photoinduced microemulsion polymerization of styrene using a specifically designed cationic amphiphilic perester photoinitiator (structure presented in Fig. 17). Due to its surface activity, this initiator would be primarily located at the interface of monomer-swollen micelles and polymer particles. Homolysis under UVA-irradiation (8 W, λ = 350 nm) would generate a radical cation and an uncharged radical. It is presumed that the first would be solubilized in the aqueous phase, add to monomer in the aqueous phase and subsequently enter into a monomer-swollen micelle or polymer particle close-by, whereas the uncharged radical would initiate polymerization within the monomer-swollen micelle or polymer particle where it was generated. In case of an anionic surfactant such as SDS, the radical cation would remain associated with the negatively charged surfactant, thereby increasing the probability for recombination with the uncharged radical. However, in case of a cationic surfactant, such as DTAB, the radical cation would exit more readily from the interfacial region (Fig. 17) due to repulsion between the two positive charges. This rationale was invoked to explain the fact that the polymer molecular weight was higher for SDS than for dodecyltrimethyl ammonium bromide (DTAB), given that a lower initiation rate would result in higher molecular weight.

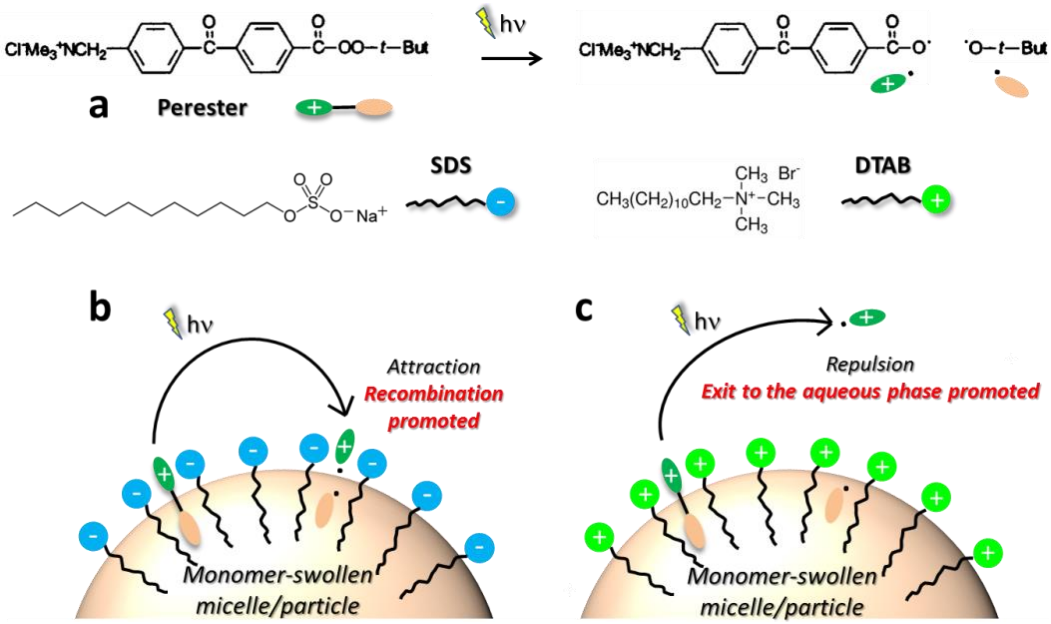

Fig 17: Positively charged amphiphilic photoinitiator used for the microemulsion photopolymerization of styrene (a). Interactions at the interface of a monomer-swollen micelle/particle upon irradiation for both types of surfactant: Negatively charged SDS (b), and positively charged DTAB (c). Reproduced from [125] with permission of the copyright owners.

In 2000, Capek [139] reported photopolymerization of microemulsions of various methacrylates in the presence of poly(ethylene oxide) methacrylate macromonomers employing a Type II radical photoinitiator (see Fig. 7b for initiation mechanism), methyldiethanolamine (MDEA) and dodecyl thioxanthone. The macromonomer gives rise to *in situ* generation of branched chains with amphiphilic character that can provide steric stabilization in addition to the electrostatic stabilization provided by SDS. The presence of the macromonomer led to an increase in particle size and a decrease in polymerization rate and molecular weight relative to the corresponding systems using SDS only. The extent of compartmentalization (segregation of propagating radicals) decreases with the increase in particle size, thus explaining the decrease in both polymerization rate and molecular weight. In both emulsion and miniemulsion polymerization, the use of nonionic surfactants tends to result in larger particle sizes. The macromonomer approach was also employed by David et al. [141], who photopolymerized microemulsions of MMA and BuMA by self-initiation under UV irradiation using a high-pressure Hg arc (300 W) in the presence of the macromonomer poly(*N*-acetylethylenimine) (PNAEI; Fig. 18). The incorporation of the macromonomer, present at the surface of the polymer particles in the form of hydrophilic branches, resulted in enhanced particle compatibility with commodity polymer matrices investigated for improvements in film formation properties.

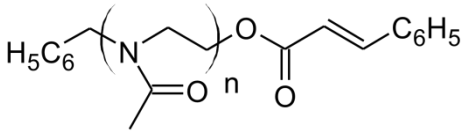

Fig 18: PNAEI macromonomer employed by David et al. [141]**.**

Jain et al. employed photoinitiated microemulsion (SDS/1-pentanol) polymerization of BA to prepare highly hydroxyl functionalized nanoparticles [142]. Functionalization was achieved by use of the photoinitiator system MDEA / Rose Bengal (RB) providing the desired chain end functionality and allowing irradiation in the VIS spectral range ($\lambda > 380$ nm). The presence of hydroxyl groups enables these polymers to act as precursors for synthesizing hybrid structures (acrylate/urethane by reaction of the hydroxyl function with isocyanate). In 2008, Wan et al. prepared nanoparticles (34 - 52 nm) of styrene-BA-silane acrylate

copolymer [143]. Subsequent film formation studies revealed inter-particle crosslinking (sol-gel process) resulting in the formation of a siloxane network.

3.2.3 Adaptation to photoinitiation: W/O microemulsion

Inverse (W/O) microemulsion polymerization involves nanoscale hydrophilic monomer droplets dispersed in a continuous organic phase. Inverse microemulsions are, just like O/W microemulsions, optically transparent due to the small micelle/particle size, and are typically employed for water soluble monomers such as acrylamide [122, 144]. These studies involved sodium dioctyl sulfosuccinate (aerosol-OT; AOT) as surfactant (Fig. 19) which is commonly employed in inverse microemulsion systems.

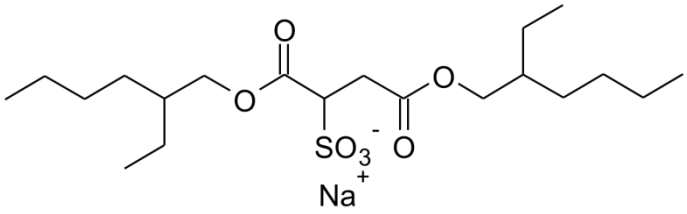

Fig 19: Sodium dioctyl sulfosuccinate (aerosol-OT; AOT)

Photoinduced inverse microemulsion polymerizations of acrylamide (acrylamide/water/toluene/ AOT/AIBN) have been investigated by Candau et al. [144, 145]. The polymerizations proceeded very rapidly (< 30 min) to full conversion, with initial micelle sizes of 4-12 nm resulting in polymer nanoparticles with diameters 28-52 nm as well as small surfactant micelles (~3 nm). This increase in size, similar to what is typically observed in O/W microemulsion polymerizations, was attributed to collision-coalescence between particles and to monomer diffusion from non-nucleated micelles. The polyacrylamide obtained was of very high molecular weight (1-5 x 10^6 g mol^{-1}) due to compartmentalization of propagating radicals. Holtzscherer et al. also reported the photopolymerization of acrylamide inverse microemulsions prepared in using *e.g.* sorbitan sesquioleate as non-ionic surfactant with particle sizes in the range 70 – 105 nm, hence, substantially larger than when using AOT [130]. Various trends were reported, such as an increase of particle size with increasing monomer content and decreasing surfactant content. A model for the photoinitiated inverse microemulsion polymerization of 2-methacryloyl oxyethyl trimethyl ammonium chloride was reported in 1998 [146].

Inverse microemulsion photopolymerization can be used to create cross-linked films by adding a crosslinking agent such as 1,6-hexanediol diacrylate to the continuous organic phase. The polymerized continuous phase and contains dispersed water droplets in its solid matrix. The synthesis and properties of such polyacrylate films were studied by Pojman and coworkers [147]. Photopolymerization affects the formation of nanostructures in the films by aggregation of water droplets or self-assembly of surfactant molecules as evidenced by small angle neutron scattering [148].

Inverse microemulsion photopolymerization has also been reported by Yagci and Matyjaszewski and coworkers using atom transfer radical polymerization (ATRP) of oligo(ethylene glycol) monomethyl ether methacrylate at room temperature with Irgacure 2959 as photoinitiator. Like RAFT or TERP mentioned above, ATRP is another example of a reversible-deactivation radical polymerization to obtain well-defined polymers in terms of molecular weight distribution and chain-end functionality. ATRP usually employs a transition metal complex Me^z/L as the catalyst (typically copper with N-containing ligands L) with an alkyl halide as the initiator (R-X, X = Cl, Br). In contrast, the authors used herein two relatively new ATRP techniques called Activators ReGenerated by Electron Transfer (ARGET) and Initiators for Continuous Activator Regeneration (ICAR), which decrease the amount of catalyst needed to only a few ppm (no photoinitiator present for the

latter) [149]. The deactivator Cu(II)/L is reduced to Cu(I)/L by radicals from the photoinitiator, and photolysis can also generate a bromine atom and Cu(I)/L from Cu(II)/L.

3.2.4 Photopolymerization in bicontinuous microemulsions

Depending on the relative amounts of surfactant, continuous phase and monomer, microemulsions may exhibit bicontinuous phases. In bicontinuous microemulsions, the dispersed phase domains are interconnected as opposed to existing merely as globular entities (Fig. 20).

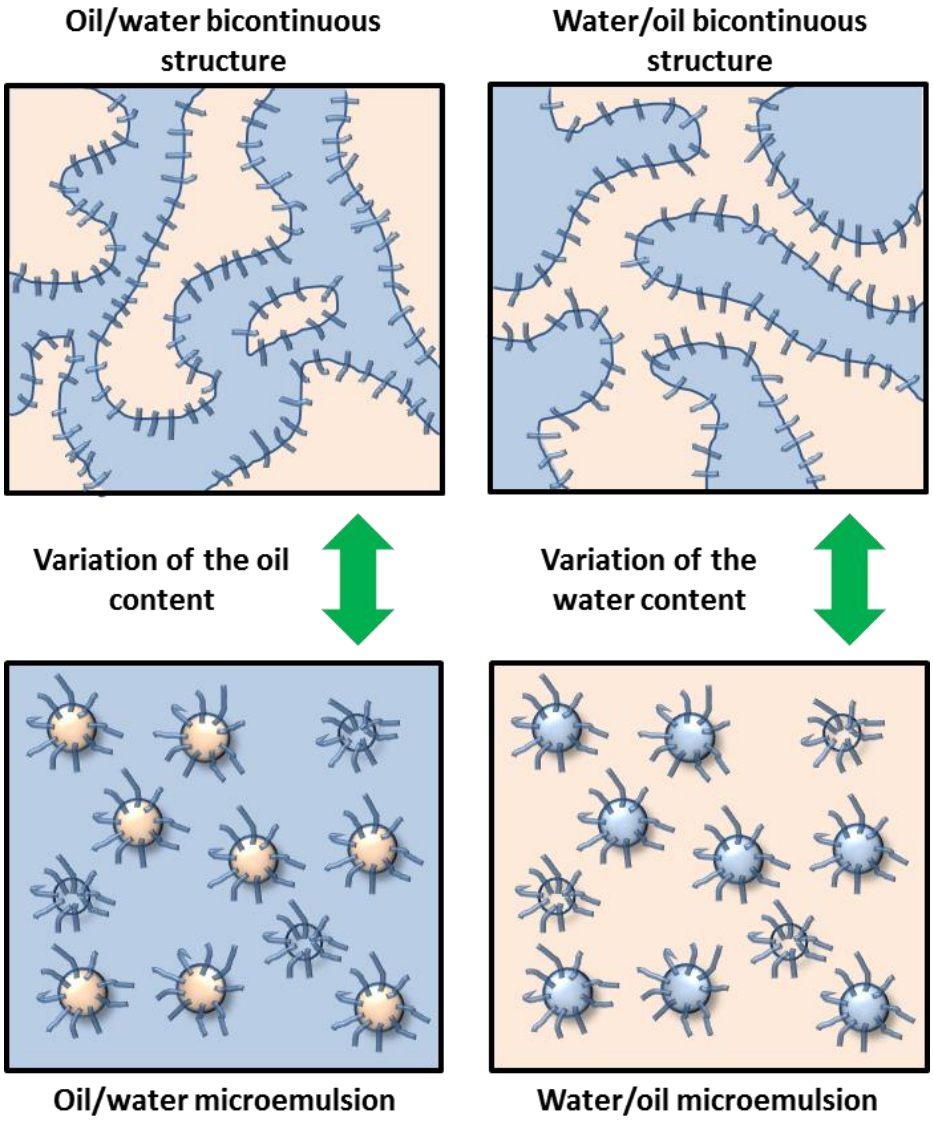

Fig 20: The various microemulsion structures obtained depending on the relative amounts of water/oil.

Polymerization of bicontinuous microemulsions enables preparation of microporous materials (pore diameter 1 - 4 nm), as reported by using photoinitiation [150, 151]. Photopolymerization of bicontinuous microemulsions of monoacrylates and diacrylates has also been studied by Peinado et al. using fluorescent probes [152] As is usually the case, photopolymerization led to changes in the monomer microemulsion structure. The nanostructure of the initial microemulsion was not retained because of the fluid template resulting in phase separation, but mesoporous materials were achieved. Photopolymerization in bicontinuous microemulsions can also be adapted to a two-phase solid medium as demonstrated by Gao and al. [153]. Porous membranes of cross-linked polymers were produced using a glucose-based dispersed phase (dehydrated to generate a solid continuous phase prior to polymerization), which is easily removed by washing with water after polymerization. This approach based on a robust solid template ensures that the

nanostructure of the initial microemulsion is maintained through the polymerization, whereas the original structures are not necessarily retained, when templating techniques are used that based on surfactant self-assembly. The pores of these structures exhibited an average size of ~25 nm.

Table 3: Summary of studies related to photopolymerization in microemulsion.

Monomer(s)	Continuous phase	Surfactant (Costabilizer)	Photoinitiator	Polymerization system / Irradiation system	Particle diameter	Ref.
MMA	Water	SDS	Saccharides	N_2 purged, 500 W, high-pressure Hg arc Phillips SP500, 250 W, high-pressure Hg arc, Osram HBO 250, λ = 313, 365 nm, external	-	[17]
Styrene	Water	SDS/DTAB	Charged perester, see Fig. 17	N_2 purged, 16 8 W, "black light" tubes, GE, F8T5-BLB, λ = 350 nm, external.	ca. 30 nm	[125]
MMA	Water	SDS	P9/P10/P13	λ = 313 nm (no details)	-	[133]
Styrene	Water	SDS/1-pentanol)	P3	Ar, 1000 W, high-pressure Hg arc, Oriel, λ = 313 nm, external, radiant exitance: 3.6 mW cm^{-2}	-	[134]
Styrene/MMA/Vinyl acetate	Water	Various (ionic and non-ionic with different HLB)	P1/P11	UV-irradiation (no details)	23 – 61 nm	[135]
BA	Water	SDS	P1/P5 Self-initiation	Ar, 250 W, medium pressure Hg arc, RVL 250 Tesla Holegovice, 125 W, medium-pressure Hg arc, RVL 250 Tesla Holegovice, λ = 313, 365 nm external	ca. 70 nm	[136-138]
Alkyl methacrylates	Water	SDS/poly (ethylene oxide) methacrylate	MDEA /dodecyl thioxanthone	Optical bench, λ = 365 nm	23 - 55 nm	[139]
MMA/BMA	Water	SDS, macromonomer (see Fig. 18)	Self-initiation	N_2, 300 W, high-pressure Hg arc, glass, external, 4 h	17 – 200 nm	[141]
BA	Water	SDS/1-pentanol)	MDEA/Rose Bengal	N_2 purged, 200 W high pressure Hg-Xe arc, λ > 380 nm, external, 5 h,	-	[142]
Styrene/BA/Silane coupling agent	Water	SDS/1-pentanol)	Benzophenone	500 W, high(?)-pressure Hg arc, glass, external, 2 – 4 h	34 – 52 nm	[143]
Acrylamide	Toluene	AOT (see Fig. 19)	P1	N_2 purged, 125 W medium pressure Hg-Xe arc, Philips HPK 125, immersed	16 - 19 nm	[144, 145]
None (water)	Dodecyl acrylate, HDDA	AOT	Irgacure 369	Film, "black light", hand-held, λ = 365 nm, external, 1 – 2 min, radiant exitance: 2.3 mW cm^{-2}	-	[147, 148]
None (water)	OEOMA	Polyethylene oxide methyl ether (Polyethylene glycol 550)	P4	Degassed (3 x) and N_2 purged, 16 UV lamps (Rayonet), λ = 350 nm, 45 mW cm^{-2}, 3 - 24 h	70 – 130 nm	[149]
MMA/AA/Ethylene glycol methacrylate (EGDMA)	Water	SDS	P5	450 W, no details, Pyrex®, external, 1 h	10 - 50 nm	[150, 151]
MMA/N,N-dimethylaminoethyl methacrylate/ EGDMA	Water	SDS/CTAB	P15	N_2, fibre guide, 450 W, medium-pressure Hg arc, Silvania, quartz, 50 min, external, radiant power: 3.13 mW	Pore : 2.3 – 2.8 µm	[152]
MMA/EGDMA	Water	SDS/CTAB	P15	Ar, 8 W, UV (no details), λ = 365 nm, external	ca. 25 nm	[153]

3.3 MINIEMULSION PHOTOPOLYMERIZATION

3.3.1 General considerations

Miniemulsions typically feature droplet sizes ranging from 40 and 400 nm [154, 155]. In the literature, they are also referred to as nanoemulsions when sub-100 nm droplets are generated. By contrast with microemulsions (10-50 nm), their preparation requires high energy input usually provided by an ultrasonifier,

static mixer or high-pressure homogenizer. This is required to overcome the surface free energy to increase the interfacial area between the dispersed monomer phase and the continuous phase. The consequence is a high demand in surfactant to stabilize the newly-formed interface, implying that micelles are generally absent in well-formulated miniemulsions. In contrast to microemulsions, miniemulsions are not thermodynamically stable but instead kinetically stable. Their stability ranges from a few hours to years depending on composition and processing conditions. Coalescence can occur when two droplets collide and finally merge, but the main destabilization route is Ostwald ripening. This occurs because of a difference in chemical potential (μ) between monomer droplets of different sizes due to different curvature radius. Smaller droplets have higher Laplace pressures (higher μ) which drives mass transfer towards the larger droplets (lower μ) through the aqueous phase [156].

Diffusional destabilization may be limited by the dissolution of a costabilizer (a compound of low molecular weight with no or very low water solubility) in the oil phase. With monomer diffusion, the costabilizer is getting concentrated in the smaller droplets, creating a gradient of composition that accounts for the appearance of a new negative term in the expression of μ (entropy of mixing) - absent when the oil droplets only contain monomer. The entropy of mixing terms tends to reduce $\Delta\mu > 0$. After a certain time of monomer diffusion, a pseudo-equilibrium is finally established ($\Delta\mu = 0$). If Ostwald ripening is retarded, predominant droplet nucleation may be achieved, and the number of the produced particles is in the same range as that of droplets. This mechanism represents the basis of miniemulsion polymerization (see stage I in Fig. 21). In contrast to emulsion polymerizations [156, 157], in miniemulsion polymerizations, there is no need for monomer transport through the aqueous phase to create polymer particles. The corollary is that droplet nucleation can be maximized, which is a distinctive feature of miniemulsion (photo)polymerization compared to other techniques of polymerization in dispersed systems. This mechanistic difference makes miniemulsion polymerization attractive for the synthesis of hybrid polymer particles [158], hollow polymer particles [159], as well as for the implementation of controlled/living radical polymerization in dispersed systems [160].

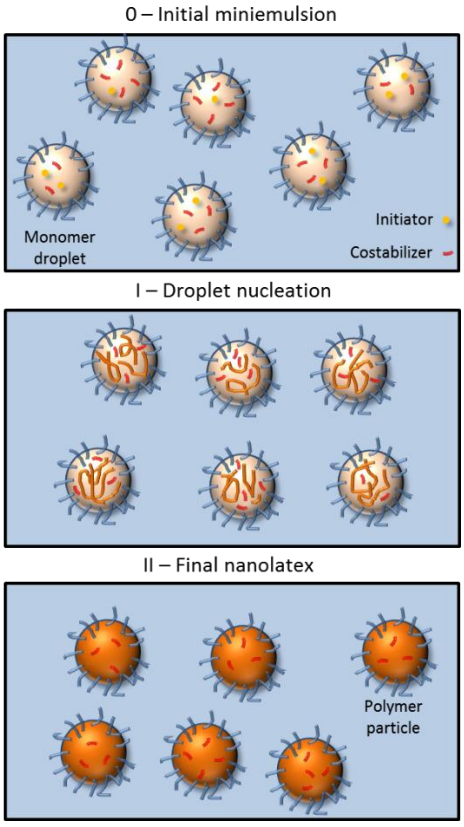

Fig 21: Schematic illustration of an ideal miniemulsion polymerization with complete droplet nucleation.

3.3.2 Adaptation to photoinitiation

The interest in miniemulsions for photopolymerization is firstly driven by the lower scattering coefficient compared to macroemulsions, when droplet sizes are decreased to 50 - 100 nm. As a result, a higher volume fraction of the reactor can be irradiated, with a positive impact on the rate of polymerization. Although monomer miniemulsions have greater droplet diameters than microemulsions (10 - 50 nm), they can be prepared at much higher solid contents (> 50 wt%), but still needing moderate surfactant concentrations (< 5 wt% with respect to monomer). In 2009, Lacroix-Desmazes et al. used for the first time miniemulsion photopolymerization for a different purpose: the polymerization at ambient temperature of VAc miniemulsions by iodine reversible transfer polymerization (IRP) using photoinitiation [161]. Mild conditions were necessary to preserve the integrity of the temperature sensitive iodinated chain ends of PVAc. Long irradiation (16 h) at low irradiance (2.5 mW cm^{-2}) resulted in a successful self-initiated photopolymerization due to the photochemical hemolysis of the C-I bonds of the diiodo-poly(dimethylsiloxane) macrophotoiniferter (I-PDMS-I, the terminology "iniferter" was given by Otsu to a class of compounds acting as radical initiators, chain-transfer agents and chain terminators, see structure in Fig. 22). The polymerization resulted in particles (160-360 nm) composed of PVAc-*b*-PDMS-*b*-PVAc triblock copolymer.

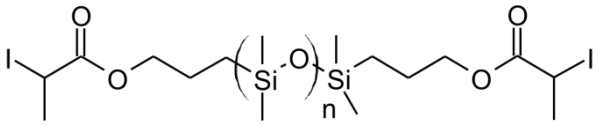

Fig. 22: Macrophotoiniferter I-PDMS-I used by Lacroix-Desmazes et al. for the synthesis of block copolymer by photopolymerization in miniemulsion [161].

Droplet nucleation is the distinctive feature of miniemulsion polymerization. It allows incorporation of hydrophobic compounds into the polymer particles, because mass transfer through the aqueous phase is avoided. Exploiting this feature, Fuchs et al. produced hybrid PMMA/gold latex [162] using benzoyl peroxide (BPO) as photoinitiator. The radiation produced by a high-pressure Hg arc (830 mW cm^{-2}) for 60 min resulted in a maximum conversion of 65 %. However, morphological studies showed only low concentrations of metal (about 0.6 wt% compared to the organic phase). Fig. 23 shows the effective incorporation of gold nanoparticles into the polymer particles. Room temperature polymerization is thought to be conducive to limit aggregation and sedimentation of particles incorporated within the polymer particles. The synthesis of magnetic iron nanoparticles encapsulated latexes has also been reported [162, 163]. For this latter investigation, miniemulsion photopolymerization of MMA was realized using Irgacure 184 (P8) as photoinitiator and a medium-pressure Hg-Xe arc (1.160 mW cm^{-2}), giving 80 % conversion in 15 min.

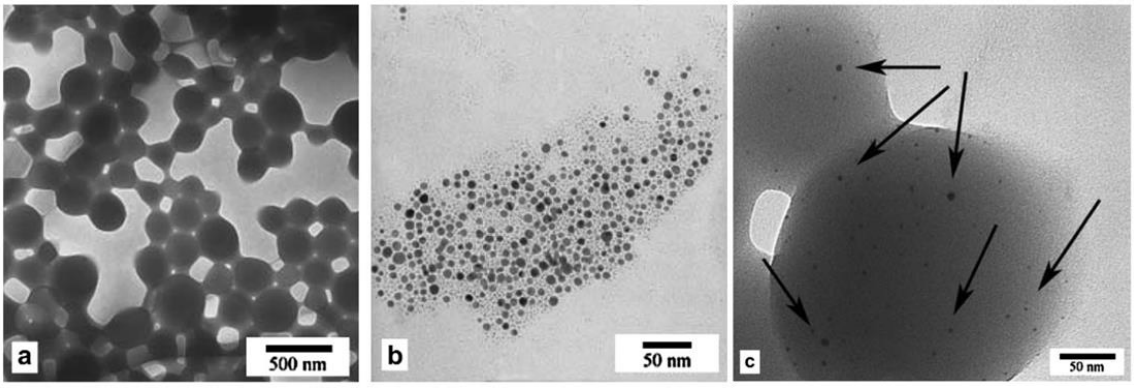

Fig. 23: Transmission electronic microscopy pictures of the PMMA latex (a), gold nanoparticles (b) and gold nanoparticles encapsulated in the latex, the arrows shows some domains including nanoparticles (c). Reproduced from [162] with permission of the copyright owners.

Film-forming nanolatexes were also obtained by Chemtob et al. from a MMA/BA/AA miniemulsion, which is a conventional formulation for coatings applications. In an exploratory study, the authors investigated the effect of the photoinitiator solubility and the influence of the solids content (5 to 20 wt%) on polymerization rates and colloidal properties [164]. Harnessing spatial control of radiation (using UV light guides) enabled in situ monitoring of particle size (via dynamic light scattering) and monomer conversion (NIR spectroscopy) throughout the photopolymerization. In 2011, Chemtob et al. conducted a detailed study of the same reaction fixing the solids content at 17 wt% [165]. The effect of various experimental parameters was studied, including droplet size, radiant power and type of photoinitiator, using a batch annular photoreactor (Fig. 24). Full conversion was achieved in less than 40 min for the more water-soluble Irgacure 2959 versus 2 h for the oil-soluble Irgacure 907. The same team also showed that photopolymerization of a MMA/BA/AA miniemulsion was possible in the absence of a photoinitiator using an INISURF (Dowfax 2A1, see definition in section 2.3.3) [166]. Initiator-free photopolymerization was also conducted with a range of self-initiating monomers, *e.g.* BA or MMA [52]. These (non-purified) monomers form initiating radicals under UV irradiation (λ < 300 nm) which may be generated in a quartz vessel by an unfiltered emission a conventional medium-pressure Hg arc.

One important remaining challenge is unveiling the complex relationship between the optical properties of a monomer emulsion and its photopolymerizability to optimize the conditions of irradiation. To this end, Chemtob and coworkers exploited spectrophotometric techniques using an integration sphere to extract absorption and scattering coefficients. The first approach used highly diluted samples (< 0.5 wt%) to avoid multiple scattering [36], while in a second step the *two-flux* theory of Kubelka-Munk was employed to directly analyze concentrated miniemulsions (30 wt%) [38]. As a complementary route, actinometry was also employed to determine the efficiency of radiation absorption in monomer nanodroplets [71]. For this purpose, a well-characterized water-insoluble chemical actinometer (Aberchrome, see *e.g.* [57]) replaced the oil-soluble photoinitiator, and was used as a probe to evaluate UV absorption in miniemulsions as a function of droplet size (40-150 nm) and organic phase content. It was found that the absorption in a miniemulsion droplet is similar to that of an equivalent organic solution regardless of the water solubility of the initiator or the level of dilution. Additionally, radiation penetration can be significantly improved by decreasing the droplet size below a threshold of 100-150 nm due to a significant decrease of scattering when using smaller droplets. A set of photoreactors displaying different sizes (micro- [60], minireactor [167]) and geometries were built and assessed for emulsion radical photopolymerization of acrylate monomers. Notably the helix-type minireactors (internal tube diameter: 1.5 mm) enabled in continuous operation a flash conversion within less than 30 s of residence time. Recently, a polysulfide latex with crystalline properties was synthesized via an innovative step-growth radical photopolymerization process (thiol-ene) [50, 168].

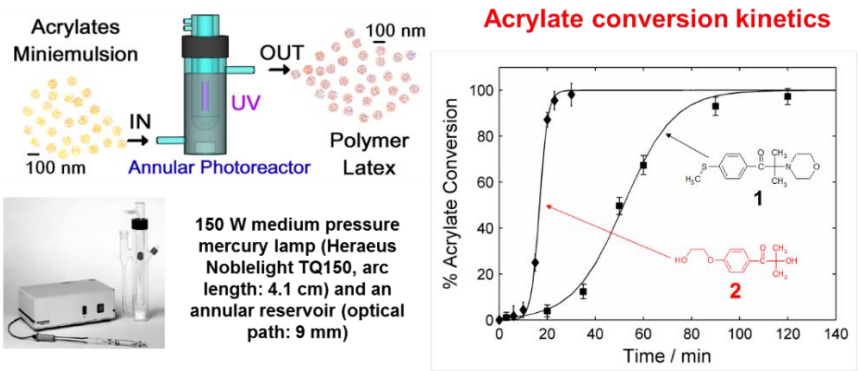

Fig. 24: Miniemulsion photopolymerization carried out in an annular photoreactor using a medium-pressure Hg arc immersed in the miniemulsion. The emitted wavelengths below 300 nm are filtered by a borosilicate sleeve. The effect of the type of photoinitiator on the polymerization rate is highlighted. Reproduced from [165] with permission of the copyright owners.

The use of photoreactors for the synthesis of high solid contents acrylic latex is the focus of research led by the group of Tomovska. Using a continuous flow tubular reactor (flow rate: 0.4 to 4.2 mL/min, inner diameter of the quartz tube: 1 mm, reactor length: 6.35 m), they studied the photoinduced synthesis of organic-inorganic hybrid latexes [46, 61]. They polymerized acrylate-based miniemulsions containing preformed polyurethane (Incorez 701) exhibiting isocyanate functional groups able to react with two MMA functional co-monomers: MAA and hydroxyethyl methacrylate, allowing the synthesis of covalently linked polyurethane/polyacrylate particles. Mild irradiance (< 7 mW cm^{-2}) was provided by 20 "Black Light" tubes (315 - 400 nm). Particle sizes ranged between 150 and 190 nm, and the photoinitiator used was the oil-soluble Irgacure 184 (P8, Table 1). They showed that high conversions (> 80 %) can be achieved for a residence time of less than 10 min using a minimum photoinitiator concentration. Molecular weights were varied (30 - 160 kDa) as well as gel contents by tuning initiator concentration or radiant power. The resulting dispersions were implemented for applications in pressure sensitive adhesives (PSA) [169]. While the first study was limited to 20 wt% solids content, an increased concentration was prone to coagulation. Such an undesired effect was attributed to a lower monomer/quartz interfacial tension compared to the aqueous phase/quartz interfacial tension. This difference drives preferential diffusion of the monomer from the droplet to the wall of the photoreactor resulting in plugging after photopolymerization [61]. This phenomenon was later investigated in further detail and shown to be related to diffusional wetting [170]. By modifying the reactor wall, they succeeded in polymerizing 40 wt% solids content styrene/BA miniemulsion [171].

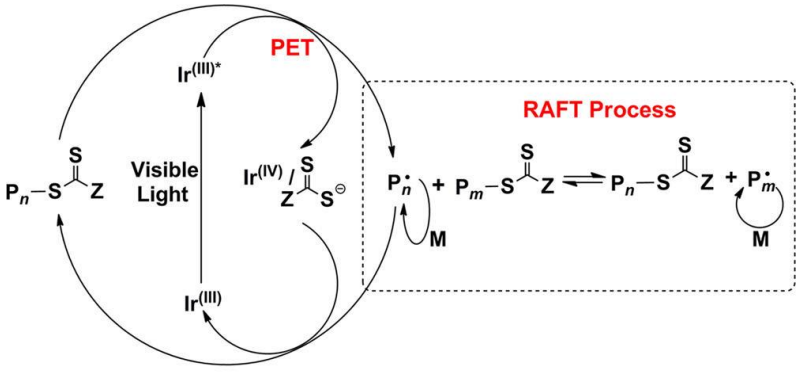

Fig 25: In a typical PET-RAFT mechanism, a photoredox catalyst (*fac*-[Ir(ppy)$_3$], Ir(III), in ref [6]) generates an excited species (Ir(III)*) under irradiation, acting as a reductor of thiocarbonylthio compounds (RAFT control agent) via a PET reaction, resulting in the production of initiating radicals ($P_n^{\bullet}$) and Ir(IV) species. In contrast to a conventional RAFT mechanism, the RAFT agent behaves both as an initiator and chain transfer agent. The radical ($P_n^{\bullet}$) may either participate in the RAFT process (dotted frame) or be oxidized by Ir(IV) species to regenerate the initial Ir(III). Reproduced from [6] with permission of the copyright owners.

Miniemulsion polymerization is probably the technique which has attracted the most attention in recent years with regards to photopolymerization in dispersed systems. The latest developments in 2016 cover the synthesis of "monodisperse" poly(hexyl acrylate) nanoparticles [172], the use of microfluidic chips as microreactor [173], as well as the cross-linking of commercial water-dispersible acrylated resins under batch (immersion-tube photoreactor) [174] and continuous (tubular photoreactor made of polyvinylchloride tubing) operation [175]. Although there is no emulsification step in this latter case, the formation of particles by oligomer "droplet" nucleation brings this study close to a miniemulsion photopolymerization. Two final studies deserving attention are that of Boyer and coworkers reporting controlled/living visible photopolymerization in miniemulsion. The first one is based on a specific photoinduced electron transfer PET-RAFT mechanism (see Fig. 25 for details on mechanism) and employs a model monomer (styrene) [6]. It stands out by different features which may shape the manner by which photopolymerization in dispersed systems will be realized in the future: use of energy-saving LEDs emitting in the VIS spectral domain, very low irradiance (< 1 mW cm^{-2}), and photoredox catalysts to be used at very low concentration (50 ppm relative to

styrene). In the second work, a visible RAFT photoiniferter was employed to polymerize butyl methacrylate miniemulsion obviating the need for catalyst or initiator [176]. Although evidences of good control/livingness are provided, the amphiphilic properties of the RAFT CTA may result in secondary nucleation, leading to loss of control at high surfactant concentration. The main works related to miniemulsion photopolymerization and their main characteristics have been summarized in Table 4.

Table 4: Main studies describing miniemulsion photopolymerization.

Monomer	Continuous phase	Surfactant (Costabilizer)	Photoinitiator	Polymerization time/Irradiation system	Particle diameter	Ref.
Vinyl acetate	Water	SDS	P1, I-PDMS-I (Fig. 22)	Ar, 125 W, Philips HPK 125, glass, immersed, irradiance: 2.5 mW cm^{-2}, irradiation time: 16 h,	160 – 360 nm	[161]
MMA	Water	Non ionic Tween 80 (Tetradecane)	Benzoyl peroxide	Ar purged, 200 W, high-pressure Hg arc, quartz, external, irradiance: 0.83 W cm^{-2}, irradiation time: 60 min	100 – 200 nm	[162]
MMA	Water	SDS (Hexadecane)	P8	300 W, medium-pressure Hg-Xe arc, λ = 350 nm, glass(?), external, radiant exitance: 1.16 mW cm^{-2}	90 - 126 nm	[163]
MMA/BA/AA	Water	Dowfax 2A1 (Hexadecane)	P15/P2/P8/P5	200 W high-pressure Hg-Xe arc, Hamamatsu L2852, quartz, external, 180 mW cm^{-2}, irradiation time: 20 - 140 min	50 – 60 nm	[164]
MMA/BA/AA	Water	SDS (Hexadecane)	P15/P2/P4/ P5/P6/P8	200 W, high-pressure Hg-Xe arc, Hamamatsu L2852, λ > 300 nm, external, radiant exitance: 4 - 200 mW cm^{-2}	60 – 90 nm	[165]
MMA/BA/AA	Water	SDS/ Dowfax 2A1 (Hexadecane)	P6 Self-initiation	200 W, high-pressure Hg-Xe arc, Hamamatsu L2852, quartz or λ > 300 nm, external, radiant exitance: 4 - 200 mW cm^{-2}, 150 W, medium-pressure Hg- arc, borosilicate, immersed, Heraeus Noblelight TQ 150, irradiation time: 20 - 140 min	55 – 75 nm	[166]
MMA/BA/AA	Water	SDS (Octadecyl acrylate)	Self-initiation	N_2 purged, 150 W, medium-pressure Hg-arc, borosilicate, immersed, Heraeus Noblelight TQ 150, irradiation time: < 6 h	40 – 115 nm	[52]
MMA/BA/AA	Water	SDS (Octadecyl acrylate)	Self-initiation	200 W, high-pressure Hg-Xe arc, Hamamatsu L2852, quartz, external, radiant exitance: 633 mW cm^{-2}	40 -300 nm	[36]
MMA/BA/AA	Water	SDS (Octadecyl acrylate)	P4/P15	200 W, high-pressure Hg-Xe arc, Hamamatsu L2852, quartz, external, λ > 300 nm, radiant exitance: 965 mW cm^{-2}, irradiation time: 1000 s	40 –300 nm	[38]
MMA/BA/AA	Water	SDS (Hexadecane)	P4	18 W, "black light" tube, Osram, λ = 280 - 410 nm, external, radiant exitance: 3 mW cm^{-2}, Residence time: 5 and 20 min	40 - 100 nm	[60]
BA/BuMA	Water	SDS (Hexadecane)	P7	18 W, "black light" tube, Osram, λ = 280 - 360 nm, external, radiant exitance: 2.6 mW cm^{-2}, Residence time: 27 s	120 nm	[167]
Dithiol-diene	Water	SDS (Hexadecane)	P4	[53]: 200 W, high-pressure Hg-Xe arc, Hamamatsu L2852, external, quartz, radiant exitance: 965 mW cm^{-2}, or λ > 300 nm, radiant exitance: 588 mW cm^{-2}, irradiation time: 5 min [165]: rradiation time: 220 min	100 – 150 nm	[50, 168]
MMA/MAA/HEMA Polyurethane (Incorez 701)	Water	SDS/ Dowfax 2A1 (Octadecyl acrylate)	P8	[49]: N_2 purged, 20 "black light" tubes, λ: 315 – 400 nm, λ_{max}: 368 nm, quartz, radiant exitance: 2.5 – 7 mW cm^{-2}, Residence time: 1.5 – 15 min	150 – 190 nm	[46, 61]
MMA/MAA/HEMA Polyurethane (Incorez 701)	Water	SDS/ Dowfax 2A1 (Octadecyl acrylate)	P2/P4/P8/P7	N_2 purged, 20 "black light" tubes, 315 – 400 nm, λ_{max}: 368 nm, quartz, Residence time: 12 - 16 min	150 nm	[169]
BA	Water	SDS (Hexadecane)	P7	18 W, "black light" tube, Osram, λ = 280 - 360 nm, external, radiant exitance: 2.6 mW cm^{-2}, Residence time: 27 s	120 nm	[170]
Styrene/BA	Water	Dowfax 2A1 (Octadecyl acrylate)	P7	N_2 purged, 20 "black light" tubes, λ: 315 – 400 nm, λ_{max}: 368 nm, quartz, radiant exitance: 2.5 – 7 mW cm^{-2}, Residence time: 1.5 – 15 min	80 – 190 nm	[171]

Hexyl acrylate	Water	SDS (Pentadecane)	Benzoin methyl ether	10 – 30 min, 5 UV tubes 8 W, λ = 365 nm, 2.2 – 3.7 mW cm^{-2}	100 - 200 nm	[172]
Styrene	Water	Lutensol AT 50 (Hexadecane)	P15	10 – 60 s, UV LED, λ = 365 nm, 44.2 - 68 mW cm^{-2}	120 – 160 nm	[173]
Oligomeric acrylated resin	Water	(Hexadecane)	P8/Benzophenone	150 W, medium-pressure Hg arc, Heraeus Noblelight, quartz, immersion, radiant exitance: 35 mW cm^{-2}, irradiation time: 60 min	40 – 500 nm	[174]
Oligomeric acrylated resin	Water	-	P8/Benzophenone	100 W, medium-pressure Hg arc, Hönle, external, PVC, λ > 340 nm, irradiation time: < 250 s	40 – 500 nm	[175]
Styrene	Water	Dowfax 8390 (Hexadecane)	Photo redox catalyst: *fac*-$[Ir(ppy)_3]$ / RAFT agent: 3-benzylsulfanylthiocarbonylsulfanyl propionic acid	LED strip , λ_{max} = 460 nm, external, 0.73 mW cm^{-2}, irradiation time: 120 h	> 200 nm	[6]
BuMA	Water	SDS (Hexadecane)	4-cyano-4[(dodecylsulfanylthiocarbonyl)sulfanyl pentanoic acid)] as photoiniferter	LED strip , λ_{max} = 530 nm, external, 0.73 mW cm^{-2}, irradiation time: 20 h	100 – 200 nm	[176]

3.4 DISPERSION PHOTOPOLYMERIZATION

3.4.1 General considerations

Dispersion polymerization stands out by its capacity to produce polymer particles in the micrometer range (0.5 – 20 µm), a size domain difficult to access with other techniques. One salient feature of dispersion polymerization relates to the chemical nature of the continuous phase. The selected solvent must dissolve the monomer(s), initiator and stabilizer before reaction, while behaving as a non-solvent of the polymer to cause an enthalpy-driven precipitation that leads to particle formation. As a result, non-aqueous or partially aqueous reaction media are generally employed, making possible a broad range of polymerizations: radical polymerization but also more water-sensitive processes such as oxidative, metathesis or step-growth polymerizations [177]. When this technique was introduced 50 years ago, the main issue was to achieve acrylic dispersions in hydrocarbon solvents [178], because of net advantages compared to their aqueous analogues, including faster evaporation rates and lower freezing points. Today, the most attractive characteristic of dispersion polymerization is the rather excellent monodispersity of the resulting micron-size particles [179], a feature sought after in niche applications such as toners, instrument calibration methods, or column packing materials for chromatography [78].

In dispersion polymerization, polymers are the preferred stabilizers since electrostatic stabilization is not effective due to the low dielectric constant of the organic reaction medium [180]. The steric stabilizer is generally a physically adsorbed linear polymer (*e.g.* PVP) or amphiphilic block copolymer. In addition, macromonomers, mainly based on PEO, have been employed extensively, because they can generate amphiphilic graft copolymers in situ upon chain extension with suitable monomers. Stabilizer grafting through chain transfer reaction is also a common mechanism of stabilization. The most broadly accepted mechanism is depicted in Fig. 26 [78]: starting from a homogeneous solution (stage **0**), the soluble linear oligomer chains grow in the continuous phase after initiation (stage **I**). When they attain a degree of polymerization exceeding the critical value for precipitation, polymer particles are formed. Nucleation stops (*i.e.* new particles are no longer generated) when a sufficient number of particles exist to capture all newly generated precipitated chain/precursor particles. Subsequent growth (stage **II**) takes place – by capture of oligomers, coagulation of unstable nuclei, and polymerization of the monomer swelling the particles – to ultimately yield sterically stabilized micron-size particles (stage **III**). The mechanism of a conventional dispersion polymerization, focusing on radical polymerization, is both complex and sensitive to numerous variables such as initiator/comonomer concentration, composition of the dispersing phase, etc. [181]. The major challenge in terms of understanding the mechanism of dispersion polymerization is the very early stage

in which particles are formed [182]. It is generally accepted that particles are formed through coagulation of single polymer chains and instable small particles. However, this stage **I** remains very short making a detailed mechanism investigation not readily accessible. Additionally, controlling the critical diameter of primary particles is challenging, while it has an important role on final particle size.

The interest for a photoinduced version of this technique arises from the transparency of the reaction medium to UV-VIS radiation before polymerization and the better control of early stages of the reaction. Dispersion photopolymerization is usually carried out in alcohol or mixed solvents (ethanol/water), using mostly PVP as stabilizer. Controlled/living radical polymerization techniques occupy a central position in the development of dispersion photopolymerization. Foremost among them is the reversible addition – fragmentation chain transfer (RAFT) polymerization due to its mild reaction conditions, the absence of heavy metals and the tolerance to a broad range of monomers and solvents. The goal is to produce polymer microparticles combining controlled molecular weight, surface functionality and narrow particle size distribution.

Dispersion photopolymerization has experienced since 2015 a renaissance when the process known as polymerization-induced self-assembly (PISA) has been extended to photopolymerization [183]. In general terms, PISA can be implemented as an emulsion or dispersion polymerization [184]. In photo-PISA, a solvophilic macromolecular chain transfer agent is subjected to photoinduced chain extension under exposure to radiation to form a second solvophobic segment. The obtained amphiphilic diblock copolymer may self-assemble to form nano-objects showing a rich morphology such as micelles, worms, vesicles and lamellae. Morphological transitions can take place during polymerization due to copolymer chain reorganization. Proceeding without external stabilizer and possibly at medium solids content (25 - 30 wt%), this mechanism of particle formation differs from a conventional dispersion polymerization. Nevertheless, the two mechanisms start both from a homogeneous solution because the added monomer that eventually forms the non-soluble block is soluble in the reaction medium. Therefore, dispersion PISA can be considered as a variant of the more general dispersion polymerization. Recent advances on photo-PISA have been reviewed by Boyer and coworkers [185]. Table 5 provides an overview of microspheres synthesized by dispersion photopolymerization. PISA can also be implemented as emulsion polymerization, but no photoinitiated version has been reported so far.

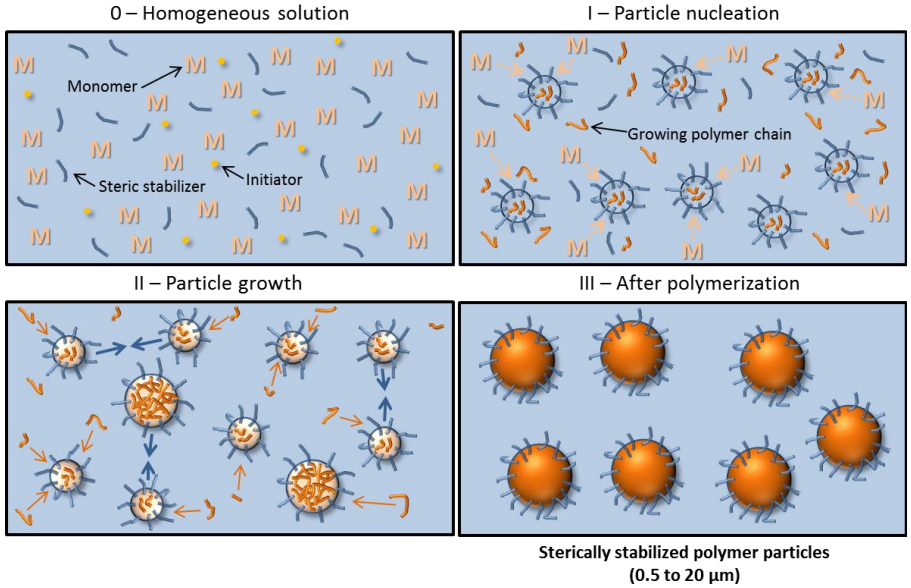

Fig. 26: Schematic mechanism of dispersion polymerization inspired from ref. [78]. In addition to stabilizer adsorption on the particle surface, depicted here, stabilization may also occur via stabilizer grafting or in situ generation of amphiphilic diblock copolymer.

3.4.2 Adaptation to photoinitiation

In 2003, Shim et al. reported RAFT dispersion photopolymerization of styrene using a dithioester control agent. This study was carried out at 50-70°C in ethanol, thereby implying that AIBN (P1, Table 1) acted both as a photo- and thermal initiator [186]. In addition, the analysis of the polymer particles revealed a lack of molecular weight control and a broad particle size distribution. Using the same experimental conditions, Ki et al. employed a PVP macro-RAFT agent as steric stabilizer, without significant improvement [187].

The first study reporting a photoinduced dispersion polymerization was published in 2008 [188]. Chen et al. photopolymerized MMA in ethanol/water employing PVP as steric stabilizer and Darocur 1173 as photoinitiator. 95 % conversion was achieved within 30 min of UV irradiation at room temperature, and the relatively monodisperse spheres (molecular-weight dispersity, Đ = 1.04) had an average diameter of 1 µm, matching the size generally obtained by dispersion polymerization. This study set out the effects of reaction conditions, such as stabilizer concentration, monomer concentration, and solvent composition on particle yield and size distribution. An analogous study was reported two years later by Huang et al. for the preparation of poly-[(MMA)-co-(MA)] COOH-functionalized microparticles [189]. Irradiation with what was most probably a "black light" tube required a long UV exposure (24 h) to achieve complete conversion. More recently, poly(styrene-co-maleic anhydride) microspheres were prepared under very similar conditions [190]. It is also worthwhile mentioning two studies standing out by their originality. Ushakova et al. investigated the effect of a magnetic field on the conversion of styrene during dispersion photopolymerization (500 W, λ > 313 nm) [191]. The concept of conducting radical polymerization under the influence of a magnetic field is discussed in detail in section 3.1. (emulsion photopolymerization). Secondly, The second publication deals with the dispersion photopolymerization of trimethylolpropane triacrylate in liquid CO_2 where poly(ethylene oxide) macromonomers were used [192].

The study by Tan et al. in 2012 is clearly the second milestone in the development of dispersion photopolymerization [193]. Highly monodisperse particles were obtained for the first time by RAFT dispersion polymerization of MMA stabilized by PVP using LEDs for irradiation and non-absorbing control agents. Control/livingness of the polymerization was demonstrated by adding a new batch of monomer at the end of the typical one-stage procedure. The process was continued by turning on the LED again (Fig. 27) to cause an increase of molecular weight in agreement with the amount of monomer added. In addition, linear growth of molecular weight during conversion was also found during the growth stage.

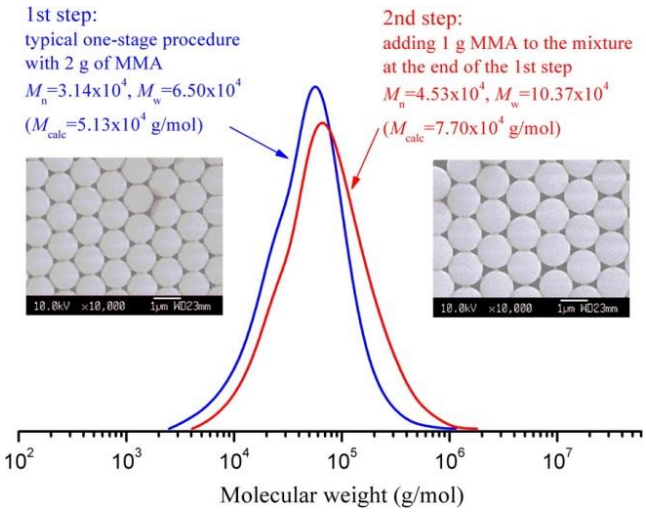

Fig. 27: GPC traces for PMMA produced in a two-step process. The first step is the RAFT dispersion photopolymerization of MMA. After 3h irradiation, a second shot of MMA was added and the reaction was continued during additional 3 h. M_{calcd} refers to the theoretical molecular weight estimated from the initial monomer and RAFT agent concentrations. Reproduced from [193] with permission of the copyright owners.

Continuing the development of RAFT dispersion photopolymerization, Tan et al. turned their attention to macroRAFT agents (Fig. 28) to stabilize PMMA microspheres through in situ formation of block copolymers [194]. Variant strategies were designed by the same group involving poly(ethylene glycol) methacrylate macromonomer [195], a range of RAFT agents [196], encapsulation of lanthanide nanoparticles [197], formation of cross-linked particles [198], as well as glycidyl-functionalized particles for post-functionalization [199].

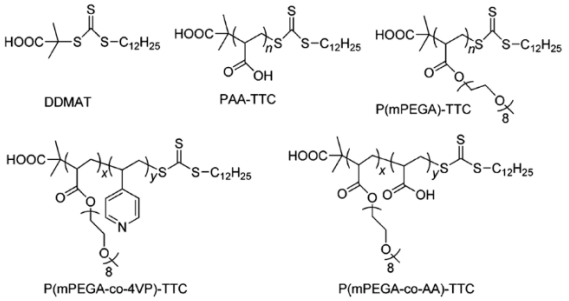

Fig 28: Macro-RAFT agents used by Tan et al. to form monodisperse microspheres by photoinduced dispersion polymerization [194]. Chemical structures taken from [194] with permission of the copyright owners.

PISA combined with photoinitiation is the latest landmark in the development of dispersion photopolymerization. While PISA by thermally induced RAFT dispersion polymerization had been known since 2011 [200], the first photo-PISA was introduced in 2015 by Cai and coworkers [201]. However, it should be noted that in 2010, Tan et al. used a stabilizing polyurethane macrophotoinitiator to polymerize MMA in dispersion conditions [80]. Despite the lack of control, monodisperse PMMA microspheres were obtained and this approach based on self-assembly of amphiphlic copolymers paved the way to photoPISA. In their pioneering study, Cai et al. photopolymerized diacetone acrylamide in water at room temperature using a well-defined poly(2-hydropropymethacrylamide) macromolecular macro-CTA to produce spherical micelles ($\lambda > 400$ nm). Shortly afterwards, Chen et al. described a similar methodology relying on the chain extension of a poly(4-vinylpyridine) macroCTA RAFT agent with styrene in methanol under UV radiation ($\lambda = 365$ nm) [202]. These two pioneering studies marked the beginning of a continuing series highlighting visible radiation-mediated RAFT dispersion PISA. Cai and coworkers diversified their initial strategy using VIS light at low radiant power by exploring other stimuli to drive PISA: polyion complex templates [203] and hydrogen-bonding [204].

Focusing on innovative means of photoinitiation, poly(oligo(ethylene glycol) methyl ether methacrylate) was chain extended in ethanol by Boyer and coworkers with benzyl methacrylate using the ruthenium-based photoredox catalyst $Ru(bpy)_3Cl_2$ [6, 205]. Importantly, the typical PISA morphologies were obtained (spheres, worms and vesicles) in this study, but polymerization rates were rather low (73 % in 24 h). More recently, the same group moved forward by reporting photo-PISA with a photochemically activable macro-RAFT agent obviating the need for external catalysts or initiators [206] or, alternatively, using zinc tetraphenylporphine (ZnTPP) as photoredox initiating system [207]. Another example of photo-PISA based on photoredox catalyst (10-phenylphenothiazine) was reported very recently by Hong et al [208].

Also very active over the last 3 years was the group of Tan at Guangdong University (China) that reported dispersion photo-PISA in methanol/water mixtures (isobornyl acrylate [209, 210] and MMA [211] for chain extension) and in water (2-hydroxylpropyl methacrylate [212-215]) as depicted in Fig. 29). Some of these studies clearly show the advantages of photo-PISA compared to conventional thermally initiated PISA. The low temperature of photo-PISA facilitated the synthesis of polymer nanoparticles encapsulating sensitive proteins [212], possessing CO_2- or thermo-responsive properties [213, 216], or containing epoxy functional groups [217]. Very recently, photo-PISA has enabled the development of novel techniques. For example,

lowering the reaction temperature to room temperature was critical to maintain good control of the polymerization using a Z-type macro-CTA, in which the RAFT reactive group is not located at the end of block copolymers, but at the center of the two blocks [218]. In addition, photo-PISA of 2-hydroxypropyl methacrylate in water was performed with an enzyme (GOx) reacting with dissolved oxygen but only active at ambient temperature. This enabled the process to be carried out in the presence of molecular oxygen in benchtop open vessels and 96-well plates without any degassing [219]. Whether as the fashion of the day or out of necessity, photo-PISA is getting a ubiquitous methodology which has become a main driver of photopolymerization in dispersed systems. The vitality of the photo-PISA methodology and an exhaustive lists of the systems investigated in this specific field are highlighted in the recent review published by Boyer and coworkers [185].

While most photoinitiated dispersion polymerization focuses on chain-growth radical polymerization, a noticeable example based on step-growth thiol–Michael Polymerization was presented by Bowman and coworkers in 2015 [220]. Handling photobase photogenerators (releasing amine or guanidine) they proved in a feasibility study the formation of cross-linked poly(thioether) microparticles by irradiating a tetrathiol/triacrylate mixture in methanol with PVP as stabilizer.

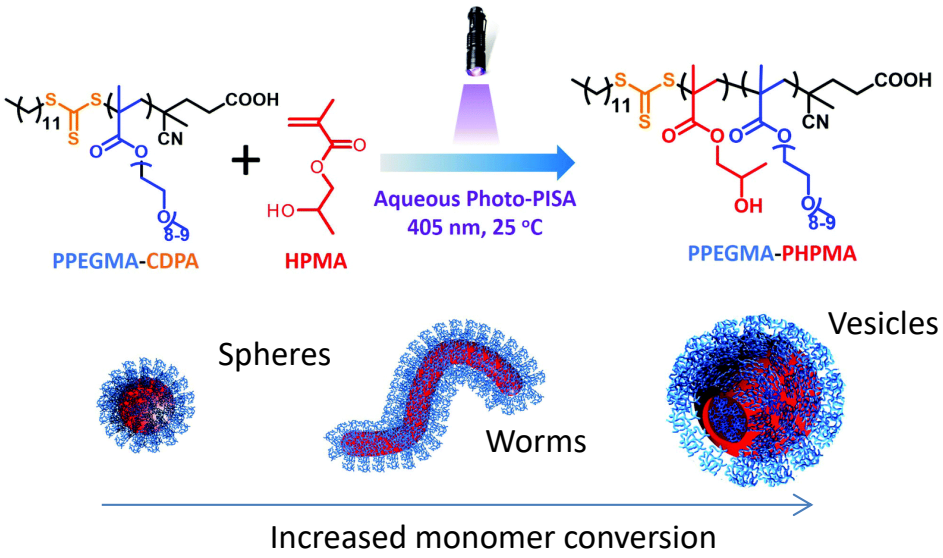

Fig 29: Photoinitiated polymerization-induced self-assembly (photo-PISA) of 2-hydroxypropyl methacrylate conducted in water using poly(poly(ethylene glycol) methyl ether methacrylate) (PPEGMA) based macro-RAFT agents. Figure was inspired from [215] and reproduced with permission of the copyright owners.

Table 5: Most significant studies on dispersion photopolymerization

Monomer	Continuous phase	Stabilizer	Photoinitiator	Polymerization time /Irradiation system	Solid content (wt %)	Particle diameter	Ref.
Styrene	Ethanol	PVP	P1	N_2 purged, Hg arc (?), 1 kW , glass, external, irradiation time: 16 h	10	0.7 – 1 µm	[186]
MMA	Ethanol/ water	PVP	P2	N_2 purged, high-pressure Hg arc, 400 W, glass, irradiance: 1.0 mW cm^{-2} (?) for λ = 320-400 nm, 30 min	10	≈ 1 µm	[188]
MMA/MAA	Ethanol/ water	PVP	P1	Hg arc or "black light" tube (?), 8 W, quartz, external, irradiance: 0.05 mW cm^{-2}	≈ 12	0.8 – 2 µm	[189]
Styrene	Isopropanol	PVP	P3	Ar, high-pressure Hg arc, DRSh-500, 500 W, glass, external, λ > 313 nm, irradiation time: 300 min	≈ 17	-	[191]
AA/trimethylol propane triacrylate	Ethanol / Liquid CO_2	PEO macromonomer	P7	CO_2, (pressurized), LED, λ = 405-410 nm, 3 W, quartz, external, irradiance: 0.8 mW cm^{-2}, reaction temperature: 0°C, irradiation time: 60 min	5	0.4 – 0.8 µm	[192]

MMA	Ethanol	PVP / Macro-RAFT CTA	P2	N_2 purged, LED, 3 W, external, λ = 365 nm, irradiance: 0.8 mW cm^{-2}, irradiation time: 45 min – 3 h	5-15	0.8 – 2 µm	[193, 194]
MMA	Ethanol/ water	Polyurethane modified Irgacure 2959 (P4)		N_2 purged, high-pressure (?) Hg arc, glass, external, irradiance (λ = 320-400 nm): 1.0 mW cm^{-2} (?), irradiation time: 1 h	10	0.9 – 1 µm	[80]
Diacetone acrylamide*	Water	Poly(2-hydropropymethacrylamide) macro-CTA	Phenyl-2,4,6-trimethyl-benzolphos-phinate	Ar purged, medium-pressure Hg arc, 400 W, external, filter: JB 400 W, λ > 400 nm, irradiance (λ = 420 nm): 0.20 mW cm^{-2}, reaction temperature: 25°C, irradiation time: 80 min	≈ 15	≈ 100 nm	[201]
Styrene*	Methanol	PVP macro-CTA	P1	UV radiation source, irradiance (λ : 365 nm): 2.50 mW cm^{-2}, irradiation time: < 10 h	≈ 50	≈ 30 nm	[202]
Benzyl methacrylate*	Ethanol	PEO methyl ether methacrylate macro-CTA	$Ru(bpy)_3Cl_2$ $6H_2O$	UV radiation source, pulsed (30 ms), external, 0.7 mW cm^{-2}, microreactor	10-20	Spherical or worm-like micelles, vesicles	[212]
Isobornyl acrylate*	Ethanol/ water	Monomethoxy PEO macro-CTA	P7	N_2 purged, LED, λ: 405 nm, external, glass, irradiance: 0.5 mW cm^{-2}, irradiation time: < 450 min	15-30	Spheres, worms, vesicles	[209]
2-hydroxylpropyl methacrylate*	Water	PEO-based macro CTA	Phenyl-2,4,6-trimethylbenzolphosphinate	N_2 purged, LED, λ: 405 nm, external, glass, irradiance: 0.5 mW cm^{-2}, irradiation time: 30 min	10-20	Spheres, worms, vesicles	[212]

* Refers to radiation-mediated controlled/radical RAFT polymerization in PISA

3.5 PRECIPITATION PHOTOPOLYMERIZATION

3.5.1 General considerations

Introduced for the first time by the group of Stöver, precipitation polymerization produces monodisperse micron-sized particles (0.5 – 15 µm) [221]. In this aspect, precipitation polymerization is barely different from dispersion polymerization. Other common points include an initial homogeneous mixture consisting of monomer, initiator and solvents, as well as the fact that particles and turbidity only arise during polymerization. However, major differences include: the absence of external stabilizer, the necessity of high amount of a cross-linker (> 95 %) and a near-θ solvent (i.e. an ideal solvent for interactions of the polymer) to avoid coagulation. All these distinctive features shed light on a very different polymerization mechanism (Fig. 30) [222].

In contrast to dispersion polymerization, the growing polymer chains do not phase separate from the continuous medium by enthalpy precipitation (unfavorable polymer-solvent interactions), but by entropic precipitation, because cross-linking prevents the polymer and solvent from freely mixing (de-solvation process). Continuous capture of oligomer species from solution contributes to particle growth from the surface, which is a significant difference to dispersion polymerization. Due to the "solvated θ" interface, such a transient polymer surface gel layer plays a key role in the colloidal stabilization of particles by a so-called “auto-steric” stabilization process. Additionally, a gentle stirring is usually recommended to avoid coagulation. In addition, high cross-linker concentration is necessary to produce “rigid” polymers able to form stable particles free of any added surfactant or stabilizer. One of the most important application areas of precipitation polymerization is the synthesis of molecularly imprinted polymers and materials for liquid chromatography.

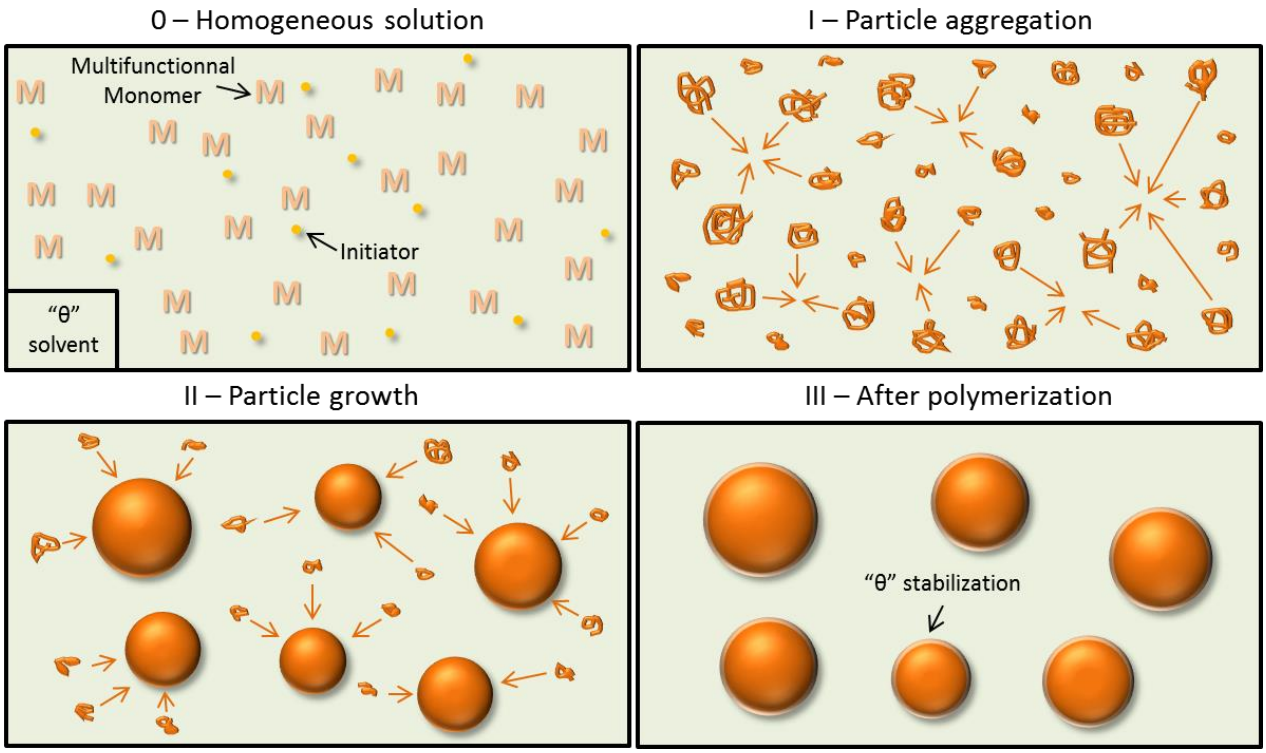

Fig 30: Particles synthesis by precipitation photopolymerization

In precipitation photopolymerization, most studies were performed at room temperature using divinylbenzene as cross-linker, and acetonitrile as θ–solvent. Fig. 31 gives a list of the main cross-linkers and monofunctional monomers used. Additionally, the characteristics of these studies on precipitation photopolymerization are summarized in Table 6. The justification for adopting this original technique is based on milder conditions, or the possibility to encapsulate temperature sensitive compounds.

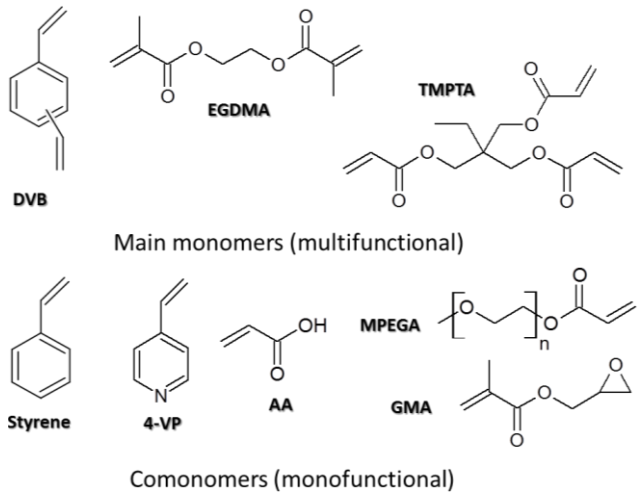

Fig 31: Main precursors used in precipitation photopolymerization

3.5.2 Adaptation to photoinitiation

In 2007, Barner et al. used AIBN (P1, Table 1), 2-methyl-4'-(methylthio)-2-morpholinopropiophenone (Irgacure 907, P6) and DMPA (P5) as radical photoinitiators for DVB precipitation polymerization in several organic solvents to obtain cross-linked microspheres [223]. Irradiation was provided by a fluorescent UV lamp. Only particle morphology was analysed and no results concerning reaction kinetics and polymer yield were reported.

Process kinetics and efficiency were addressed by Limé et al., who synthesized highly monodisperse cross-linked microparticles based on DVB and DVB/styrene in acetonitrile using AIBN as photoinitiator and a 150 W Xe arc [224]. Fig. 32 shows a schematic drawing of the photoreactor setup. The non-optimized photopolymerization conditions account for sluggish polymerization rates and long polymerization times extending up to 1 week. In 2009, Limé et al. showed that the use of a cosolvent (THF or 1-decanol) may afford porous monodisperse microparticles [225]. Interestingly, the change of the continuous phase had a positive impact on the polymerization times that were reduced to 48 h, but this result was not explained. 2,3-epoxymethacrylate was also used as co-monomer to design functional particles, and the resulting materials were used and tested as immobile phase in chromatography [226]. In 2013, other cross-linked microparticles were obtained by replacing DVB by multifunctional acrylate monomers: *e.g.* ethylene glycol dimethacrylate [227] or trimethylolpropane triacrylate [228].

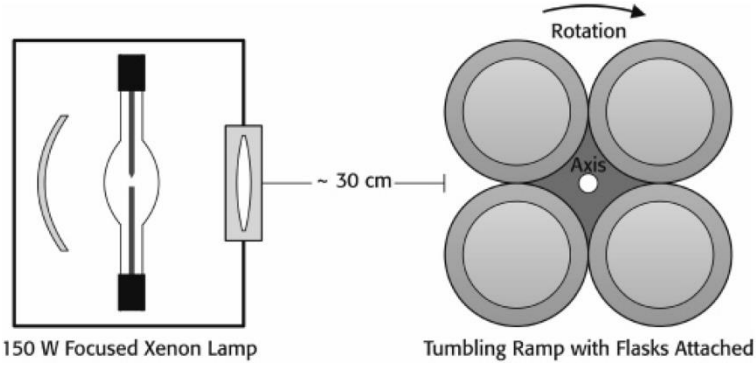

Fig. 32: Schematic drawing of the photopolymerization setup where 4 polypropylene or Teflon flasks were mounted on a rotating bracket. The flasks were rotating at 5-15 turns/min under the focused radiation of a Xe arc. Figure was reproduced from [224] with permission of the copyright owners.

Table 6: Main studies describing precipitation photopolymerization.

Monomers (Fig. 34)	**Continuous phase**	**Photoinitiator**	**Polymerization time/ Irradiation system**	**Particle diameter**	**Ref.**
DVB	Acetonitrile	P1/P5/P6	N_2 purged and degassed, "black light" tube (?) tube, UVP 3UV-38 "longwave", external, glass, radiant exitance: 0.015 mW (?), irradiation time: 24 h	1 – 3 µm	[223]
DVB/Styrene	Acetonitrile	P1	N_2 purged, Xe arc, 150 W, periodic (4 to 12 s), external, polypropylene, irradiation time: 6 – 40 h	1.4 – 4 µm	[224]
DVB/Glycidyl methacrylate	Acetonitrile/THF	P1	N_2 purged, Xe arc, 150 W, periodic (4 to 12 s), external, polypropylene, irradiation time: 12 – 24 h	0.8 – 5.1 µm	[225]
Ethylene glycol dimethacrylate/4-Vinylpyridine	Ethanol	Photoiniferter : benzyl dithiocarbamate	Ar purged, medium-pressure Hg arc, 400 W, glass, external, , irradiation time: 10 h	0.3 – 1.4 µm	[227]
Trimethylolpropane triacrylate /Styrene	Ethanol	P1	N_2 purged, Xe arc, 150 W, external, quartz, irradiation time: 120 h	0.7 – 2.9 µm	[228]

3.6 SUSPENSION PHOTOPOLYMERIZATION

3.6.1 General considerations

Suspension polymerization is, in terms of tonnage, the most important industrial polymerization process in dispersed systems [10]. Firstly, monomer emulsification is performed by simple mechanical stirring (Fig. 33). The interplay between droplet coalescence and break-up determines the droplet size distribution that is usually broad, ranging between 50 µm and 1 mm. The initiator is dissolved in the dispersed phase, and can be hydrophobic in the case of an oil-in-water type suspension (O/W) (most common), or hydrophilic in the case of a water-in-oil system (W/O). A stabilizer is usually added - often a water-soluble polymer - to prevent macroscopic phase separation. After the polymerization process, the polymer microparticles, often referred to as beads or pearls due to their large size, are recovered by filtration and dried. They usually have a similar

size distribution as the drops from which they are formed [229]. In this sense, a suspension polymerization bears more resemblance to a miniemulsion polymerization than to an emulsion polymerization, as particles are formed directly from monomer droplets. However, it should be stressed that the kinetics is very different due to radical compartmentalization in the case of miniemulsion. Smaller particles (0.2 to 20 microns) can be produced by microsuspension polymerization by increasing the stabilizer content and the stirring rate.

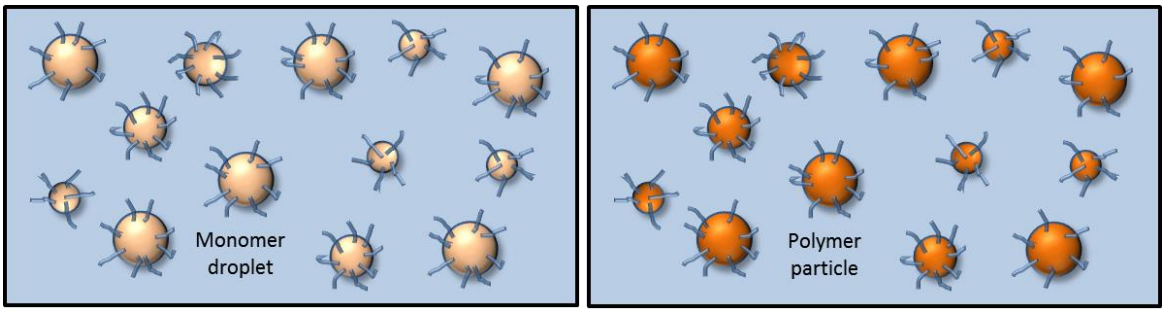

Fig. 33: Suspension polymerization process.

3.6.2 Adaptation to photoinitiation

There are relatively few examples of suspension photopolymerization; the main characteristics of these cases are summarized in Table 7. An inverse suspension photopolymerization was used by Pishko et al. in 2001 for the synthesis of cross-linked hydrogel beads able to release proteins [230]. The initial hydrophilic microdroplets contained pentaerythritol triacrylate (PETA), poly(ethylene glycol diacrylate) (PEG-DA) acting as a reactive costabilizer (Fig. 34) as well as a Type I photoinitiator, DMPA (P5). A mineral oil served as continuous phase. After UV exposure, cross-linked microspheres ranging in size from 500 to 900 µm were obtained.

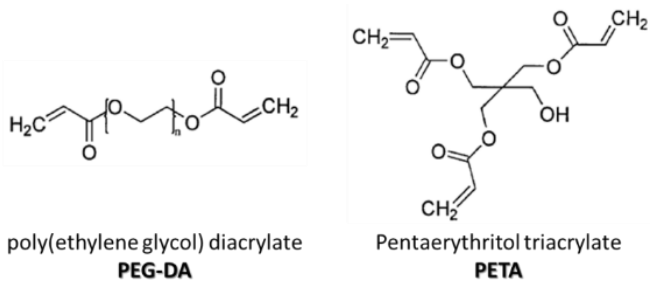

Fig. 34: Monomers used in suspension photopolymerization by Pishko et al. [230].

Crivello et al. synthesized epoxy-functional microspheres using cationic photopolymerization in aqueous and non-aqueous media. The waterborne suspensions based on dicyclohexyl epoxy monomers were stabilized by PVA, while the solvent-borne suspensions did not contain any stabilizer. A modified iodonium salt bearing a lipophilic chain was employed to ensure complete solubilization in the dispersed phase (Fig. 35). Despite the tendency of water to act as transfer agent, cross-linking occurred in these aqueous suspensions when the droplet diameters were greater than 1 µm. This result clearly demonstrates the importance of minimizing the surface-to-volume ratio to favor propagation over secondary reactions in the case of cationic polymerization. The aqueous suspension resulted in particles within the size range of 1 to 40 µm. Porogen agents were also introduced into the dispersed monomer phase to induce a macroporous structure of the particles. The porosity of the microspheres could be finely tailored by using different non-volatile porogen agents that are soluble in the monomer droplets and insoluble in the polymer [85, 231]. Another example of photoinitiated cationic polymerization of vinyl ethers in a dispersed system close to

suspension polymerization was reported by Yagci and coworkers [232]. The aqueous phase contained diphenyliodonium iodide and the water-tolerant Lewis acid (ytterbium triflate), while the monomer was dissolved in an acetonitrile organic phase. A highly exothermic polymerization takes place leading to precipitation due to the absence of surfactant.

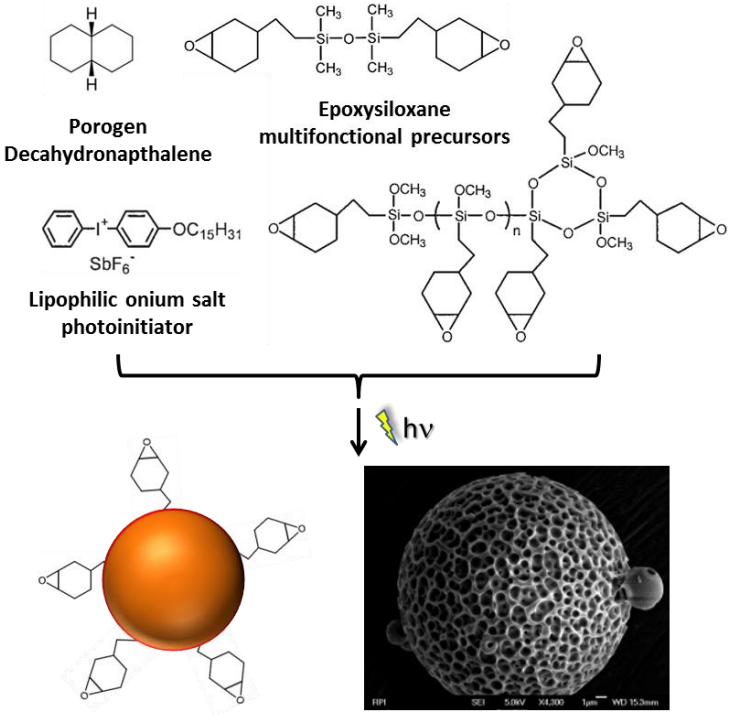

Fig. 35: Photoinduced process for the synthesis of porous microspheres in suspension developed by Crivello and Falk [85]. Monomer structures and TEM images were taken from reference [85] and reproduced with permission of the copyright owners. The epoxy functionality at the particle surface can be modified to have access to other functionalities [231].

Radical mediated thiol-ene step-growth photopolymerization was employed in 2012 by Shipp et al. to prepare cross-linked polysulfide microspheres from a waterborne monomer suspension containing polythiol and polyene monomers at equimolar ratios of ene/thiol functionality. This study marks the first use of thiol-ene photopolymerization in a dispersed system [233]. Unconventional experimental conditions were reported with the use of ultrasonication, organic diluents (toluene) and a costabilizer. A second study reported in 2014 was more similar to the conventional conditions of suspension polymerization by emulsifying a thiol-ene monomer phase by mechanical agitation in order to create monomer droplets. The study focused on the influence of different stabilizers, including anionic, cationic, and nonionic surfactants, which are nevertheless not usual in suspension systems [234]. This process was recently optimized by the replacement of the surfactants mentioned with water-soluble gum suspending agents such as gum Arabic, guar gum, and xanthan gum, demonstrating their efficient stabilizing properties even at very low concentration (0.005-0.5 wt%) [235].

More recently, functionalized thiol microparticles were created by using a slightly nonstoichiometric mixture (1.1:1 thiol:ene mol. equiv.). Successful capping of microparticles was subsequently performed with C60 (fullerene) to create a recyclable supported sensitizer for singlet-oxygen reactions [236]. For the production of supported sensitizers and phoocatalysts which is largely inspired by the protocol established by Shipp et al., the synthesis of porous microparticles containing different amounts of linear polymer porogen (poly(methyl methacrylates), PMMA) in the monomer organic phase was reported [237].

Table 7: Main studies describing suspension photopolymerization.

Monomer(s)	Continuous phase	Protective colloid	Photoinitiator	Polymerization time/ Irradiation system	Particle diameter	Ref.
Poly(ethylene glycol) diacrylate/pentaerythritol triacrylate	Mineral oil	-	P5	High-pressure Hg arc, 100 W, external, radiant exitance: 20 W cm^{-2}, irradiation time: 3 s	560 – 840 µm	[230]
Epoxysiloxane oil (Fig. 35)	Water Mineral oil	IPVA	Various diaryliodonium and triaryl sulfonium salts	Medium-pressure Hg arc, Hanovia, 679A36, 200 W, external, quartz, irradiance: 0.9 mW cm^{-2}, irradiation time: 5 to 15 min	10 – 50 µm	[85, 231]
Thiol/ene/yne multifunctional	Organic solvents	SDS	P5	"black light" tube, 9 W, λ = 320 - 400 nm, external, glass, irradiance: 2.5 mW cm^{-2}, irradiation time: < 1h	210 - 600 µm	[233]
Thiol/ene/yne multifunctional	Water	Various ionic and non-ionic surfactants	P8	UV radiation source, 365 nm, external, glass, irradiance: 11 mW cm^{-2}, irradiation time: 5 min	50 – 500 µm	[234]
Thiol/ene multifunctional	Water	Gum arabic, Guar gum, Xanthan gum	P8	UV radiation source, 365 nm, external, glass, irradiance: 11 mW cm^{-2}, irradiation time: 5 min	50 – 500 µm	[235]
Thiol/ene multifunctional	Water	Chitosan (Low molecular weight)	Irgacure 651	16 fluorescent tubes, λ = 350 nm, external, glass, Rayonet Photoreactor, irradiation time: 1 - 3 h	3 – 27 µm	[236]
Thiol/ene multifunctional	Water	SDS	P8	UV spotlight Lightningcure L8868 (Hamamtsu), irradiance: 18 mW cm^{-2}, external, glass, 30 s – 15 min	100- 600 µm	[237]

3.7 AEROSOL PHOTOPOLYMERIZATION

3.7.1 General considerations

Aerosol processing refers to the polymerization of monomer droplets dispersed in a gas phase (*e.g.* nitrogen or helium). Compared to a wet chemical route which is the mainstream approach to generate polymer particles, aerosol polymerization offers significant advantages: continuous production without the need of additives (surfactants, solvent), droplet nucleation implying that the final particle size is predetermined by the initial droplet size, high production rates, and straightforward collection of particles. Originally, aerosol technology was developed for the large scale manufacture of a broad variety of high utility inorganic nanoparticles (powders), including carbon black, titanium dioxide, and fumed silica [238]. Today, conventional aerosol processing remains intimately linked to flame reactors and very high temperatures processing, which are obviously not compatible with the synthesis of organic (nano)particles [239]. For a successful transposition into the domain of polymer, heat-induced aerosol polymerization has proved to be inadequate due to the negligible heat capacity of gases limiting heat exchange between the phases, as well as to the low stability of the aerosol monomer droplets. By contrast, photochemically induced aerosol polymerization appears to be a much better platform because of two specific features: the high cross-linking rates even at ambient temperature and the UV-visible transparency of many carrier gases used for aerosol production. Whatever the process, aerosol polymerization is useful for the preparation of hard polymer particles.

3.7.2 Adaptation to photoinitiation

The first results published in this field were obtained by Matijevic et al., and date back to the early 1980s. A complex tubular photoreactor set-up including multiple chambers was used to synthesize various dry polymer particles. In a first step, a monodisperse monomer (styrene or divinylbenzene) aerosol was generated by condensing vapor on condensation nuclei flowing through a temperature-controlled tube. Subsequently, a laminar flow stream was generated and contacted with the vapor of trifluoromethanesulfonic acid to initiate a cationic polymerization [240]. Monodisperse particles in the range

of 10-20 microns were achieved. However, heating was required to increase the relatively low reaction rates, and the irradiation conditions were not thoroughly described. During the same period, two other studies were conducted to synthesize microparticles based on poly-*p*-tertiarybutylstyrene [76] and mixed polyurea/metal oxide microspheres [241]. To investigate the very high rates associated with monomer droplet photopolymerization, single particle studies were also performed. A single entity was created by levitation of a small droplet in an electrodynamic balance, and the kinetics were monitored by fluorescence [242] or Raman spectroscopy [243].

In 1996, Esen et al. provided significant technical improvements: the use of a simpler tubular reactor fitted with external "black light" tubes, and a spray nozzle to generate monomer aerosol droplets [244]. Starting with a range of highly reactive multifunctional acrylate monomers dissolved in a highly volatile solvent (acetone, diethyl ether), monodisperse polymer particles with diameters of 5 to 50 µm were achieved by radical photopolymerization. Similar results were obtained by Gao and al. in 2007 using an analogous process [245].

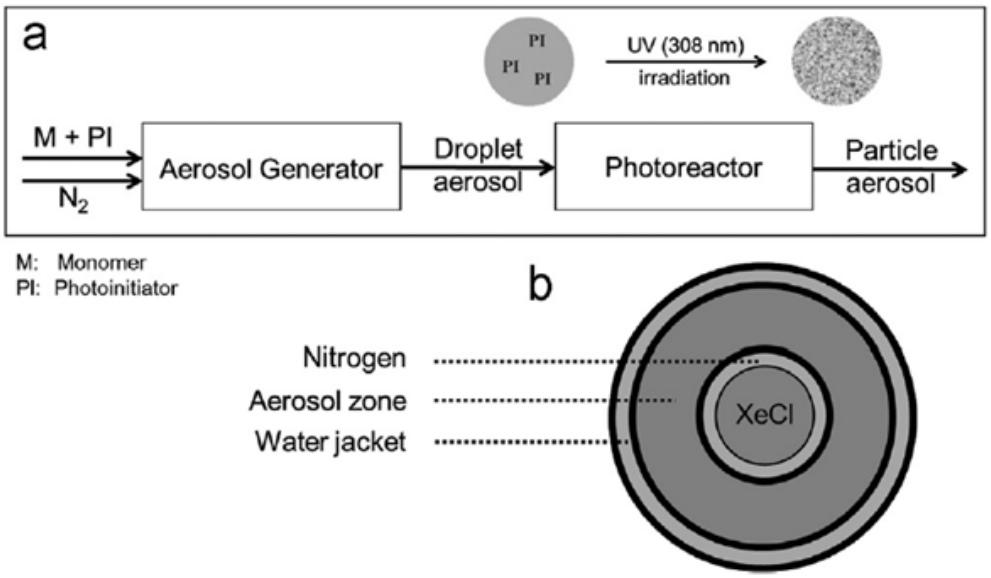

Fig. 36: Aerosol photopolymerization setup by spraying taken from reference [246] and reproduced with permission of the copyright owners. Schematic outline of the setup (a) and cross sectional view of the photoreactor (b).

The team of Wörner made intense research efforts from 2007 onwards to emphasize the new opportunities offered by aerosol processing with regard to particle morphology and composition [246]. Initial experiments were carried out using an annular photochemical reactor fitted with a cylindrical excimer radiation source (Fig. 36). While the radical homopolymerization of MMA aerosol droplets did not result in particles, two approaches relying on cross-linking (MMA/1,6-hexanediol diacrylate) and copolymerization (MMA/BA aerosol droplets) led to the successful formation of polymer particles. Interestingly, the process was extended to cationic photopolymerization [247] following the pioneering studies by Vorderbruggen et al. in 1996 [248]. The use of an inert gas carrier facilitated the implementation of this water-sensitive polymerization process. In this case, the aerosol droplets comprised multifunctional vinyl ether or epoxy monomers that were irradiated externally with a set of six "black light" fluorescent tubes. Recently, Wörner et al. fully exploited the technique when synthesizing a range of nanostructured particles, including mosaic nanoparticles caused by the phase separation of non-volatile porogen agent, or nanocapsules containing an active compound (caffeine) [249]. Organic-inorganic ZnO/polyacrylate nanoparticles were also produced by exploiting the photocatalytic properties of these inorganic semiconductor nanoparticles to trigger radical initiation [250]. Complex core-shell structure were finally obtained by merging two separate streams of

oppositely charged inorganic nanoparticle (core: silica, gold) and aerosol monomer droplets to generate the polymer shell [251]. The different works related to aerosol photopolymerization and their main characteristics are summarized in Table 8.

Table 8: Main studies on aerosol photopolymerization.

Monomer(s)	Continuous Phase	Photoinitiator	Polymerization time/ Irradiation system	Particle diameter	Reference
Styrene/DVB	He	TFSA photoactivated	Xe arc, 75 W, irradiation time: < 5 min,	5 - 30 µm	[240]
SOMOS 3100 (photopolymerizable resin based on di and triacrylates)	N_2	Type I, contained in SOMOS 3100	N_2, 8 "black light" tubes, 36 W, external	5 - 50 µm	[244]
SOMOS 10220 (photopolymerizable resin based on di and triacrylates)	N_2	Type I, contained in SOMOS 10220	N_2, 8 "black light" tubes, 40 W, external	5 -100 µm	[245]
MMA/BA/Hexanediol diacrylate	N_2	P6	N_2, XeCl excimer radiation source, HSQ 300 quartz, immersed, λ: 308 nm, radiant exitance: 10 mW cm^{-2}, irradiation time: 15 – 60 s	200 nm - 2 µm	[246]
Tri(ethylene glycol)divinyl ether, cyclohexene oxide	N_2	Triarylsulfonium salt	N_2, 6 fluorescent tubes, λ: 270-360 nm, external, irradiance: 5 mW cm^{-2}	200 nm - 2 µm	[247]
Diepoxysiloxane	N_2	Diphenyliodonium salt	Medium-pressure Hg arc, Hanovia, 400 W, external, salt plates, irradiation time: 1 s – 10 min	≈ 31 µm	[248]
MMA/BA/Hexanediol diacrylate + Porogen agent	N_2	P6	a) N_2, XeCl excimer radiation source, HSQ 300 quartz, immersed, λ: 308 nm, radiant exitance: ≤ 10 mW cm^{-2}, irradiation time: 1 min b) N_2, 6 fluorescent tubes, λ: 270-360 nm, external, irradiance: 5 mW cm^{-2}	1 -3 µm	[249]
MMA/BA/Hexanediol diacrylate + ZnO nanoparticles	N_2	P6	a) N_2, XeCl excimer radiation source, HSQ 300 quartz, immersed, λ: 308 nm, radiant exitance: ≤ 10 mW cm^{-2}, irradiation time: 1 min b) N_2, 6 fluorescent tubes, λ: 270-360 nm, external, irradiance: 5 mW cm^{-2}	200 nm- 2 µm	[250]
MMA/BA/Hexanediol diacrylate + Silica nanoparticles	N_2	P6	N_2, 6 fluorescent tubes, λ: 270-360 nm, external, irradiance: 5 mW cm^{-2}, irradiation time: 20 or 60 s	≈ 195 nm	[251]

4 CONCLUSION AND PROSPECTS

Over the past three decades, more stringent environmental and health regulations have placed greater emphasis on polymerizations in dispersed systems. Although most dispersed polymer products are particles dispersed in water, there is a wide variety of materials in terms of the types of polymers produced (thermosets, thermoplastics), of the size of the particles prepared (ranging from nanometer to millimeter scale) as well as of the available structures (functionalized, cross-linked or porous spheres, core-shell or hybrid particles, adhesive or protective films, etc.). This impressive versatility is rendered possible as a direct result of the wide array of different polymerization processes in dispersed systems. Although further progress will be made in the next years, the advances will be limited by the boundaries imposed by the chemistry of chain-growth radical polymerization using thermal or redox initiators.

As a "driver for change", photochemical initiation has proved to be well suited for polymerizations in dispersed systems as evidenced by the number of studies (approx. 200) that have been published in this domain since the 1980s. The perhaps seemingly minor alteration to a process to make it a photopolymerization – in most cases simply changing the initiation system and using a radiation source – can in fact lead to considerable added value. At present, the main advantage exploited by the polymer scientists is a polymerization conducted at room temperature with the goals of lowering energy consumption. Additional attractive features include both spatial and temporal control, or more recently, the possibility to perform some polymerizations facilitated under radiation activation (for e.g. thiol-ene step-growth

polymerization) or mediated by radiation (for e.g. photo-catalyzed radical initiation). In some cases, energetic dosage of radiation has demonstrated its ability to control the molecular-weight dispersity and the distribution of particle sizes. These attractive features should fuel a broader utilization in photopolymerization, whose principal application today concerns film curing technology. Additionally, the large-scale development of UV and VIS LEDs is another driving force behind the growth of photopolymerization techniques in general. However, one of the main obstacles for the development of photoinitiated polymerization processes in dispersed systems is radiation attenuation. The main consequence is a non-uniform radiation distribution, and in the worst conditions, a minimal irradiated reactor volume fraction that may lead to plugging problems and low efficiency of the photochemical initiation. Limited radiation penetration can be a major problem, when the system involves a high concentration of strongly scattering dispersed entities (i.e. monomer droplets and/or polymer particles being greater than approximately 100 nm in diameter), which are routine conditions in emulsion polymerization for example. Therefore, research on photopolymerization in dispersed systems started about 35 years ago, but crucially never succeeded in getting established as a solid alternative to conventional emulsion polymerization. However, very few photopolymerizations in dispersed systems described in this review were carried with an effort for optimizing utilization of radiation. Consequently, there is a considerable room for improvement, and clearly, many specific features offered by photoinitiation have yet to be realized.

With regard to prospects, a number of areas (many of them highlighted in this review) stand out. The issue of radiation attenuation is currently being addressed mainly by the design and use of new photoreactors suitable for highly absorbing media such as falling film or tubular reactors. To mitigate this problem, VIS light initiated polymerizations may another lever because in this spectral range, scattering is decreased compared to UV radiation. Some recent advances include three different approaches based on VIS photoinitiator, photoiniferter or photocatalysts. Furthermore, there is the question of the most suitable processes for a photopolymerization in dispersed system. Firstly, recent years have seen very few works on emulsion photopolymerization, which is however, one of the most established polymerization processes in dispersed systems. We foresee that the development of novel water-soluble photoinitiators may unlock its significant potential for innovation, with the additional benefit that radical recombination is minimized compared to organo-soluble photoinitiators that are predominantly micellized by surfactant species. Miniemulsion photopolymerization may be a second suitable process because it may feature, in the best cases, low-scattering monomer nanodroplets (40-100 nm). However, such nanosize range is not systematically achieved, and generally requires an energy-intensive emulsification stage clashing with the energy-saving features of a photoinitiated polymerization. In this regard, dispersion PISA is attractive as particles are formed via a self-assembly process, and the initial polymerization mixture is homogeneous (non-scattering). Photo-PISA is now being developed and explored within the context of RAFT polymerization. Of note is the fact that this polymerization technique falls in the category of controlled/living radical polymerization, and the role played by radiation is not simply to cause decomposition of a radical photoinitiator, but typically to regulate the activation/deactivation process (of propagating radicals) that is central to these systems. This specific area of research remains in its infancy, and it is envisaged that there is significant potential for development of photochemical systems that may greatly expand the scope of polymer particle synthesis. As a final comment, radiation is noninvasive (VIS light) for many biological systems – this is an important advantage in regards to the use of photochemical initiation for of polymer (nano)particles for pharmaceutical and medical applications such as drug delivery.

5. VITAE

Florent Jasinski obtained his Master degree at the University of Haute-Alsace (France). In 2014, he defended his PhD on the topic of photopolymerization in dispersed systems, at the University of Haute-Alsace (France). In 2015, he moved to the Centre for Advanced Macromolecular Design (CAMD) at UNSW (Sydney, Australia) where he is currently working as a postdoctoral research associate. His research focuses on gradient morphology nanoparticles used in advanced coatings applications.

Per Zetterlund graduated from KTH in Stockholm (Sweden), obtained his Ph.D. at Leeds University (UK), and conducted postdoctoral research at Griffith University (Brisbane, Australia). In 1999, he became Assistant Professor at Osaka City University (Japan), and moved to Kobe University (Japan) in 2003. Since 2009, he is working at The Centre for Advanced Macromolecular Design (CAMD) at UNSW (Sydney, Australia), where he is full Professor and CAMD co-Director. His research is concerned with synthesis of well-defined polymer, polymeric nanoparticles of various morphologies, and hybrid materials (graphene). He has published more than 175 peer-reviewed papers.

André M. Braun retired in 2006 from his chair at the Department of Chemical and Process Engineering of the University of Karlsruhe (now Karlsruhe Institute of Technology), Germany. He received his chemistry diploma in 1964 and his Ph.D. in 1966 from the University of Basel, Switzerland. From 1967 to 1969, he was a postdoctoral fellow at the California Institute of Technology and at Yale University. From 1969 to 1977, he worked as a research chemist at the Central Research Department of J.R. Geigy AG, later Ciba-Geigy AG in Basel. In 1977, he joined the Institute of Physical Chemistry of the Ecole Polytechnique Fédérale de Lausanne (EPFL), Switzerland. After his habilitation in 1978, he led as a privatdocent a research group focused on industrial applications of photochemistry until 1992, when he was called to head the Hewlett-Packard sponsored “Lehrstuhl für Umweltmesstechnik” at the University of Karlsruhe. His research interests include mechanistic and preparative photochemistry, design and scaling of photochemical reactors for industrial applications, and photophysics and photochemistry applied to environmental analysis and pollutant degradation. For his commitment to share experience and equipment with research groups in the framework

of international bilateral research contracts, he received in 2013 a honorary PhD of the Universidad Nacional del Litoral, Santa Fe, Argentina, and was nominated honorary professor of the Universidad Nacional de La Plata, Argentina, in 2014.

Abraham Chemtob obtained a PhD degree (Polymer Chemistry) in 2003 at the University of Bordeaux (France) on the development of ring-opening metathesis polymerization in dispersed systems. After two postdoctoral positions (University of Sydney - Australia, University of Basque Country - Spain), he became lecturer in 2006 (University of Haute Alsace - France). He currently works at the Institut de Sciences des Matériaux de Mulhouse (IS2M, CNRS). He is author of 75 refereed publications and his research activities have focused on innovative photopolymerization mechanisms and processes with 3 main topics: radical photopolymerization in dispersed systems, sol-gel inorganic photopolymerization, and step-growth photopolymerizations.

6. REFERENCES

[1] Asua JM. Chapter 1. Introduction to Polymerization Processes. In: Asua JM, editor. Polymer Reaction Engineering: Blackwell Publishing Ltd; 2008. p. 1-28.

[2] Anonymous, Freedonia Group. Freedonia World Emulsion Polymers, Study 2929, Industry study with Forecasts for 2016-2021. Cleveland: Freedonia; 2012. 319 pp.

[3] Schnabel W. Photopolymerization. Polymers and Light: Wiley-VCH, Weinheim; 2007. p. 273-304.

[4] Schwalm R. UV Coatings Basics, Recent Developments and New Applications. First ed. Amsterdam, The Netherlands: Elsevier; 2007 . 322 pp.

[5] Turro NJ, Chow M-F, Chung C-J, Tung C-H. An efficient, high conversion photoinduced emulsion polymerization. Magnetic field effects on polymerization efficiency and polymer molecular weight. J Am Chem Soc. 1980;102:7391-3.

[6] Jung K, Xu JT, Zetterlund PB, Boyer C. Visible-Light-Regulated Controlled/Living Radical Polymerization in Miniemulsion. ACS Macro Lett. 2015;4:1139-43.

[7] Mathers RT, Meier MAR. Green Polymerization Methods: Renewable Starting Materials, Catalysis and Waste Reduction. Weinheim, Germany: Wiley VCH;2011. 380 pp.

[8] Asua JM. Emulsion Polymerization: From Fundamental Mechanisms to Process Developments. J Polym Sci Part A Polym Chem. 2004;42:1025-41.

[9] Chern C-S. Principles and Applications of Emulsion Polymerization. Hoboken, USA: John Wiley and Sons; 2008. 272 pp.

[10] Brooks BW. Suspension Polymerization Processes. Chem Eng Techno. 2010;33:1737-44.

[11] Tauer K. Latex Particles. Colloids and Colloid Assemblies: Wiley-VCH Verlag; 2003. p. 1-51.

[12] Urban D, Takamura K. Polymer Dispersions and their Industrial Applications.Darmstadt: Wiley-VCH Verlag; 2002. 408 pp.

[13] Asua JM. Challenges and Opportunities in Continuous Production of Emulsion Polymers: a Review. Macromol React Eng. 2016;10:311-23.

[14] Fouassier JP, Lalevée J. Photoinitiators for Polymer Synthesis: Scope, Reactivity, and Efficiency. New York: John Wiley & Sons Inc, 2013. 494 pp.

[15] Jones FN, Nichols ME, Pappas SP. Organic Coatings: Science and Technology Hoboken, USA: John Wiley & Sons, Inc.; 2017. 512 pp.

[16] Turro NJ, Grätzel M, Braun AM. Photophysical and Photochemical Processes in Micellar Systems. Angew Chem Int Ed. 1980;19:675-96.

[17] Merlin A, Fouassier JP. Emulsion photopolymerization of MMA in the presence of saccharide. J Polym Sci Part A Polym Chem. 1981;19:2357-9.
[18] Baigl D. Photo-actuation of liquids for light-driven microfluidics: state of the art and perspectives. Lab Chip. 2012;12:3637-53.
[19] Silvares AFM, Nascimento CAO, Oliveros E, Bossmann SH, Braun AM. Optimization of the photochemically initiated polymerization of methyl methacrylate. Chem Eng Process Process Intensif. 2006;45:1001-10.
[20] Beuermann S, Buback M. Rate coefficients of free-radical polymerization deduced from pulsed laser experiments. Prog Polym Sci. 2002;27:191-254.
[21] Silvares AFM, do Nascimento CAO, Oliveros E, Bossmann SH, Braun AM. Pulsed XeCl Excimer Radiation for Optimizing the Polydispersity of Methyl Methacrylate Pre-Polymers. Ind Eng Chem Res. 2007;46:7436-47.
[22] Fouassier JP. Photoinitiation, Photopolymerization, and Photocuring: Fundamentals and Applications. New York: Hanser-Gardner Publications; 1995. 375 pp.
[23] Schnabel W. Technical Developments Related to Photopolymerization. Polymers and Light: Wiley-VCH, Weinheim; 2007. p. 305-33.
[24] Bouquey M, Serra C, Berton N, Prat L, Hadziioannou G. Microfluidic synthesis and assembly of reactive polymer beads to form new structured polymer materials. Chem Eng J. 2008;135:S93-S8.
[25] Nie ZH, Li W, Seo M, Xu SQ, Kumacheva E. Janus and ternary particles generated by microfluidic synthesis: Design, synthesis, and self-assembly. J Am Chem Soc. 2006;128:9408-12.
[26] Pregibon DC, Toner M, Doyle PS. Multifunctional encoded particles for high-throughput biomolecule analysis. Science. 2007;315:1393-6.
[27] Marre S, Jensen KF. Synthesis of micro and nanostructures in microfluidic systems. Chem Soc Rev. 2010;39:1183-202.
[28] Decker C, Moussa K. A new method for monitoring ultra-fast photopolymerizations by real-time infra-red (RTIR) spectroscopy. Makromol Chem. 1988;189:2381-94.
[29] Satuf ML, Brandi RJ, Cassano AE, Alfano OM. Experimental method to evaluate the optical properties of aqueous titanium dioxide suspensions. Ind Eng Chem Res. 2005;44:6643-9.
[30] Sun L, Bolton JR. Determination of the Quantum Yield for the Photochemical Generation of Hydroxyl Radicals in TiO2 Suspensions. J Phys Chem. 1996;100:4127-34.
[31] van de Hulst HC. Light Scattering by Small Particles. New York: John Wiley & Sons, Inc; 1957. 496 pp.
[32] Bohren CF, Huffman DR. Absorption and Scattering of Light by Small Particles. Weinheim: Wiley-VCH Verlag GmbH; 2007. 530 pp.
[33] Weiner I, Rust M, Donnelly TD. Particle size determination: An undergraduate lab in Mie scattering. Am J Phys. 2001;69:129-36.
[34a] Prahl S. Mie Scattering theory http://omlc.ogi.edu/software/mie/, 2018. 1 pp.
[34b] Prahl S. Mie Scattering Calculator http://omlc.ogi.edu/calc/mie_calc.html, 2018. 1 pp.
[35] Cox AJ, DeWeerd AJ, Linden J. An experiment to measure Mie and Rayleigh total scattering cross sections. Am J Phys. 2002;70:620-5.
[36] Jasinski F, Lobry E, Chemtob A, Croutxé-Barghorn C, Criqui A. Photopolymerizable Monomer Miniemulsions: Why Does Droplet Size Matter? Macromol Chem Phys. 2013;214:1669-76.
[37] Kubelka P. New Contributions to the Optics of Intensely Light-Scattering Materials. Part I. J Opt Soc Am. 1948;38:448-57.
[38] Lobry E, Jasinski F, Penconi M, Chemtob A, Ley C, Croutxé-Barghorn C, et al. Absorption and Scattering in Concentrated Monomer Miniemulsions: Static and Dynamic Investigations. Macromol Chem Phys. 2014;215:1201-11.
[39] Withaker S, Cassano AE. Concepts an Design of Chemical Reactors. Montreux, Switzerland: Gordon and Breach Science Publishers; 1986. 572 pp.
[40] Pareek VK, Adesina AA. Light intensity distribution in a photocatalytic reactor using finite volume. AIChE J. 2004;50:1273-88.
[41] Pareek V, Chong SH, Tade M, Adesina AA. Light intensity distribution in heterogenous photocatalytic reactors. Asia-Pac J Chem Eng. 2008;3:171-201.
[42] Moreira J, Serrano B, Ortiz A, de Lasa H. TiO2 absorption and scattering coefficients using Monte Carlo method and macroscopic balances in a photo-CREC unit. Chem Eng J. 2011;66:5813-21.

[43] Romero RL, Alfano OM, Cassano AE. Cylindrical photocatalytic reactors. Radiation absorption and scattering effects produced by suspended fine particles in an annular space. Ind Eng Chem Res. 1997;36:3094-109.
[44] Duran JE, Taghipour F, Mohseni M. Irradiance modeling in annular photoreactors using the finite-volume method. J Photochem Photobiol, A. 2010;215:81-9.
[45] Fischer M. Industrial Applications of Photochemical Synthesis. Angew Chem Int Ed Engl. 1978;17:16-26.
[46] Daniloska V, Tomovska R, Asua JM. Hybrid miniemulsion photopolymerization in a continuous tubular reactor—A way to expand the characteristics of polyurethane/acrylics. Chem Eng J. 2012;184:308-14.
[47] Xu J, Boyer C. Visible Light Photocatalytic Thiol–Ene Reaction: An Elegant Approach for Fast Polymer Postfunctionalization and Step-Growth Polymerization. Macromolecules. 2015;48:520-9.
[48] Dong S, Suzuki Y, Nik Hadzir NH, Lucien FP, Zetterlund PB. Radical polymerization of miniemulsions induced by compressed gases. RSC Adv. 2016;6:50650-7.
[49] Thompson KL, Lane JA, Derry MJ, Armes SP. Non-aqueous Isorefractive Pickering Emulsions. Langmuir. 2015;31:4373-6.
[50] Jasinski F, Lobry E, Tarablsi B, Chemtob A, Croutxé-Barghorn C, Le Nouen D, et al. Light-Mediated Thiol–Ene Polymerization in Miniemulsion: A Fast Route to Semicrystalline Polysulfide Nanoparticles. ACS Macro Lett. 2014;3:958-62.
[51] Amato DN, Amato DV, Narayanan J, Donovan BR, Douglas JR, Walley SE, et al. Functional, Composite Polythioether Nanoparticles via Thiol-Alkyne Photopolymerization in Miniemulsion. Chem Commun. 2015;51:10910-3.
[52] Jasinski F, Lobry E, Lefevre L, Chemtob A, Croutxe-Barghorn C, Allonas X, et al. Acrylate nanolatex via self-initiated photopolymerization. J Polym Sci Part A Polym Chem. 2014;52:1843-53.
[53] Lobry E, Bah A, Vidal L, Oliveros E, Braun AM, Criqui A, et al. Colloidal and Supported TiO2: Toward Nonextractable and Recyclable Photocatalysts for Radical Polymerizations in Aqueous Dispersed Media. Macromol Chem Phys. 2016;217:2321-9.
[54] Kohut-Svelko N, Pirri R, Asua JM, Leiza JR. Redox Initiator Systems for Emulsion Polymerization of Acrylates. J Polym Sci Part A Polym Chem. 2009;47:2917-27.
[55] Wang S. Redox-Initiated Adiabatic Emulsion Polymerization.Theses and Dissertations Paper 1294. Lehigh: Lehigh University; 2013. 246 pp.
[56] Mao D, Yang QL, Zhang X, Cheng Y. UV-Enhanced Gas-Solid Chlorination of Polyvinyl Chloride for Cleaner Production of Chlorinated Polyvinyl Chloride. Chem Eng Techno. 2016;39:834-40.
[57] Braun AM, Maurette MT, Oliveros E. Photochemical technology. New York: John Wiley & Sons Inc, 1991. 580 pp.
[58] Li Z, Chen WJ, Zhang ZB, Zhang LF, Cheng ZP, Zhu XL. A surfactant-free emulsion RAFT polymerization of methyl methacrylate in a continuous tubular reactor. Polym Chem. 2015;6:1937-43.
[59] Knowles JP, Elliott LD, Booker-Milburn KI. Flow photochemistry: Old light through new windows. Beil J Org Chem. 2012;8:2025-52.
[60] Lobry E, Jasinski F, Penconi M, Chemtob A, Croutxé-Barghorn C, Oliveros E, et al. Continuous-flow synthesis of polymer nanoparticles in a microreactor via miniemulsion photopolymerization. RSC Adv. 2014;4:43756-9.
[61] Daniloska V, Tomovska R, Asua JM. Designing tubular reactors to avoid clogging in high solids miniemulsion photopolymerization. Chem Eng J. 2013;222:136-41.
[62] Chemtob A, Lobry E, Rannee A, Jasinski F, Penconi M, Oliveros E, et al. Flash Latex Production in a Continuous Helical Photoreactor: Releasing the Brake Pedal on Acrylate Chain Radical Polymerization. Macromol React Eng. 2016;10:261-8.
[63] Stannett V, Gervasi JA, Kearney JJ, Araki K. Radiation-induced emulsion polymerization of vinyl acetate and styrene. J Appl Polym Sci. 1969;13:1175-89.
[64] Bradley M, Grieser F. Emulsion Polymerization Synthesis of Cationic Polymer Latex in an Ultrasonic Field. J Colloid Interface Sci. 2002;251:78-84.
[65] Bradley MA, Prescott SW, Schoonbrood HAS, Landfester K, Grieser F. Miniemulsion Copolymerization of Methyl Methacrylate and Butyl Acrylate by Ultrasonic Initiation. Macromolecules. 2005;38:6346-51.
[66] Korkut I, Bayramoglu M. Various Aspects of Ultrasound Assisted Emulsion Polymerization Process. Ultrason Sonochem. 2014;21:1592-9.

[67] Ooi SK, Biggs S. Ultrasonic initiation of polystyrene latex synthesis. Ultrason Sonochem. 2000;7:125-33.
[68] Correa R, Gonzalez G, Dougar V. Emulsion polymerization in a microwave reactor. Polymer. 1998;39:1471-4.
[69] Grassie N, Scott G. Polymer Degradation and Stabilisation. Cambridge: Cambridge University Press; 1985. 222 pp.
[70] Murov SL, Carmichael I, Hug GL. Handbook of Photochemistry, 2nd ed. New York: Marcel Dekker Inc, 1993. 664 pp.
[71] Penconi M, Lobry E, Jasinski F, Chemtob A, Croutxe-Barghorn C, Criqui A, et al. The use of chemical actinometry for the evaluation of the light absorption efficiency in scattering photopolymerizable miniemulsions. Photochem Photobiol Sci. 2015;14:308-19.
[72] Dixon JC. The Shock Absorber Handbook Appendix C: Properties of Water. John Wiley & Sons Ltd, 2007. p. 379-80.
[73] Quickenden TI, Irvin JA. The ultraviolet absorption spectrum of liquid water. J Chem Phys. 1980;72:4416-28.
[74] Campo J, Desmet F, Wenseleers W, Goovaerts E. Highly sensitive setup for tunable wavelength hyper-Rayleigh scattering with parallel detection and calibration data for various solvents. Opt Express. 2009;17:4587-604.
[75] Zhou Z, He D, Guo Y, Cui Z, Zeng L, Li GZ, et al. Photo-induced polymerization in ionic liquid medium: 1. Preparation of polyaniline nanoparticles. Polym Bull. 2009;62:573-80.
[76] Partch R, Matijević E, Hodgson AW, Aiken BE. Preparation of polymer colloids by chemical reactions in aerosols. I. Poly(p-tertiarybutylstyrene). J Polym Sci Part A Polym Chem. 1983;21:961-7.
[77] Napper DH, Netschey A. Studies of the steric stabilization of colloidal particles. J Colloid Interface Sci. 1971;37:528-35.
[78] Kawaguchi S, Ito K. Dispersion Polymerization. In: Okubo M, editor. Polymer Particles: Springer Berlin New York; 2005. p. 299-328.
[79] Pinto MCC, Santos JGF, Machado F, Pinto JC. Suspension Polymerization Processes In: Encyclopedia of Polymer Science and Technology, John Wiley & Sons, Inc. https://doi.org/10.1002/0471440264.pst597; 2013. 31 pp
[80] Tan J, Wu B, Yang J, Zhu Y, Zeng Z. Photoinitiated dispersion polymerization using polyurethane based macrophotoinitiator as stabilizer and photoinitiator. Polymer. 2010;51:3394-401.
[81] Holmberg K, editor.Novel Surfactants: Preparation Applications And Biodegradability, 2nd Ed. New York: Marcel Dekker; 2003. 648 pp.
[82] Haga N, Takayanagi H. Mechanisms of the Photochemical Rearrangement of Diphenyl Ethers. J Org Chem. 1996;61:735-45.
[83] Turro NJ. Chapters 10.3 and 13.2. Modern Molecular Photochemistry. Mill Valley, CA: University Science Books; 1991.628 pp.
[84] Firme CL, Garden SJ, de Lucas NC, Nicodem DE, Correa RJ. Theoretical Study of Photochemical Hydrogen Abstraction by Triplet Aliphatic Carbonyls by Using Density Functional Theory. J Phys Chem A. 2013;117:439-50.
[85] Falk B, Crivello JV. Synthesis of Epoxy-Functional Microspheres by Cationic Suspension Photopolymerization. Chem Mater. 2004;16:5033-41.
[86] Gilbert RG. Emulsion Polymerization: A Mechanistic Approach. London: Academic Press; 1995. 362 pp.
[87] Liska R. Photoinitiators with functional groups. v. new water-soluble photoinitiators containing carbohydrate residues and copolymerizable derivatives thereof. J Polym Sci Part A Polym Chem. 2002;40:1504-18.
[88] Ullrich G, Ganster B, Salz U, Moszner N, Liska R. Photoinitiators with functional groups. IX. Hydrophilic bisacylphosphine oxides for acidic aqueous formulations. J Polym Sci Part A Polym Chem. 2006;44:1686-700.
[89] Benedikt S, Wang J, Markovic M, Moszner N, Dietliker K, Ovsianikov A, et al. Highly Efficient Water-Soluble Visible Light Photoinitiators. J Polymer Sci Part A Polym Chem. 2016;54:473-9.
[90] Pawar AA, Saada G, Cooperstein I, Larush L, Jackman JA, Tabaei SR, et al. High-performance 3D printing of hydrogels by water-dispersible photoinitiator nanoparticles. Sci Adv. 2016;2:1501381/1-8.
[91] Dadashi-Silab S, Doran S, Yagci Y. Photoinduced Electron Transfer Reactions for Macromolecular Syntheses. Chem Rev. 2016;116:10212-75.

[92] Dietliker K. A compilation of photoinitiators commercially available for UV today. Edinbergh, London: SITA Technology Ltd. 2002. 250 pp.
[93] Thickett SC, Gilbert RG. Emulsion polymerization: State of the art in kinetics and mechanisms. Polymer. 2007;48:6965-91.
[94] Luo YW, Schork FJ. Emulsion and miniemulsion polymerizations with an oil-soluble initiator in the presence and absence of an aqueous-phase radical scavenger. J Polym Sci Part A Polym Chem. 2002;40:3200-11.
[95] Zetterlund PB. Controlled/living radical polymerization in nanoreactors: compartmentalization effects. Polym Chem. 2011;2:534-49.
[96] Turro NJ, Chow MF, Chung CJ, Tung CH. Magnetic field and magnetic isotope effects on photoinduced emulsion polymerization. J Am Chem Soc. 1983;105:1572-7.
[97] Turro NJ, Arora KS. Magnetic effects on photoinduced emulsion polymerization. Effects of lanthanide ion addition. Macromolecules. 1986;19:42-6.
[98] Turro NJ, Pierola IF, Chung C-J. Stereochemistry of photoinitiated emulsion polymerization. J Polym Sci, Part A: Polym Chem. 1983;21:1085-96.
[99] Bradley F, Johnston LJ, De Mayo P, King Wong S. Surface photochemistry: generation of benzyl radical pairs on dry silica gel. Can J Chem. 1983;62:403-10.
[100] Salikhov KM. Magnetic Isotope Effect in Radical Reactions: An Introduction. Wien: Springer; 1996. 149 pp.
[101] Chiriac AP, Simionescu CI. Magnetic field polymerisation. Prog Polym Sci. 2000;25:219-58.
[102] Britton D, Heatley F, Lovell PA. Chain transfer to polymer in free-radical bulk and emulsion polymerization of vinyl acetate studied by NMR spectroscopy. Macromolecules. 1998;31:2828-37.
[103] Mah S, Koo D, Jeon H, Kwon S. Photo-induced emulsion polymerization of vinyl acetate in the presence of poly(oxyethylene)10 nonyl phenyl ether ammonium sulfate, an anionic emulsifier (I). J Appl Polym Sci. 2002;84:2425-31.
[104] Mah S, Lee D, Koo D, Kwon S. Photo-induced emulsion polymerization of vinyl acetate in the presence of poly(oxyethylene) nonyl phenyl ether, a nonionic emulsifier (II). J Appl Polym Sci. 2002;86:2153-8.
[105] Kwak J, Lacroix-Desmazes P, Robin JJ, Boutevin B, Torres N. Synthesis of mono functional carboxylic acid poly(methyl methacrylate) in aqueous medium using sur-iniferter. Application to the synthesis of graft copolymers polyethylene-g-poly(methyl methacrylate) and the compatibilization of LDPE/PVDF blends. Polymer. 2003;44:5119-30.
[106] Otsu T. Iniferter concept and living radical polymerization. J Polym Sci Part A Polym Chem. 2000;38:2121-36.
[107] Matyjaszewski K. A commentary on "Role of initiator-transfer agent-terminator (Iniferter) in radical polymerizations: polymer design by organic disulfides as iniferters" by T. Otsu, M. Yoshida (Macromol. rapid commun. 1982,3,127-132). Macromol Rapid Commun. 2005;26:135-6.
[108] Shim SE, Shin Y, Jun JW, Lee K, Jung H, Choe S. Living-Free-Radical Emulsion Photopolymerization of Methyl Methacrylate by a Surface Active Iniferter (Suriniferter). Macromolecules. 2003;36:7994-8000.
[109] Quinn JF, Barner L, Barner-Kowollik C, Rizzardo E, Davis TP. Reversible addition-fragmentation chain transfer polymerization initiated with ultraviolet radiation. Macromolecules. 2002;35:7620-7.
[110] Fan W, Tosaka M, Yamago S, Cunningham MF. Living ab initio Emulsion Polymerization of Methyl Methacrylate in Water Using a Water-Soluble Organotellurium Chain Transfer Agent under Thermal and Photochemical Conditions. Angew Chem Int Ed. 2018;57:962-6.
[111] Hu X, Zhang J, Yang W. Preparation of transparent polystyrene nano-latexes by an UV-induced routine emulsion polymerization. Polymer. 2009;50:141-7.
[112] Nunes JDS, Asua JM. Synthesis of High Solids Content Low Surfactant/Polymer Ratio Nanolatexes. Langmuir. 2013;29:3895-902.
[113] Pignatello JJ, Oliveros E, Mackay A. Advanced oxidation processes for organic contaminant destruction based on the Fenton reaction and related chemistry. Crit Rev Environ Sci Technol. 2006;36:1-84.
[114] Zhang H, Zang L, Luo J, Guo J. Preparation of poly(methyl methacrylate) nano-latexes via UV irradiation in the presence of iron aqueous solution. e-polymers 2012. p. 376-85.

[115] Müller G, Zalibera M, Gescheidt G, Rosenthal A, Santiso-Quinones G, Dietliker K, et al. Simple One-Pot Syntheses of Water-Soluble Bis(acyl)phosphane Oxide Photoinitiators and Their Application in Surfactant-Free Emulsion Polymerization. Macromol Rapid Commun. 2015;36:553-7.
[116] Chicoma DL, Carranza V, Giudici R. Synthesis of Core-Shell Particles of Polystyrene and Poly(methyl methacrylate) Using Emulsion Photopolymerization. Makromol Chem Macromol. 2013;324:124-33.
[117] Lu Y, Wittemann A, Ballauff M, Drechsler M. Preparation of Polystyrene-Poly(N-isopropylacrylamide) (PS-PNIPA) Core-Shell Particles by Photoemulsion Polymerization. Macromol Rapid Commun. 2006;27:1137-41.
[118] Krüger K, Tauer K, Yagci Yf, Moszner N. Photoinitiated Bulk and Emulsion Polymerization of Styrene – Evidence for Photo-Controlled Radical Polymerization. Macromolecules. 2011;44:9539-49.
[119] Laurino P, Hernandez HF, Bräuer J, Krüger K, Grützmacher H, Tauer K, et al. Snowballing Radical Generation Leads to Ultrahigh Molecular Weight Polymers. Macromol Rapid Commun. 2012;33:1770-4.
[120] Le Quéméner F, Subervie D, Morlet-Savary F, Lalevée J, Lansalot M, Bourgeat-Lami E, et al. Visible-light Emulsion Photopolymerization of Styrene. Angew Chem. 2018;57:957-61.
[121] Nomura M, Suzuki K. A new kinetic interpretation of the styrene microemulsion polymerization. Macromol Chem Phys. 1997;198:3025-39.
[122] Candau F. Microemulsion Polymerization. In: Asua JM, editor. Polymeric Dispersions: Principles and Applications: Springer Netherlands; 1997. p. 127-40.
[123] Chow PY, Gan LM.Microemulsion polymerizations and reactions. In: Okubo M, editor. Polymer Particles: Springer Berlin New York; 2005. p. 257-98.
[124] Guo JS, El-Aasser MS, Vanderhoff JW. Microemulsion polymerization of styrene. J Polym Sci Part A Polym Chem. 1989;27:691-710.
[125] Wang L, Liu X, Li Y. Synthesis and Evaluation of a Surface-Active Photoinitiator for Microemulsion Polymerization. Macromolecules. 1998;31:3446-53.
[126] Full AP, Kaler EW, Arellano J, Puig JE. Microemulsion polymerization of styrene: The effect of salt and structure. Macromolecules. 1996;29:2764-75.
[127] Capek I. Microemulsion polymerization of styrene in the presence of anionic emulsifier. Adv Colloid Interface Sci. 1999;82:253-73.
[128] Capek I. Radical polymerization of polar unsaturated monomers in direct microemulsion systems. Adv Colloid Interface Sci. 1999;80:85-149.
[129] Capek I, Juraniĉová V. On kinetics of microemulsion copolymerization of butyl acrylate and acrylonitrile. J Polym Sci Part A Polym Chem. 1996;34:575-85.
[130] Holtzscherer C, Durand JP, Candau F. Polymerization of acrylamide in nonionic microemulsions: Characterization of the microlatices and polymers formed. Colloid Polym Sci. 1987;265:1067-74.
[131] Kukulj D, Davis TP, Gilbert RG. Chain transfer to monomer in the free-radical polymerizations of methyl methacrylate, styrene, and alpha-methylstyrene. Macromolecules. 1998;31:994-9.
[132] Kubota H, Ogiwara Y, Matsuzaki K. Photopolymerization of methyl methacrylate in the presence of saccharide. J Appl Polym Sci. 1976;20:1405-12.
[133] Encinas MV, Lissi EA, Olea AE. Polymerization photoinitiated by carbonyl compounds. V. Dependence of the initiation efficiency on the sensitizer distribution in emulsion polymerization. J Polym Sci Part A Polym Chem. 1983;21:2157-9.
[134] Kuo PL, Turro NJ, Tseng CM, El-Aasser MS, Vanderhoff JW. Photoinitiated polymerization of styrene in microemulsions. Macromolecules. 1987;20:1216-21.
[135] Larpent C, Tadros TF. Preparation of microlatex dispersions using oil-in-water microemulsions. Colloid Polym Sci. 1991;269:1171-83.
[136] Capek I. Photopolymerization of butyl acrylate microemulsions 1. Post-polymerization. Polym Int. 1996;40:41-9.
[137] Capek I. Photopolymerization of butyl acrylate microemulsion. Effect of reaction conditions and additives on fates of desorbed radicals. Polym J. 1996;28:400-6.
[138] Capek I, Fouassier JP. Kinetics of photopolymerization of butyl acrylate in direct micelles. Eur Polym J. 1997;33:173-81.
[139] Capek I. Photopolymerization of alkyl(meth)acrylates and polyoxyethylene macromonomers in fine emulsions. Eur Polym J. 2000;36:255-63.

[140] Buback M, Huckestein B, Russell GT. Modeling of termination in intermediate and high conversion free radical polymerizations. Macromol Chem Phys. 1994;195:539-54.
[141] David G, Özer F, Simionescu BC, Zareie H, Pişkin E. Microemulsion photopolymerization of methacrylates stabilized with sodium dodecyl sulfate and poly(N-acetylethylenimine) macromonomers. Eur Polym J. 2002;38:73-8.
[142] Jain K, Klier J, Scranton AB. Photopolymerization of butyl acrylate-in-water microemulsions: Polymer molecular weight and end-groups. Polymer. 2005;46:11273-8.
[143] Wan T, Hu ZW, Ma XL, Yao J, Lu K. Synthesis of silane monomer-modified styrene–acrylate microemulsion coatings by photopolymerization. Prog Org Coat. 2008;62:219-25.
[144] Candau F, Leong YS, Pouyet G, Candau S. Inverse microemulsion polymerization of acrylamide: Characterization of the water-in-oil microemulsions and the final microlatexes. J Colloid Interface Sci. 1984;101:167-83.
[145] Leong YS, Candau F. Inverse microemulsion polymerization. J Phys Chem. 1982;86:2269-71.
[146] Buruaga ASD, Capek I, Cal JCDL, Asua JM. Kinetics of the photoinitiated inverse microemulsion polymerization of 2-methacryloyl oxyethyl trimethyl ammonium chloride. J Polym Sci A Polym Chem. 1998;36:737-48.
[147] Marszalek JE, Pojman JA, Aultman KL, Hoyle CE, Whitehead JB. Humidity-responsive polymeric films based on AOT-water reverse microemulsions. J Appl Polym Sci. 2007;106:1957-63.
[148] Marszalek JE, Pojman JA, Page KA. Neutron Scattering Study of the Structural Change Induced by Photopolymerization of AOT/D2O/Dodecyl Acrylate Inverse Microemulsions. Langmuir. 2008;24:13694-700.
[149] Ciftci M, Tasdelen MA, Li W, Matyjaszewski K, Yagci Y. Photoinitiated ATRP in Inverse Microemulsion. Macromolecules. 2013;46:9537-43.
[150] Raj WRP, Sasthav M, Cheung HM. Formation of porous polymeric structures by the polymerization of single-phase microemulsions formulated with methyl methacrylate and acrylic acid. Langmuir. 1991;7:2586-91.
[151] Raj WRP, Sasthav M, Cheung HM. Synthesis of porous polymeric membranes by polymerization of micro-emulsions. Polymer. 1993;34:3305-12.
[152] Peinado C, Bosch P, Martín V, Corrales T. Photoinitiated polymerization in bicontinuous microemulsions: Fluorescence monitoring. J Polym Sci Part A Polym Chem. 2006;44:5291-303.
[153] Gao F, Ho C-C, Co CC. Polymerization in Bicontinuous Microemulsion Glasses. Macromolecules. 2006;39:9467-72.
[154] Asua JM. Challenges for Industrialization of Miniemulsion Polymerization. Prog Polym Sci. 2014;39:1797-826.
[155] Antonietti M, Landfester K. Polyreactions in miniemulsions. Prog Polym Sci. 2002;27:689-757.
[156] Landfester K, Bechthold N, Förster S, Antonietti M. Evidence for the preservation of the particle identity in miniemulsion polymerization. Macromol Rapid Commun. 1999;20:81-4.
[157] Alduncin JA, Forcada J, Asua JM. Miniemulsion Polymerization Using Oil-Soluble Initiators. Macromolecules. 1994;27:2256-61.
[158] Landfester K. Miniemulsion Polymerization and the Structure of Polymer and Hybrid Nanoparticles. Angew Chem Int Ed. 2009;48:4488-507.
[159] Tiarks F, Landfester K, Antonietti M. Preparation of polymeric nanocapsules by miniemulsion polymerization. Langmuir. 2001;17:908-18.
[160] Zetterlund PB, Thickett SC, Perrier S, Bourgeat-Lami E, Lansalot M. Controlled/Living Radical Polymerization in Dispersed Systems: An Update. Chem Rev. 2015;115:9745-800.
[161] Tonnar J, Pouget E, Lacroix-Desmazes P, Boutevin B. Synthesis of Poly(vinyl acetate)-block-poly(dimethylsiloxane)-block-poly(vinyl acetate) Copolymers by Iodine Transfer Photopolymerization in Miniemulsion. Macromol Symp. 2009;281:20-30.
[162] Fuchs AV, Will GD. Photo-initiated miniemulsion polymerization as a route to the synthesis of gold nanoparticle encapsulated latexes. Polymer. 2010;51:2119-24.
[163] Dou J, Zhang Q, Jian L, Gu Ji. Magnetic nanoparticles encapsulated latexes prepared with photo-initiated miniemulsion polymerization. Colloid Polym Sci. 2010;288:1751-6.
[164] Chemtob A, Kunstler B, Croutxé-Barghorn C, Fouchard S. Photoinduced miniemulsion polymerization. Colloid Polym Sci. 2010;288:579-87.

[165] Hoijemberg PA, Chemtob A, Croutxé-Barghorn C, Poly J, Braun AM. Radical Photopolymerization in Miniemulsions. Fundamental Investigations and Technical Development. Macromolecules. 2011;44:8727-38.
[166] Hoijemberg PA, Chemtob A, Croutxé-Barghorn C. Two routes towards photoinitiator-free photopolymerization in miniemulsion: Acrylate self-initiation and photoactive surfactant. Macromol Chem Phys. 2011;212:2417-22.
[167] Chemtob A, Lobry E, Rannée A, Jasinski F, Penconi M, Oliveros E, et al. Flash Latex Production in a Continuous Helical Photoreactor: Releasing the Brake Pedal on Acrylate Chain Radical Polymerization. Macromol React Eng. 2016;10:261-8.
[168] Jasinski F, Rannée A, Schweitzer J, Fischer D, Lobry E, Croutxé-Barghorn C, et al. Thiol–Ene Linear Step-Growth Photopolymerization in Miniemulsion: Fast Rates, Redox-Responsive Particles, and Semicrystalline Films. Macromolecules. 2016;49:1143-53.
[169] Daniloska V, Carretero P, Tomovska R, Asua JM. High performance pressure sensitive adhesives by miniemulsion photopolymerization in a continuous tubular reactor. Polymer. 2014;55:5050-6.
[170] Chemtob A, Rannée A, Chalan L, Fischer D, Bistac S. Continuous flow reactor for miniemulsion chain photopolymerization: Understanding plugging issue. Eur Polym J. 2016;80:247-55.
[171] Tomovska R, de la Cal JC, Asua JM. Miniemulsion Photo-Copolymerization of Styrene/Butyl Acrylate in a Continuous Tubular Reactor. Ind Eng Chem Res. 2014;53:7313-20.
[172] Saadé J, Bordes C, Raffin G, Hangouët M, Marote P, Faure K. Response surface optimization of miniemulsion: application to UV synthesis of hexyl acrylate nanoparticles. Colloid Polym Sci. 2016;294:27-36.
[173] Radtke CP, Delbé M, Wörner M, Hubbuch J. Photoinitiated miniemulsion polymerization in microfluidic chips on automated liquid handling stations: Proof of concept. Eng Life Sci. 2016;16:505-14.
[174] Roose P, Berlier M, De Doncker P, Baurant JN, Walters P. UV-nanoparticles: Photopolymerized polymer colloids from aqueous dispersions of acrylated oligomers. Prog Org Coat. 2014;77:1569-76.
[175] Roose P, Berlier M, Lazzaroni R, Leclère P. Dispersion Photopolymerization of Acrylated Oligomers Using a Flexible Continuous Reactor. Macromol React Eng. 2016;10:502-9.
[176] Jung K, Boyer C, Zetterlund PB. RAFT iniferter polymerization in miniemulsion using visible light. Polym Chem. 2017;8:3965-70.
[177] Chemtob A, Heroguez V, Gnanou Y. Dispersion ring-opening metathesis polymerization of norbornene using PEO-based stabilizers. Macromolecules. 2002;35:9262-9.
[178] Osmond DWJ, Thompson HH. Dispersion polymerisation of an acrylate in the presence of a rubber and a non-polar organic solvent and product obtained. US Patent 3257340 A; 1963.
[179] Ober CK, Lok KP, Hair ML. Monodispersed, micron-sized polystyrene particles by dispersion polymerization. J Polym Sci Part C Polym Lett. 1985;23:103-8.
[180] Sudol ED. Dispersion Polymerization. In: Asua JM, editor. Polymeric Dispersions: Principles and Applications. Dordrecht: Springer Science+Business Media. 1997. p. 141-53.
[181] Wang DN, Dimonie VL, Sudol ED, El-Aasser MS. Dispersion polymerization of n-butyl acrylate. J Appl Polym Sci. 2002;84:2692-709.
[182] Fehrenbacher U, Ballauff M. Kinetics of the early stage of dispersion polymerization in supercritical CO2 as monitored by turbidimetry. 2. Particle formation and locus of polymerization. Macromolecules. 2002;35:3653-61.
[183] Charleux B, Delaittre G, Rieger J, D'Agosto F. Polymerization-Induced Self-Assembly: From Soluble Macromolecules to Block Copolymer Nano-Objects in One Step. Macromolecules. 2012;45:6753-65.
[184] Canning SL, Smith GN, Armes SP. A Critical Appraisal of RAFT-Mediated Polymerization-Induced Self Assembly. Macromolecules. 2016;49:1985-2001.
[185] Yeow J, Boyer C. Photoinitiated Polymerization-Induced Self-Assembly (Photo-PISA): New Insights and Opportunities. Adv Sci. 2017;4:1700137/1-14.
[186] Shim SE, Jung H, Lee H, Biswas J, Choe S. Living radical dispersion photopolymerization of styrene by a reversible addition–fragmentation chain transfer (RAFT) agent. Polymer. 2003;44:5563-72.
[187] Ki B, Yu YC, Jeon HJ, Yu WR, Ryu HW, Youk JH. Dispersion polymerization of styrene using poly(4-vinylpyridine) macro-RAFT agent under UV radiation. Fibers Polym. 2012;13:135-8.
[188] Chen J, Zeng Z, Yang J, Chen Y. Photoinitiated dispersion polymerization of methyl methacrylate: A quick approach to prepare polymer microspheres with narrow size distribution. J Polym Sci Part A Polym Chem. 2008;46:1329-38.

[189] Huang Z, Sun F, Liang S, Wang H, Shi G, Tao L, et al. Photo-Initiated Dispersion Polymerization of Copolymer Microspheres in a Closed System: Poly(MMA-co-MAA). Macromol Chem Phys. 2010;211:1868-78.
[190] Zhu ZM, Sun FQ, Yang LT, Gu KY, Li WS. Poly (styrene-co-maleic anhydride) microspheres prepared in ethanol/water using a photochemical method and their application in Ni^{2+} adsorption. Chem Eng J. 2013;223:395-401.
[191] Ushakova MA, Chernyshev AV, Taraban MB, Petrov AK. Observation of magnetic field effect on polymer yield in photoinduced dispersion polymerization of styrene. Eur Polym J. 2003;39:2301-6.
[192] Wu B, Tan J, Yang J, Zeng Z. Photoinitiated precipitation polymerization in liquid CO_2: Fast formation of crosslinked poly(acrylic acid-co-methoxy polyethylene glycol acrylate) microspheres. J Polym Sci Part A Polym Chem. 2011;49:4660-7.
[193] Tan J, Rao X, Wu X, Deng H, Yang J, Zeng Z. Photoinitiated RAFT Dispersion Polymerization: A Straightforward Approach toward Highly Monodisperse Functional Microspheres. Macromolecules. 2012;45:8790-5.
[194] Tan J, Rao X, Yang J, Zeng Z. Synthesis of Highly Monodisperse Surface-Functional Microspheres by Photoinitiated RAFT Dispersion Polymerization Using Macro-RAFT Agents. Macromolecules. 2013;46:8441-8.
[195] Tan JB, Zhao GY, Lu YJ, Zeng ZH, Winnik MA. Synthesis of PMMA Microparticles with a Narrow Size Distribution by Photoinitiated RAFT Dispersion Polymerization with a Macromonomer as the Stabilizer. Macromolecules. 2014;47:6856-66.
[196] Tan JB, Rao X, Jiang D, Yang JW, Zeng ZH. One-stage photoinitiated RAFT dispersion polymerization - Reaction parameters for achieving high particle size uniformity. Polymer. 2014;55:2380-8.
[197] Tan J, Zhao G, Zeng Z, Winnik MA. PMMA Microspheres with Embedded Lanthanide Nanoparticles by Photoinitiated Dispersion Polymerization with a Carboxy-Functional Macro-RAFT Agent. Macromolecules. 2015;48:3629-40.
[198] Tan JB, Rao X, Yang JW, Zeng ZH. Monodisperse highly cross-linked "living" microspheres prepared via photoinitiated RAFT dispersion polymerization. RSC Adv. 2015;5:18922-31.
[199] Tan JB, Fu LL, Zhang XC, Bai YH, Zhang L. Photosynthesis of poly(glycidyl methacrylate) microspheres: a component for making covalently cross-linked colloidosomes and organic/inorganic nanocomposites. J Mater Sci. 2016;51:9455-71.
[200] Sugihara S, Blanazs A, Armes SP, Ryan AJ, Lewis AL. Aqueous Dispersion Polymerization: A New Paradigm for in Situ Block Copolymer Self-Assembly in Concentrated Solution. J Am Chem Soc. 2011;133:15707-13.
[201] Jiang YY, Xu N, Han J, Yu QP, Guo L, Gao P, et al. The direct synthesis of interface-decorated reactive block copolymer nanoparticles via polymerisation-induced self-assembly. Polym Chem. 2015;6:4955-65.
[202] Liu ZZ, Zhang GJ, Lu W, Huang YJ, Zhang JW, Chen T. UV light-initiated RAFT polymerization induced self-assembly. Polym Chem. 2015;6:6129-32.
[203] Yu QP, Ding Y, Cao H, Lu XH, Cai YL. Use of Polyion Complexation for Polymerization-Induced Self-Assembly in Water under Visible Light Irradiation at 25 degrees C. ACS Macro Lett. 2015;4:1293-6.
[204] Gao P, Cao H, Ding Y, Cai M, Cui ZG, Lu XH, et al. Synthesis of Hydrogen-Bonded Pore-Switchable Cylindrical Vesicles via Visible-Light-Mediated RAFT Room-Temperature Aqueous Dispersion Polymerization. ACS Macro Lett. 2016;5:1327-31.
[205] Yeow J, Xu JT, Boyer C. Facile Synthesis of Worm-like Micelles by Visible Light Mediated Dispersion Polymerization Using Photoredox Catalyst. J Vis Exp. 2016;112:e54269/1-6.
[206] Yeow J, Sugita OR, Boyer C. Visible Light-Mediated Polymerization-Induced Self-Assembly in the Absence of External Catalyst or Initiator. ACS Macro Lett. 2016;5:558-64.
[207] Yeow J, Shanmugam S, Corrigan N, Kuchel RP, Xu JT, Boyer C. A Polymerization-Induced Self-Assembly Approach to Nanoparticles Loaded with Singlet Oxygen Generators. Macromolecules. 2016;49:7277-85.
[208] Zhou J, Hong C, Pan C. The photo-controlled polymerization-induced self-assembly and reorganization process for fabrication of polymeric nanomaterials. Mater Chem Front. 2017;1:1200-6.
[209] Tan JB, Huang CD, Liu DD, Zhang XC, Bai YH, Zhang L. Alcoholic Photoinitiated Polymerization-Induced Self-Assembly (Photo-PISA): A Fast Route toward Poly(isobornyl acrylate)-Based Diblock Copolymer Nano-Objects. ACS Macro Lett. 2016;5:894-9.

[210] Tan J, He J, Li X, Xu Q, Huang C, Liu D, et al. Rapid synthesis of well-defined all-acrylic diblock copolymer nano-objects via alcoholic photoinitiated polymerization-induced self-assembly (photo-PISA). Polym Chem. 2017;8:6853-64.
[211] Tan J, Peng Y, Liu D, Huang C, Yu M, Jiang D, et al. Facile Preparation of Monodisperse Poly(2-hydroxyethyl acrylate)-Grafted Poly(methyl methacrylate) Microspheres via Photoinitiated RAFT Dispersion Polymerization. Macromol Chem Phys. 2016;217:1723-8.
[212] Tan JB, Sun H, Yu MG, Sumerlin BS, Zhang L. Photo-PISA: Shedding Light on Polymerization-Induced Self-Assembly. ACS Macro Lett. 2015;4:1249-53.
[213] Tan JB, Bai YH, Zhang XC, Huang CD, Liu DD, Zhang L. Low-Temperature Synthesis of Thermoresponsive Diblock Copolymer Nano-Objects via Aqueous Photoinitiated Polymerization-Induced Self-Assembly (Photo-PISA) using Thermoresponsive Macro-RAFT Agents. Macromol Rapid Commun. 2016;37:1434-40.
[214] Yu MG, Tan JB, Yang JW, Zeng ZH. Z-type and R-type macro-RAFT agents in RAFT dispersion polymerization - another mechanism perspective on PISA. Polym Chem. 2016;7:3756-65.
[215] Tan JB, Bai YH, Zhang XC, Zhang L. Room temperature synthesis of poly(poly(ethylene glycol) methyl ether methacrylate)-based diblock copolymer nano-objects via Photoinitiated Polymerization-Induced Self-Assembly (Photo-PISA). Polym Chem. 2016;7:2372-80.
[216] Tan J, Zhang X, Liu D, Bai Y, Huang C, Li X, et al. Facile Preparation of CO2-Responsive Polymer Nano-Objects via Aqueous Photoinitiated Polymerization-Induced Self-Assembly (Photo-PISA). Macromol Rapid Commun. 2017;38:1600508/1-8
[217] Tan J, Liu D, Huang C, Li X, He J, Xu Q, et al. Photoinitiated Polymerization-Induced Self-Assembly of Glycidyl Methacrylate for the Synthesis of Epoxy-Functionalized Block Copolymer Nano-Objects. Macromol Rapid Commun. 2017;38:1700195/1-7.
[218] Tan JB, Li XL, Zeng RM, Liu DD, Xu Q, He J, et al. Expanding the Scope of Polymerization-Induced Self-Assembly: Z-RAFT-Mediated Photoinitiated Dispersion Polymerization. ACS Macro Lett. 2018;7:255-62.
[219] Tan JB, Liu DD, Bai YH, Huang CD, Li XL, He J, et al. Enzyme-Assisted Photoinitiated Polymerization-Induced Self-Assembly: An Oxygen-Tolerant Method for Preparing Block Copolymer Nano-Objects in Open Vessels and Multiwell Plates. Macromolecules. 2017;50:5798-806.
[220] Wang C, Zhang XP, Podgorski M, Xi WX, Stansbury J, Bowman CN. Monodispersity/Narrow Polydispersity Cross-Linked Microparticles Prepared by Step-Growth Thiol-Michael Addition Dispersion Polymerizations. Macromolecules. 2015;48:8461-70.
[221] Li K, Stöver HDH. Synthesis of monodisperse poly(divinylbenzene) microspheres. J Polym Sci Part A Polym Chem. 1993;31:3257-63.
[222] Downey JS, Frank RS, Li WH, Stover HDH. Growth mechanism of poly(divinylbenzene) microspheres in precipitation polymerization. Macromolecules. 1999;32:2838-44.
[223] Joso R, Pan EH, Stenzel MH, Davis TP, Barner-Kowollik C, Barner L. Ambient temperature synthesis of well-defined microspheres via precipitation polymerization initiated by UV-irradiation. J Polym Sci Part A Polym Chem. 2007;45:3482-7.
[224] Limé F, Irgum K. Monodisperse Polymeric Particles by Photoinitiated Precipitation Polymerization. Macromolecules. 2007;40:1962-8.
[225] Limé F, Irgum K. Preparation of Divinylbenzene and Divinylbenzene-co-Glycidyl Methacrylate Particles by Photoinitiated Precipitation Polymerization in Different Solvent Mixtures. Macromolecules. 2009;42:4436-42.
[226] Nordborg A, Limé F, Shchukarev A, Irgum K. A cation-exchange material for protein separations based on grafting of thiol-terminated sulfopropyl methacrylate telomers onto hydrophilized monodisperse divinylbenzene particles. J Sep Sci. 2008;31:2143-50.
[227] Zhao M, Zhang H, Ma F, Zhang Y, Guo X, Zhang H. Efficient synthesis of monodisperse, highly crosslinked, and “living” functional polymer microspheres by the ambient temperature iniferter-induced “living” radical precipitation polymerization. J Polym Sci Part A Polym Chem. 2013;51:1983-98.
[228] Gu X, Sun H, Kong X, Fu C, Yu H, Li J, et al. A green protocol to prepare monodisperse poly(TMPTMA–styrene) microspheres by photoinitiated precipitation polymerization in low-toxicity solvent. Colloid Polym Sci. 2013;291:1771-9.
[229] VivaldoLima E, Wood PE, Hamielec AE, Penlidis A. An updated review on suspension polymerization. Ind Eng Chem Res. 1997;36:939-65.

[230] Mellott MB, Searcy K, Pishko MV. Release of protein from highly cross-linked hydrogels of poly(ethylene glycol) diacrylate fabricated by UV polymerization. Biomaterials. 2001;22:929-41.
[231] Falk B, Crivello JV. Synthesis and modification of epoxy- and hydroxy-functional microspheres. J Appl Polym Sci. 2005;97:1574-85.
[232] Kahveci MU, Tasdelen MA, Cook WD, Yagci Y. Photoinitiated Cationic Polymerization of Mono and Divinyl Ethers in Aqueous Medium Using Ytterbium Triflate as Lewis Acid. Macromol Chem Phys. 2008;209:1881-6.
[233] Durham OZ, Krishnan S, Shipp DA. Polymer Microspheres Prepared by Water-Borne Thiol–Ene Suspension Photopolymerization. ACS Macro Lett. 2012;1:1134-7.
[234] Durham OZ, Shipp DA. Suspension Thiol-Ene Photopolymerization: Effect of Stabilizing Agents on Particle Size and Stability. Polymer. 2014;55:1674-80.
[235] Durham OZ, Shipp DA. Suspension "click" polymerizations: thiol-ene polymer particles prepared with natural gum stabilizers. Colloid Polym Sci. 2015;293:2385-94.
[236] Barker EM, Buchanan JP. Thiol-ene polymer microbeads prepared under high-shear and their successful utility as a heterogeneous photocatalyst via C-60-capping. Polymer. 2016;92:66-73.
[237] Tan J, Li C, Zhou J, Yin C, Zhang B, Gu J, et al. Fast and facile fabrication of porous polymer particles via thiol-ene suspension photopolymerization. RSC Adv. 2014;4:13334-9.
[238] Gurav A, Kodas T, Pluym T, Xiong Y. Aerosol Processing of Materials. Aerosol Sci Techno. 1993;19:411-52.
[239] Pratsinis SE, Vemury S. Particle formation in gases: A review. Powder Techno. 1996;88:267-73.
[240] Nakamura K, Partch RE, Matijević E. Preparation of polymer colloids by chemical reactions in aerosols: II. Large particles. J Colloid Interface Sci. 1984;99:118-27.
[241] Partch RE, Nakamura K, Wolfe KJ, Matijević E. Preparation of polymer colloids by chemical reactions in aerosols. III. Polyurea and mixed polyurea-metal oxide particles. J Colloid Interface Sci. 1985;105:560-9.
[242] Ward TL, Zhang SH, Allen T, Davis EJ. Photochemical polymerization of acrylamide aerosol particles. J Colloid Interface Sci. 1987;118:343-55.
[243] Widmann JF, Davis EJ. Photochemical initiated polymerization of single microdroplets. Colloid Polym Sci. 1996;274:525-31.
[244] Esen C, Schweiger G. Preparation of Monodisperse Polymer Particles by Photopolymerization. J Colloid Interface Sci. 1996;179:276-80.
[245] Gao Z, Grulke EA, Ray AK. Synthesis of monodisperse polymer microspheres by photopolymerization of microdroplets. Colloid Polym Sci. 2007;285:847-54.
[246] Akgün E, Hubbuch J, Wörner M. Perspectives of aerosol-photopolymerization: Nanoscale polymer particles. Chem Eng Sci. 2013;101:248-52.
[247] Akgun E, Muntean A, Hubbuch J, Worner M, Sangermano M. Cationic Aerosol Photopolymerization. Macromol Mater Eng. 2015;300:136-9.
[248] Vorderbruggen MA, Wu K, Breneman CM. Use of Cationic Aerosol Photopolymerization To Form Silicone Microbeads in the Presence of Molecular Templates. Chem Mater. 1996;8:1106-11.
[249] Akgun E, Hubbuch J, Worner M. Perspectives of Aerosol-Photopolymerization: Nanostructured Polymeric Particles. Macromol Mater Eng. 2014;299:1316-28.
[250] Akgun E, Hubbuch J, Worner M. Perspectives of aerosol-photopolymerization: organic-inorganic hybrid nanoparticles. Colloid Polym Sci. 2014;292:1241-7.
[251] Sigmund S, Akgun E, Meyer J, Hubbuch J, Worner M, Kasper G. Defined polymer shells on nanoparticles via a continuous aerosol-based process. J Nanoparticle Res. 2014;16.